

Extended-soft-core Baryon-Baryon Model ESC08

II. Hyperon-Nucleon Interactions

M.M. Nagels

*Institute of Mathematics, Astrophysics, and Particle Physics
University of Nijmegen, Nijmegen, The Netherlands*

Th.A. Rijken

*Institute of Mathematics, Astrophysics, and Particle Physics
University of Nijmegen, Nijmegen, The Netherlands and
Nishina Center for Accelerator-Based Science, Institute for Physical
and Chemical Research (RIKEN), Wako, Saitama, 351-0198, Japan*

Y. Yamamoto

*Nishina Center for Accelerator-Based Science, Institute for Physical
and Chemical Research (RIKEN), Wako, Saitama, 351-0198, Japan*

(Dated: version of: September 11, 2018)

The YN results are presented from a new version of the Extended-soft-core (ESC) potential model for Baryon-baryon (BB) scattering. The potentials consist of local- and non-local-potentials due to (i) One-boson-exchanges (OBE), which are the members of nonets of pseudoscalar-, vector-, scalar-, and axial-vector mesons, (ii) Pomeron and Odderon exchanges, (iii) Two pseudoscalar exchange (PS-PS), and (iv) Meson-Pair-exchange (MPE). Both the OBE- and Pair-vertices are regulated by gaussian form factors producing potentials with a soft behavior near the origin. The assignment of the cut-off masses for the BBM-vertices is dependent on the $SU(3)$ -classification of the exchanged mesons for OBE, and a similar scheme for MPE. In addition to these standard ingredients of the ESC-models also the possible short range repulsion due to the quark Pauli-principle in the BB-channels is included in the analysis, for the first time in a systematic way, in this paper.

The present version of the ESC-model, called ESC08, describes nucleon-nucleon (NN) and hyperon-nucleon (YN) as well as the $S=-2$ hyperon-hyperon/nucleon (YY) in a unified way using broken $SU(3)$ -symmetry. Major novel ingredients with respect to the former version ESC04 are the inclusion of (i) short-range gaussian odderon-potentials corresponding to the odd number gluon-exchange, (ii) exceptional short range repulsion in specific YN and YY channels due to Pauli-forbidden six-quark cluster $(0s)^6$ -configurations. Further new elements are (i) the extension of the $J^{PC} = 1^{++}$ axial-vector meson coupling, (ii) the inclusion of the $J^{PC} = 1^{+-}$ axial-vector mesons, and (iii) a completion of the $1/M$ -corrections for the meson-pair-exchange (MPE) potentials. Like in the ESC04-model, the octet and singlet coupling constants and $F/(F+D)$ -ratio's of the model are conform the predictions of the quark-antiquark pair-creation (QPC) model with dominance of the 3P_0 -mechanism. This not only for the OBE-couplings but also for the MPE-couplings and $F/(F+D)$ -ratio's.

Broken $SU(3)$ -symmetry serves to connect the NN , the YN and the YY channels. The fitting of NN dominates the determination of the couplings and the cut-off masses. Only a few parameters are strongly influenced by the YN data, and by the constraints for the YY -interactions following from G-matrix analyses of hypernuclei. In particular, the meson-baryon coupling constants are calculated via $SU(3)$ using the coupling constants of the NN -analysis as input. In contrast to ESC04, we do not consider medium strong flavor-symmetry-breaking (FSB) of the coupling constants. The charge-symmetry-breaking (CSB) in the Λp and Λn channels, which is an $SU(2)$ isospin breaking, is included in the OBE-, TME-, and MPE-potentials.

For the ESC08-model we performed a simultaneous fit to the combined NN and YN scattering data, supplied with constraints on the YN and YY interaction originating from the G-matrix information on hypernuclei. In addition to the usual set of 35 YN-data and 3 $\Sigma^+ p$ cross-sections from a recent KEK-experiment E289, we added 11 elastic and inelastic Λp and 3 elastic $\Sigma^- p$ cross-sections at higher energy. We obtained within this simultaneous fit $\chi^2/NN_{data} = 1.081$ and $\chi^2/YN_{data} = 1.08$. In particular, we were able to fit the precise experimental datum $r_R = 0.468 \pm 0.010$ for the inelastic $\Sigma^- p$ capture ratio at rest rather well.

Besides the results for the fit to the scattering data, which defines the model largely, also the application to hypernuclear systems, using the G-matrix method, is rather important in establishing the ESC-model. Different versions of e.g. the ESC08-model give different results for hypernuclei. The reported G-matrix calculations are performed for YN (ΛN , ΣN , ΞN) pairs in nuclear matter and also for some hypernuclei. The obtained well depths (U_Λ , U_Σ , U_Ξ) reveal distinct features of the ESC-model.

The inclusion of a quark core Pauli-repulsion can make the Σ -nucleus interaction sufficiently repulsive, as seems to be required by the available experimental evidence. Furthermore, the ESC08-

model gives small spin-orbit splittings in Λ -hypernuclei, which is also indicated by experiment.

PACS numbers: 13.75.Cs, 12.39.Pn, 21.30.+y

I. INTRODUCTION

This is the second in a series of papers [1–3], henceforth referred to I, II, and III respectively, on the results of the Extended-soft-core (ESC) model for low and intermediate energy baryon-baryon interactions using the ESC08-model. The first results on the BB-channels and applications to hypernuclei were given in the review [4]. With the ESC04-models [5–7], it was shown that a very successful description of the presently available baryon-baryon scattering data could be achieved within the ESC-approach to the nuclear force problem. Also, such a description was obtained with meson-baryon coupling parameters which can be understood rather nicely within the context of the 3P_0 -quark-pair creation mechanism [8, 9]. This latter mechanism has been shown to be dominant in the framework of lattice QCD [10]. The simultaneous and unified treatment of the NN and YN channels in ESC04, using broken $SU(3)$ -flavor, has given already a rather successful potential model for the low and intermediate energy baryon-baryon scattering data. Furthermore, the basic ingredients of the model are physically motivated by the quark-model (QM) and QCD.

The G-matrix calculations showed that basic features of hypernuclear data are also reproduced rather well, improving several weak points of the soft-core OBE-models [11–13]. However, there remained the problem that the meson-exchange models seem to be unable to give a positive well depth U_Σ . A second problem posed the very small spin-orbit splittings in Λ -hypernuclei [14, 15]. In this paper we extend and refine the ESC-model in order to provide improvements and answers to these issues.

First, we list the new ingredients of the here presented version ESC08c, which are more or less in line with the ESC-approach as presented so far. In this category, the following additions to the ESC04-model are made for the present ESC08-model:

- (i) For the axial-vector mesons with $J^{PC} = 1^{++}$, the A -mesons, next to the $\gamma_5\gamma_\mu$ -coupling also the derivative $\gamma_5 k_\mu$ -coupling is exploited.
- (ii) The axial-vector mesons with $J^{PC} = 1^{+-}$, the B -mesons, are included as well. The latter have potentials of the same type as the pseudo-scalar mesons, but have an opposite sign. We notice that now the set of the exchanged quantum numbers for OBE-potentials is identical to that for MPE-potentials.
- (iii) For the meson-exchange we have included the Brown-Downs-Iddings anti-symmetric spin-orbit potentials from pseudoscalar-, vector-, scalar-, and axial- meson exchange [16].
- (iv) We have completed the $1/M$ -corrections for meson-pair-exchange (MPE), in particular for the $J^{PC} = 1^{++}$ - and $J^{PC} = 1^{+-}$ -axial pairs. This also leads to new important contributions to the anti-symmetric-spin-orbit

interaction [17].

(v) For the diffractive contribution we have next to the Pomeron-exchange [18] added the Odderon-exchange [19]. Whereas in QCD the Pomeron can be associated with colorless even number (2,4, ...) of gluon-exchanges, the Odderon is associated with the colorless odd number (3,5, ...) of gluon-exchanges. At low energies the Pomeron has $J^{PC} = 0^{++}$, but the Odderon has $J^{PC} = 1^{--}$.

Secondly, we have opened the possibility to incorporate possible effects of a 'structural' or channel-dependent repulsion due to Pauli-blocking. This repulsion originates from a 'forbidden-state' in the $SU(6)_{fs}$ Quark-Cluster-Model (QCM) [20, 21]. This is the analog of a well known effect in $\alpha\alpha$ -scattering discovered in the sixties [22]. This 'forbidden-state' is the $[51]$ -irrep and this irrep occurs with a large weight in the two $J^P = 1/2^+$ -baryon states in the $SU(3)_f$ -irreps $\{10\}$ and $\{8_s\}$. These irreps are prominent in the $\Sigma^+p(^3S_1)$ - respectively the $\Sigma N(^1S_0)$ -states. These are precisely the states where according to e.g. the G-matrix calculations the ESC-models possibly lack some repulsion. This repulsion seems to be indicated by experiment [23, 24]. The $[51]$ -irrep also occurs in the other NN -, YN -, and YY -channels, but with roughly equal weights, see [20], apart from a few $S=-2$ channels, e.g. $\Xi N(I=1, S=0)$.

We account for the 'exceptional-repulsion' in a phenomenological way by enhancing the "pure" Pomeron-coupling. So the effective Pomeron-repulsion consists of the pure Pomeron-exchange contribution augmented with a fraction of Pauli-blocking repulsion, which varies for the different BB-channels. (The other typical quark-cluster effects like e.g. one-gluon-exchange (OGE) annex quark-interchange is in ESC-models taken care of by meson exchange.) In this work we try to determine the strength of this Pauli-blocking effect in BB-channels. The fit to NN determines the sum of both the pure Pomeron-repulsion and the Pauli-blocking repulsion. The fit to YN determines the fraction of Pauli-blocking in it.

The ESC08-model realizes a fusion between the soft-core meson-exchange potentials and QCM-aspects of the baryon-baryon interactions and can be called a 'hybrid' ESC-model. The soft-core meson-exchange model has been described in detail in previous papers, [5–7]. Therefore, we may refer here to those papers for a description of (a) the physical background, (b) the employed formalism, (c) the description of the potentials, either in details or in references to papers where further information may be obtained. In this paper we will derive (i) the new OBE-potentials employed here for the first time in the context of the ESC-model, (ii) the Odderon-potentials, and (iii) a derivation of the short-range phenomenology connected to the quark Pauli principle within the context

of the $SU(3)_f$ -formalism as used in the Nijmegen potentials. Next to these items, we will also give the new $1/M$ -corrections for the axial-meson-pair-exchange potentials, where we restrict ourselves to the spin-spin and tensor contributions. The YN symmetric and anti-symmetric spin-orbit potentials will be described in another paper.

In [5, 6] a detailed description of the basic features of the ESC-models has been given and motivated. Many of these were already present in the Nijmegen soft-core [12] and hard-core [25] OBE-models. We refer the reader to these references for the description and discussion of the items such as: (broken) $SU(3)$ -flavor, charge-symmetry-breaking (CSB) in YN , meson-mixing in the pseudo-scalar-, vector-, scalar- meson $SU(3)$ -nonets, the role of the quark-antiquark pair-creation 3P_0 -model for BBM- and BBMP-couplings. Also, in e.g. [6] one finds a recapitulation of the goals of our continued investigation of the baryon-baryon systems.

In the soft-core Nijmegen OBE- and ESC-models the form factors are taken to be of the gaussian-type. In the (non-relativistic) QM's a gaussian behavior of the form factors for ground-state baryons is most natural. The two-particle branchpoints, corresponding to e.g. $\pi\pi, \pi\rho, K\rho$ -etc., are in the ESC-models accounted for by the MPE-potentials. Gaussian residue functions are used in regge-pole models for two-particle reactions at high-energy and low momentum-transfers.

As pointed out in [5, 6] $SU(3)$ -symmetry and the QPC-model give strong constraints on the coupling parameters. The 3P_0 -model also offers the possibility to introduce a scheme for hypercharge breaking a la Gell-Mann-Okubo for the BBM-couplings. In order to keep some more flexibility in distinguishing the NN - and the $YN(S = -1)$ -channels, such a medium-strong breaking was explored in the NSC97 [13] and ESC04 [6]. In the present study we do not apply such a breaking. The results show that a scheme of $SU(3)$ symmetric couplings with only mass breaking can give an excellent description of all BB interactions.

The content of this paper is as follows. In section II we review very briefly the scattering formalism, the Lippmann-Schwinger equation for the T- and V-matrices. Similarly, in section III the NN and $S = -1$ YN -channels on the isospin and particle basis, and the use of the multi-channel Schrödinger equation is mentioned. The potentials in momentum and configuration space are defined by referring to the description given in [5]. Also $SU(3)$ -breaking is reviewed briefly. In section IV on the OBE-potentials, the additions for ESC08 in comparison with the ESC04-model are described. Here, we give the new potentials in momentum and configuration space. In section V the $SU(3)$ structure of the MPE-potentials is given and the additions in comparison with the ESC04-model are listed. The latter are the axial $J^{PC} = 1^{+-}$ ($\pi\omega$)-pair potentials, which is the content of Appendix B. In section VI the short-range phenomenology is discussed. We derive the incorporation of the 'exceptional' Pauli-repulsion, which shows up 'exceptionally' large in the

$SU(3)$ -irreps $\{10\}$ and $\{8_s\}$.

In section VII the simultaneous $NN \oplus YN \oplus YY$ fitting procedure is reviewed. In section VIII the results for the coupling constants and $F/(F + D)$ -ratios for OBE and MPE are given. They are discussed and compared with the predictions of the QPC-model. Here, also the values of the BBM -couplings are displayed for pseudo-scalar, vector, scalar, and axial-vector mesons.

In section IX the YN -results for ESC08c from the combined $NN \oplus YN \oplus YY$ -fit are discussed. In section X we discuss the fit to the YN scattering data. In section XI, the hypernuclear properties of ESC08 are studied through the G-matrix calculations for YN ($\Lambda N, \Sigma N, \Xi N$) and their partial-wave contributions. Here, the implications of possible three-body effects for the nuclear saturation and baryon well-depths are discussed. Also, the $\Lambda\Lambda$ interactions in ESC08 are demonstrated to be consistent with the observed data of ${}^6_{\Lambda\Lambda}\text{He}$. In section XII we finish by a final discussion, draw some conclusions, and an outlook. In Appendix A we display the full $SU(3)$ contents of the MPE-couplings, and in Appendix B for completeness the $J^{PC} = 1^{+-}$ axial-pair potentials are given. Finally, in Appendix C the antisymmetric spin-orbit potentials are derived explicitly for strange meson-exchange K, K^*, κ , and K_1 .

II. SCATTERING FORMALISM, THE LIPPMANN-SCHWINGER EQUATION, POTENTIALS

In this paper we treat the nucleon-nucleon (NN) and hyperon-nucleon (YN) reactions with strangeness $S = 0, -1$. Since in general there are both 'direct' and 'exchange' potentials, the ordering of the baryons in the incoming and outgoing states needs special attention. For keeping this ordering clear, we consider for definiteness the hyperon-nucleon reactions

$$Y(p_1, s_1) + N(p_2, s_2) \rightarrow Y'(p'_1, s'_1) + N'(p'_2, s'_2) . \quad (2.1)$$

Like in [12], whose conventions we will follow in this paper, we will also refer to Y and Y' as particles 1 and 3 and to N and N' as particles 2 and 4. The four momentum of particle i is $p_i = (E_i, \mathbf{k}_i)$ where $E_i = \sqrt{\mathbf{k}_i^2 + M_i^2}$ and M_i is the mass/ The transition amplitude matrix M is related to the S -matrix via

$$\langle f|S|i\rangle = \langle f|i\rangle - i(2\pi)^4\delta^4(P_f - P_i)\langle f|M|i\rangle , \quad (2.2)$$

where $P_i = p_1 + p_2$ and $P_f = p'_1 + p'_2$ represent the total four momentum for the initial state $|i\rangle$ and the final state $|f\rangle$. The latter refer to the two-particle states, which we normalize in the following way

$$\begin{aligned} \langle \mathbf{p}'_1, \mathbf{p}'_2 | \mathbf{p}_1, \mathbf{p}_2 \rangle &= (2\pi)^3 2E(\mathbf{k}_1) \delta^3(\mathbf{p}'_1 - \mathbf{p}_1) \cdot \\ &\times (2\pi)^3 2E(\mathbf{k}_2) \delta^3(\mathbf{p}'_2 - \mathbf{p}_2) . \end{aligned} \quad (2.3)$$

We follow section II of [12] in detail. The transformation to the non-relativistic normalization of the two-particle states leads to states with

$$(\mathbf{p}'_1, s'_1; \mathbf{p}'_2, s'_2 | \mathbf{p}_1, s_1; \mathbf{p}_2, s_2) = (2\pi)^6 \delta^3(\mathbf{p}'_1 - \mathbf{p}_1) \cdot \times \delta^3(\mathbf{p}'_2 - \mathbf{p}_2) \delta_{s'_1, s_1} \delta_{s'_2, s_2} . \quad (2.4)$$

For these states we define the T -matrix by

$$(f|T|i) = \{4M_{34}(E_3+E_4)\}^{-\frac{1}{2}} \langle f|M|i \rangle \{4M_{12}(E_1+E_2)\}^{-\frac{1}{2}} , \quad (2.5)$$

which satisfies the Lippmann-Schwinger equation [12]

$$(3, 4|T|1, 2) = (3, 4|V|1, 2) + \frac{1}{(2\pi)^3} \sum_n \int d^3k_n \cdot \times (3, 4|V|n_1, n_2) \frac{2M_{n_1, n_2}}{\mathbf{p}_n^2 - \mathbf{k}_n^2 + i\varepsilon} (n_1, n_2|T|1, 2) , \quad (2.6)$$

and where analogously to Eq. (2.5) the potential V is defined as

$$(f|V|i) = \{4M_{34}(E_3+E_4)\}^{-\frac{1}{2}} \langle f|W|i \rangle \{4M_{12}(E_1+E_2)\}^{-\frac{1}{2}} . \quad (2.7)$$

Above, we denoted the initial- and final-state CM-momenta by \mathbf{p}_i and \mathbf{p}_f . Using rotational invariance and parity conservation we expand the T -matrix, which is a 4×4 -matrix in Pauli-spinor space, into a complete set of Pauli-spinor invariants ([12, 26])

$$T = \sum_{i=1}^8 T_i(\mathbf{p}_f^2, \mathbf{p}_i^2, \mathbf{p}_i \cdot \mathbf{p}_f) P_i . \quad (2.8)$$

Introducing

$$\mathbf{q} = \frac{1}{2}(\mathbf{p}_f + \mathbf{p}_i), \quad \mathbf{k} = \mathbf{p}_f - \mathbf{p}_i, \quad \mathbf{n} = \mathbf{p}_i \times \mathbf{p}_f = \mathbf{q} \times \mathbf{k} \quad (2.9)$$

with, of course, $\mathbf{n} = \mathbf{q} \times \mathbf{k}$, we choose for the operators P_i in spin-space

$$P_1 = 1 , \quad (2.10a)$$

$$P_2 = \boldsymbol{\sigma}_1 \cdot \boldsymbol{\sigma}_2 , \quad (2.10b)$$

$$P_3 = (\boldsymbol{\sigma}_1 \cdot \mathbf{k})(\boldsymbol{\sigma}_2 \cdot \mathbf{k}) - \frac{1}{3}(\boldsymbol{\sigma}_1 \cdot \boldsymbol{\sigma}_2) \mathbf{k}^2 , \quad (2.10c)$$

$$P_4 = \frac{i}{2}(\boldsymbol{\sigma}_1 + \boldsymbol{\sigma}_2) \cdot \mathbf{n} , \quad (2.10d)$$

$$P_5 = (\boldsymbol{\sigma}_1 \cdot \mathbf{n})(\boldsymbol{\sigma}_2 \cdot \mathbf{n}) , \quad (2.10e)$$

$$P_6 = \frac{i}{2}(\boldsymbol{\sigma}_1 - \boldsymbol{\sigma}_2) \cdot \mathbf{n} , \quad (2.10f)$$

$$P_7 = (\boldsymbol{\sigma}_1 \cdot \mathbf{q})(\boldsymbol{\sigma}_2 \cdot \mathbf{k}) + (\boldsymbol{\sigma}_1 \cdot \mathbf{k})(\boldsymbol{\sigma}_2 \cdot \mathbf{q}) \quad (2.10g)$$

$$P_8 = (\boldsymbol{\sigma}_1 \cdot \mathbf{q})(\boldsymbol{\sigma}_2 \cdot \mathbf{k}) - (\boldsymbol{\sigma}_1 \cdot \mathbf{k})(\boldsymbol{\sigma}_2 \cdot \mathbf{q}) . \quad (2.10h)$$

Here we follow [12, 26], except that we have chosen here P_3 to be a purely ‘tensor-force’ operator.

Similarly to (2.9) the potentials are expanded as

$$V = \sum_{i=1}^6 V_i(\mathbf{k}^2, \mathbf{q}^2) P_i . \quad (2.11)$$

The potentials in configuration space are described in Pauli-spinor space as follows

$$V(r) = V_C(r) + V_\sigma(r) \boldsymbol{\sigma}_1 \cdot \boldsymbol{\sigma}_2 + V_T(r) S_{12} + V_{SL}(r) \cdot \times \mathbf{L} \cdot \mathbf{S}_+ + V_{AL}(r) \mathbf{L} \cdot \mathbf{S}_- + V_Q(r) Q_{12} , \quad (2.12)$$

where $\mathbf{S}_\pm = (\boldsymbol{\sigma}_1 \pm \boldsymbol{\sigma}_2)/2$, and see e.g. [12] for a definition of the operators S_{12} and Q_{12} .

III. CHANNELS, POTENTIALS, AND $SU(3)$ SYMMETRY

A. Channels and Potentials

On the physical particle basis, there are three charge NN-channels:

$$q = +2, +1, 0 : \quad pp \rightarrow pp , \quad pn \rightarrow pn , \quad nn \rightarrow nn \quad (3.1)$$

Similarly, there are four charge YN-channels:

$$\begin{aligned} q = +2 : & \quad \Sigma^+ p \rightarrow \Sigma^+ p , \\ q = +1 : & \quad (\Lambda p, \Sigma^+ n, \Sigma^0 p) \rightarrow (\Lambda p, \Sigma^+ n, \Sigma^0 p) , \\ q = 0 : & \quad (\Lambda n, \Sigma^0 n, \Sigma^- p) \rightarrow (\Lambda n, \Sigma^0 n, \Sigma^- p) , \\ q = -1 : & \quad \Sigma^- n \rightarrow \Sigma^- n . \end{aligned} \quad (3.2)$$

Like in [12, 13], the potentials are calculated on the isospin basis. For $S = 0$ nucleon-nucleon systems there are two isospin-channels, namely $I = 1$ and $I = 0$. For $S = -1$ hyperon-nucleon systems there are also two isospin channels: (i) $I = \frac{1}{2}$: $(\Lambda N, \Sigma N \rightarrow \Lambda N, \Sigma N)$, and (ii) $I = \frac{3}{2}$: $\Sigma N \rightarrow \Sigma N$.

For the OBE-part of the potentials the treatment of $SU(3)$ for the BBM interaction Lagrangians and the coupling coefficients of the OBE-graphs has been given in detail in previous work of the Nijmegen group, e.g. [12] and [13]. For the TME- and the MPE-parts the calculation of the coupling coefficients has been exposed in our paper on the ESC04-model [6]. There we described the method of an automatic computerized calculation of these coefficients by exploiting the ‘cartesian-octet’-representation.

Also in this work we do not solve the Lippmann-Schwinger equation, but the multi-channel Schrödinger equation in configuration space, completely analogous to [12]. The multichannel Schrödinger equation for the configuration-space potential is derived from the Lippmann-Schwinger equation through the standard Fourier transform, and the equation for the radial wave function is found to be of the form [12]

$$u''_{l,j} + (p_i^2 \delta_{i,j} - A_{i,j}) u_{l,j} - B_{i,j} u'_{l,j} = 0 , \quad (3.3)$$

where $A_{i,j}$ contains the potential, nonlocal contributions, and the centrifugal barrier, while $B_{i,j}$ is only present when non-local contributions are included. The solution in the presence of open and closed channels is given, for example, in Ref. [27]. The inclusion of the Coulomb interaction in the configuration-space equation is well known and included in the evaluation of the scattering matrix.

The momentum space and configuration space potentials for the ESC-models have been described in paper I [5] for baryon-baryon in general. Here, we will only give the new contributions to these potentials, both in momentum and configuration space.

B. SU(3)-Symmetry and -Breaking, Form Factors

The treatment of the mass differences among the baryons is handled in the same way as for ESC04, which is exactly that of other Nijmegen models [12, 13, 25]. Also, exchange potentials related to strange meson exchange K, K^* etc., can be found in these references.

The breaking of SU(3)-symmetry occurs in several places. The physical masses of the baryons and mesons are used. Noticable is the $SU(2) \subset SU(3)$ breaking due to $\Lambda - \Sigma^0$ -mixing [28]. This $\Lambda - \Sigma^0$ -mixing leads also to a non-zero coupling of the Λ to the other $I = 1$ mesons: $\rho(760), a_0(980), a_1(1270)$, as well as to the $I = 1$ -pairs. For the details of these OBE-couplings see e.g. [13], equations (2.15)-(2.17). Like in ESC04, the corresponding so-called CSB-potentials are included in the ESC08-model for OBE, TME, and MPE.

The medium-strong SU(3)-symmetry breaking of the BBM-coupling constants is not tried in ESC08. In the ESC04-model this was considered optional, and regulated by the 3P_0 -model by a differentiation between the $s\bar{s}$ -quark pair and the creation of a non-strange quark-antiquark pair. Of course, we could contemplate about such an option here, but we did not investigate this option.

The baryon mass differences in the intermediate states for TME- and MPE- potentials have been neglected for YN-scattering. This, although possible in principle, becomes rather laborious and is not expected to change the characteristics of the baryon-baryon potentials much.

Also in this work, like ESC04- [5–7] and in the NSC97-models [13], the form factors depend on the SU(3) assignment of the mesons. In principle, we introduce form factor masses, i.e. cut-off's, Λ_8 and Λ_1 for the $\{8\}$ and $\{1\}$ members of each meson nonet, respectively. In the application to YN and YY, we could allow for SU(3)-breaking, by using different cut-offs for the strange mesons K, K^* , and κ . However, in the ESC08-model we do not exploit this possible breaking, but assign for the strange $I = 1/2$ -mesons the same cut-off as for the $I = 1$ -mesons. Moreover, for the $I = 0$ -mesons we assign the cut-offs as if there were no meson-mixing. For example we assign Λ_1 for the dominant singlet mesons η', ω, ϵ , and Λ_8 for η, ϕ, S^* , etc. This means a very slight form of

SU(3)-symmetry breaking.

IV. OBE-POTENTIALS IN ESC08

The OBE-potentials in ESC08 are those contained already in ESC04 [5, 6], and some new additional contributions. The additions to the OBE-potentials w.r.t. the ESC04-models consist of the following elements: (i) extension of the baryon-baryon-meson vertex of the axial-vector mesons ($J^{PC} = 1^{++}$) by adding the derivative coupling, (ii) inclusion of the axial-vector mesons of the 2nd kind, having $J^{PC} = 1^{+-}$. In paper I [1] the potentials for non-strange meson exchange have been given. Here, we list the additions and the basic potentials for meson exchange with non-zero strangeness.

A. Additions to the OBE-Potentials in ESC08

The interaction Hamiltonian densities for the new couplings are

a) Axial-vector-meson exchange ($J^{PC} = 1^{++}, 1^{st}$ kind):

$$\mathcal{H}_A = g_A [\bar{\psi} \gamma_\mu \gamma_5 \psi] \phi_A^\mu + \frac{if_A}{\mathcal{M}} [\bar{\psi} \gamma_5 \psi] \partial_\mu \phi_A^\mu. \quad (4.1)$$

In ESC04 the g_A -coupling was included, but not the derivative f_A -coupling.

b) Axial-vector-meson exchange ($J^{PC} = 1^{+-}, 2^{nd}$ kind):

$$\mathcal{H}_B = \frac{if_B}{m_B} [\bar{\psi} \sigma_{\mu\nu} \gamma_5 \psi] \partial_\nu \phi_B^\mu. \quad (4.2)$$

In ESC04 this coupling was not included. Like for the axial-vector mesons of the 1^{st} -kind we include a SU(3)-nonet with members $b_1(1235), h_1(1170), h_1(1380)$. In the quark-model they are $Q\bar{Q}({}^1P_1)$ -states.

The inclusion of the gaussian form factors is discussed in previous papers [12] etc. For the approximations made in deriving the potentials from the relativistic Born-Approximation we refer also to [12]. Due to these approximations the dependence on \mathbf{q}^2 is linearized and we write

$$V_i(\mathbf{k}^2, \mathbf{q}^2) = V_{ia}(\mathbf{k}^2) + V_{ib}(\mathbf{k}^2) \mathbf{q}^2, \quad (4.3)$$

where $i = 1 - 8$. It turns out that to order \mathbf{q}^2 only $V_{1b} \neq 0$. The additional OBE-potentials are obtained in the standard way, see [11, 12]. We write the potential functions V_i of (2.11) in the form

$$V_i(\mathbf{k}^2, \mathbf{q}^2) = \sum_X \Omega_i^{(X)}(\mathbf{k}^2) \cdot \Delta^{(X)}(\mathbf{k}^2, m^2, \Lambda^2), \quad (4.4)$$

where m denotes the mass of the meson, Λ the cut-off in the gaussian form factor, and $X = S, A, B$, and O

(S= scalar, A= axial-vector, B= axial-vector, and O = diffractive/odderon). For the additions when X=S,B the propagator is

$$\Delta^{(X)}(\mathbf{k}^2, m^2, \Lambda^2) = (1 - \mathbf{k}^2/U^2)e^{-\mathbf{k}^2/\Lambda^2}/(\mathbf{k}^2 + m^2), \quad (4.5)$$

and for the additions in the cases X=A,O the propagator is

$$\Delta^{(O)}(\mathbf{k}^2, m^2, \Lambda^2) = \frac{1}{\mathcal{M}^2}e^{-\mathbf{k}^2/4m_O^2}. \quad (4.6)$$

Here, \mathcal{M} is a universal scaling mass, taken to be the proton mass, which we also use in the derivative couplings above, as well as in the f_V -coupling of the vector-mesons. We note that the pole for the derivative coupling of the axial-vector exchange is canceled because of a factor $k^\mu (g_{\mu\nu} - k_\mu k_\nu/m_A^2)$.

B. Meson-exchange with Non-zero Strangeness ($\Delta Y \neq 0$)

For the non-strange mesons the mass differences at the vertices are neglected, we take at the YYM - and the NNM -vertex the average hyperon and the average nucleon mass respectively. This implies that we do not include contributions to the Pauli-invariants P_7 and P_8 . For vector-, and diffractive OBE-exchange we refer the reader to Ref. [12], where the contributions to the different $\Omega_i^{(X)}$'s for baryon-baryon scattering are given in detail. These exchanges lead to the so-called 'exchange-potentials'. For the invariants O_1, \dots, O_6 , the expressions analogous to those for the non-strange mesons given above apply. This with the amendments that (i) in momentum and configuration space there is a complete symmetric appearance of M_Y and M_N , (ii) in configuration space there appears the baryon-exchange operator $\mathcal{P} = -\mathcal{P}_x \mathcal{P}_\sigma$ operator, and (iii) for the antisymmetric spin-orbit potential $\mathcal{P} \rightarrow \mathcal{P}_x$. The details are given in Appendix C. Therefore, the $\Omega_i^{(X)}$ for these potentials can be obtained from those given in paper I Eqs. (4.9)-(4.13), by replacing both M_Y and M_N by $(M_Y M_N)^{1/2}$, and adding a (-)-sign. Furthermore, in the case of using the Proca-formalism [29], we get non-negligible contributions from the second part of the vector-meson propagator $(k_\mu k_\nu/m^2)$ of the K^* meson giving

$$-V_i^{K^*} = V_i^{(V)} - \frac{(M_3 - M_1)(M_4 - M_2)}{m^2} V_i^{(S)}, \quad (4.7)$$

where in $V_i^{(S)}$ the vector-meson-couplings have to be used, and M_Y and M_N must be replaced by $(M_Y M_N)^{1/2}$. In (4.7) $M_1 = M_4 = M_Y$ and $M_2 = M_3 = M_N$. Then the additional terms are

$$-V_i^{K_A} = V_i^{(A)} - \frac{(M_3 - M_1)(M_4 - M_2)}{m^2} V_i^{(P)}, \quad (4.8)$$

For the axial-vector meson K_B there is no contribution from the second-term in the propagator.

For the mesons with non-zero strangeness, K, K^*, κ, K_A and K_B , the mass differences at the vertices are not neglected, we take into account at the YNM -vertices the differences between the average hyperon and the average nucleon mass. This implies that we do include contributions to the Pauli-invariants P_8 . There do not occur contributions to P_7 .

(a) Pseudoscalar K-meson exchange:

$$\Omega_2^{(P)} = -g_{13}^P g_{24}^P \left(\frac{\mathbf{k}^2}{12M_Y M_N} \right), \quad \Omega_3^{(P)} = -g_{13}^P g_{24}^P \left(\frac{1}{4M_Y M_N} \right). \quad (4.9)$$

(b) Vector-meson K^* -exchange:

$$\begin{aligned}
\Omega_{1a}^{(V)} &= \left\{ g_{13}^V g_{24}^V \left(1 - \frac{\mathbf{k}^2}{8M_Y M_N} \right) - (g_{13}^V f_{24}^V + f_{13}^V g_{24}^V) \frac{\mathbf{k}^2}{4\mathcal{M}\sqrt{M_Y M_N}} \right. \\
&\quad \left. + f_{13}^V f_{24}^V \frac{\mathbf{k}^4}{16\mathcal{M}^2 M_Y M_N} \right\} \\
\Omega_{1b}^{(V)} &= g_{13}^V g_{24}^V \left(\frac{3}{2M_Y M_N} \right), \quad \Omega_2^{(V)} = -\frac{2}{3}\mathbf{k}^2 \Omega_3^{(V)} \\
\Omega_3^{(V)} &= \left\{ (g_{13}^V g_{24}^V + (g_{13}^V f_{24}^V + g_{24}^V f_{13}^V) \frac{\sqrt{M_Y M_N}}{\mathcal{M}}) + f_{13}^V f_{24}^V \frac{M_Y M_N}{\mathcal{M}^2} \left(1 - \frac{\mathbf{k}^2}{M_Y M_N} \right) \right\} / (4M_Y M_N) \\
\Omega_4^{(V)} &= - \left\{ 12g_{13}^V g_{24}^V + 8(g_{13}^V f_{24}^V + f_{13}^V g_{24}^V) \frac{\sqrt{M_Y M_N}}{\mathcal{M}} - f_{13}^V f_{24}^V \frac{3\mathbf{k}^2}{\mathcal{M}^2} \right\} / (8M_Y M_N) \\
\Omega_5^{(V)} &= - \left\{ g_{13}^V g_{24}^V + 4(g_{13}^V f_{24}^V + f_{13}^V g_{24}^V) \frac{\sqrt{M_Y M_N}}{\mathcal{M}} + 8f_{13}^V f_{24}^V \frac{M_Y M_N}{\mathcal{M}^2} \right\} / (16M_Y^2 M_N^2) \\
\Omega_6^{(V)} &= - \left\{ (g_{13}^V f_{24}^V - f_{13}^V g_{24}^V) \frac{1}{\sqrt{\mathcal{M}^2 M_Y M_N}} \right\}. \tag{4.10}
\end{aligned}$$

(c) Scalar-meson κ -exchange:

$$\begin{aligned}
\Omega_1^{(S)} &= -g_{13}^S g_{24}^S \left(1 + \frac{\mathbf{k}^2}{8M_Y M_N} - \frac{\mathbf{q}^2}{2M_Y M_N} \right), \quad \Omega_4^{(S)} = -g_{13}^S g_{24}^S \frac{1}{2M_Y M_N} \\
\Omega_5^{(S)} &= g_{13}^S g_{24}^S \frac{1}{16M_Y^2 M_N^2}, \quad \Omega_6^{(S)} = 0. \tag{4.11}
\end{aligned}$$

(d) Axial-vector K_1 -exchange $J^{PC} = 1^{++}$:

$$\begin{aligned}
\Omega_2^{(A)} &= -g_{13}^A g_{24}^A \left[1 - \frac{2\mathbf{k}^2}{3M_Y M_N} \right] + \left[\left(g_{13}^A f_{24}^A + f_{13}^A g_{24}^A \right) \frac{\sqrt{M_Y M_N}}{\mathcal{M}} - f_{13}^A f_{24}^A \frac{\mathbf{k}^2}{2\mathcal{M}^2} \right] \frac{\mathbf{k}^2}{6M_Y M_N} \\
\Omega_{2b}^{(A)} &= -g_{13}^A g_{24}^A \left(\frac{3}{2M_Y M_N} \right) \\
\Omega_3^{(A)} &= -g_{13}^A g_{24}^A \left[\frac{1}{4M_Y M_N} \right] + \left[\left(g_{13}^A f_{24}^A + f_{13}^A g_{24}^A \right) \frac{\sqrt{M_Y M_N}}{\mathcal{M}} - f_{13}^A f_{24}^A \frac{\mathbf{k}^2}{2\mathcal{M}^2} \right] \frac{1}{2M_Y M_N} \\
\Omega_4^{(A)} &= -g_{13}^A g_{24}^A \left[\frac{1}{2M_Y M_N} \right], \quad \Omega_5^{(A)'} = -g_{13}^A g_{24}^A \left[\frac{2}{M_Y M_N} \right], \quad \Omega_6^{(A)} = 0. \tag{4.12}
\end{aligned}$$

Here, we used the B-field description with $\alpha_r = 1$, see paper I, Appendix A. The detailed treatment of the potential proportional to P'_5 , i.e. with $\Omega_5^{(A)'}$, is given in paper I, Appendix B.

(e) Axial-vector mesons with $J^{PC} = 1^{+-}$:

$$\begin{aligned}
\Omega_2^{(B)} &= +f_{13}^B f_{24}^B \frac{(M_N + M_Y)^2}{m_B^2} \left[\left(1 - \frac{\mathbf{k}^2}{4M_Y M_N} \right) + 3 \frac{(\mathbf{q}^2 + \mathbf{k}^2/4)}{2M_Y M_N} \right] \left(\frac{\mathbf{k}^2}{12M_Y M_N} \right) \\
\Omega_3^{(B)} &= +f_{13}^B f_{24}^B \frac{(M_N + M_Y)^2}{m_B^2} \left[\frac{1}{4M_Y M_N} \right]. \tag{4.13}
\end{aligned}$$

(f) Diffractive-exchange (pomeron, $K_2(J=0)$):

The pomeron carries no strangeness. Therefore, the contribution to the potentials comes from the $J=0$ -part of K_2 -exchange [18]. The Ω_i^D are the same as for scalar-meson-exchange Eq.(4.11), but with $\pm g_{13}^S g_{24}^S$ replaced by $\mp g_{13}^D g_{24}^D$, and except for the zero in the form factor. Since in ESC08-models $g_{NNa_2} = 0$ there is no contribution to the exchange with non-zero strangeness.

(g) Odderon-exchange: Since the gluons carry no strangeness, there is no contribution to the potentials.

As in Ref. [12] in the derivation of the expressions for $\Omega_i^{(X)}$, given above, M_Y and M_N denote the mean hyperon and nucleon mass, respectively $M_Y = (M_1 + M_3)/2$ and $M_N = (M_2 + M_4)/2$, and m denotes the mass of the exchanged meson. Moreover, the approximation $1/M_N^2 + 1/M_Y^2 \approx 2/M_N M_Y$, is used, which is rather good since the mass differences between the baryons are not large.

C. One-Boson-Exchange Interactions in Configuration Space I

In configuration space the BB-interactions are described by potentials of the general form

$$V = \left\{ V_C(r) + V_\sigma(r) \boldsymbol{\sigma}_1 \cdot \boldsymbol{\sigma}_2 + V_T(r) S_{12} + V_{SO}(r) \mathbf{L} \cdot \mathbf{S} + V_Q(r) Q_{12} + V_{ASO}(r) \frac{1}{2} (\boldsymbol{\sigma}_1 - \boldsymbol{\sigma}_2) \cdot \mathbf{L} - \frac{1}{2} \left(\nabla^2 \phi(r) + \phi(r) \nabla^2 \right) \right\} \cdot \mathcal{P}, \quad (4.14)$$

where

$$S_{12} = 3(\boldsymbol{\sigma}_1 \cdot \hat{r})(\boldsymbol{\sigma}_2 \cdot \hat{r}) - (\boldsymbol{\sigma}_1 \cdot \boldsymbol{\sigma}_2), \quad (4.15a)$$

$$Q_{12} = \frac{1}{2} \left[(\boldsymbol{\sigma}_1 \cdot \mathbf{L})(\boldsymbol{\sigma}_2 \cdot \mathbf{L}) + (\boldsymbol{\sigma}_2 \cdot \mathbf{L})(\boldsymbol{\sigma}_1 \cdot \mathbf{L}) \right], \quad (4.15b)$$

$$\phi(r) = \phi_C(r) + \phi_\sigma(r) \boldsymbol{\sigma}_1 \cdot \boldsymbol{\sigma}_2, \quad (4.15c)$$

For the basic functions for the Fourier transforms with gaussian form factors, we refer to Refs. [11, 12]. For the details of the Fourier transform for the potentials with P'_5 , which occur in the case of the axial-vector mesons with $J^{PC} = 1^{++}$, we refer to paper I, Appendix B.

(a) Pseudoscalar-meson K-exchange:

$$V_{PS}(r) = \frac{m}{4\pi} \left[g_{13}^P g_{24}^P \frac{m^2}{4M_Y M_N} \left(\frac{1}{3} (\boldsymbol{\sigma}_1 \cdot \boldsymbol{\sigma}_2) \phi_C^1 + S_{12} \phi_T^0 \right) \right] \mathcal{P}. \quad (4.16)$$

(b) Vector-meson K^* -exchange:

$$\begin{aligned} V_V(r) = & \frac{m}{4\pi} \left\{ g_{13}^V g_{24}^V \left[\phi_C^0 + \frac{m^2}{2M_Y M_N} \phi_C^1 - \frac{3}{4M_Y M_N} (\nabla^2 \phi_C^0 + \phi_C^0 \nabla^2) \right] \right. \\ & + (g_{13}^V f_{24}^V + f_{13}^V g_{24}^V) \frac{m^2}{4\mathcal{M} \sqrt{M_Y M_N}} \phi_C^1 + f_{13}^V f_{24}^V \frac{m^4}{16\mathcal{M}^2 M_Y M_N} \phi_C^2 \Big\} \\ & + \frac{m^2}{6M_Y M_N} \left\{ \left[g_{13}^V g_{24}^V + (g_{13}^V f_{13}^V + g_{24}^V f_{13}^V) \frac{\sqrt{M_Y M_N}}{\mathcal{M}} + f_{13}^V f_{24}^V \frac{M_Y M_N}{\mathcal{M}^2} \right] \phi_C^1 + f_{13}^V f_{24}^V \frac{m^2}{8\mathcal{M}^2} \phi_C^2 \right\} (\boldsymbol{\sigma}_1 \cdot \boldsymbol{\sigma}_2) \\ & - \frac{m^2}{4M_Y M_N} \left\{ \left[g_{13}^V g_{24}^V + (g_{13}^V f_{24}^V + g_{24}^V f_{13}^V) \frac{\sqrt{M_Y M_N}}{\mathcal{M}} \right] \phi_T^0 + f_{13}^V f_{24}^V \frac{m^2}{8\mathcal{M}^2} \phi_T^1 \right\} S_{12} \\ & - \frac{m^2}{M_Y M_N} \left\{ \left[\frac{3}{2} g_{13}^V g_{24}^V + (g_{13}^V f_{24}^V + f_{13}^V g_{24}^V) \frac{\sqrt{M_Y M_N}}{\mathcal{M}} \right] \phi_{SO}^0 + \frac{3}{8} f_{13}^V f_{24}^V \frac{m^2}{\mathcal{M}^2} \phi_{SO}^1 \right\} \mathbf{L} \cdot \mathbf{S} \\ & + \frac{m^4}{16M_Y^2 M_N^2} \left\{ \left[g_{13}^V g_{24}^V + 4(g_{13}^V f_{24}^V + f_{13}^V g_{24}^V) \frac{\sqrt{M_Y M_N}}{\mathcal{M}} + 8f_{13}^V f_{24}^V \frac{M_Y M_N}{\mathcal{M}^2} \right] \right\} \\ & \times \frac{3}{(mr)^2} \phi_T^0 Q_{12} + \frac{m^2}{M_Y M_N} \left\{ (g_{13}^V f_{24}^V - f_{13}^V g_{24}^V) \frac{\sqrt{M_Y M_N}}{\mathcal{M}} \phi_{SO}^0 \right\} \cdot \frac{1}{2} (\boldsymbol{\sigma}_1 - \boldsymbol{\sigma}_2) \cdot \mathbf{L} \mathcal{P}_\sigma \Big\} \mathcal{P}. \end{aligned} \quad (4.17)$$

(c) Scalar-meson κ -exchange:

$$\begin{aligned} V_S(r) = & -\frac{m}{4\pi} \left[g_{13}^S g_{24}^S \left\{ \left[\phi_C^0 - \frac{m^2}{4M_Y M_N} \phi_C^1 \right] + \frac{m^2}{2M_Y M_N} \phi_{SO}^0 \mathbf{L} \cdot \mathbf{S} + \frac{m^4}{16M_Y^2 M_N^2} \right. \right. \\ & \times \frac{3}{(mr)^2} \phi_T^0 Q_{12} + \frac{1}{4M_Y M_N} (\nabla^2 \phi_C^0 + \phi_C^0 \nabla^2) \Big\} \Big] \mathcal{P}. \end{aligned} \quad (4.18)$$

(d) Axial-vector K_1 -meson exchange $J^{PC} = 1^{++}$:

$$\begin{aligned}
V_A(r) = & -\frac{m}{4\pi} \left[\left\{ g_{13}^A g_{24}^A \left(\phi_C^0 + \frac{2m^2}{3M_Y M_N} \phi_C^1 \right) + \frac{m^2}{6M_Y M_N} (g_{13}^A f_{24}^A + f_{13}^A g_{24}^A) \frac{\sqrt{M_Y M_N}}{\mathcal{M}} \phi_C^1 \right. \right. \\
& + f_{13}^A f_{24}^A \frac{m^4}{12M_Y M_N \mathcal{M}^2} \phi_C^2 \left. \right\} (\boldsymbol{\sigma}_1 \cdot \boldsymbol{\sigma}_2) - \frac{3}{4M_Y M_N} (\nabla^2 \phi_C^0 + \phi_C^0 \nabla^2) (\boldsymbol{\sigma}_1 \cdot \boldsymbol{\sigma}_2) \\
& - \frac{m^2}{4M_Y M_N} \left\{ \left[g_{13}^A g_{24}^A - 2 (g_{13}^A f_{24}^A + f_{13}^A g_{24}^A) \frac{\sqrt{M_Y M_N}}{\mathcal{M}} \right] \phi_T^0 - f_{13}^A f_{24}^A \frac{m^2}{2\mathcal{M}^2} \phi_T^1 \right\} S_{12} \\
& + \frac{m^2}{2M_Y M_N} g_{13}^A g_{24}^A \phi_{SO}^0 \mathbf{L} \cdot \mathbf{S} \left. \right] \mathcal{P}.
\end{aligned} \tag{4.19}$$

(e) Axial-vector-meson exchange $J^{PC} = 1^{+-}$:

$$\begin{aligned}
V_B(r) = & -\frac{m}{4\pi} \frac{(M_N + M_Y)^2}{m^2} \left[f_{13}^B f_{24}^B \left\{ \frac{m^2}{12M_Y M_N} \left(\phi_C^1 + \frac{m^2}{4M_Y M_N} \phi_C^2 \right) \right. \right. \\
& \left. \left. - \frac{m^2}{8M_Y M_N} (\nabla^2 \phi_C^1 + \phi_C^1 \nabla^2) + \left[\frac{m^2}{4M_Y M_N} \right] \phi_T^0 S_{12} \right\} \right] \mathcal{P}.
\end{aligned} \tag{4.20}$$

(f) Diffractive-exchange: Since in the ESC08-model the diffractive pomeron and odderon exchanges are SU(3) singlets there are no contribution to $S \neq 0$ -exchange potentials.

Above, in Eq.'s (4.16-4.20) the exchange operator is defined as

$$\mathcal{P} = -\mathcal{P}_x \mathcal{P}_\sigma, \tag{4.21}$$

where \mathcal{P}_x and \mathcal{P}_σ are the space- and spin-exchange operators respectively. The extra $(-\mathcal{P}_\sigma)$ -operator in (4.17) for the antisymmetric spin-orbit potential is explained in Appendix C. We note that $-\mathcal{P}_\sigma \mathcal{P} = \mathcal{P}_x$, which is well defined for the coupled singlet-triplet systems.

D. One-Boson-Exchange Interactions in Configuration Space II

Here we give the extra potentials due to the zero's in the scalar and axial-vector form factors.

a) Again, for $X = V, D$ we refer to the configuration space potentials in Ref. [12]. For $X = S$ we give here the additional terms w.r.t. those in [12], which are due to the zero in the scalar form factor. They are

$$\begin{aligned}
\Delta V_S(r) = & -\frac{m}{4\pi} \frac{m^2}{U^2} \left[g_{13}^S g_{24}^S \left\{ \left[\phi_C^1 - \frac{m^2}{4M_Y M_N} \phi_C^2 \right] + \frac{m^2}{2M_Y M_N} \phi_{SO}^1 \mathbf{L} \cdot \mathbf{S} \right. \right. \\
& \left. \left. + \frac{m^4}{16M_Y^2 M_N^2} \phi_T^1 Q_{12} \right\} \right] \mathcal{P}.
\end{aligned} \tag{4.22}$$

b) For the axial-vector mesons, the configuration space potential corresponding to (4.12) is

$$\begin{aligned}
V_A^{(1)}(r) = & -\frac{g_A^2}{4\pi} m \left[\phi_C^0 (\boldsymbol{\sigma}_1 \cdot \boldsymbol{\sigma}_2) - \frac{1}{12M_Y M_N} (\nabla^2 \phi_C^0 + \phi_C^0 \nabla^2) (\boldsymbol{\sigma}_1 \cdot \boldsymbol{\sigma}_2) \right. \\
& \left. + \frac{3m^2}{4M_Y M_N} \phi_T^0 S_{12} + \frac{m^2}{2M_Y M_N} \phi_{SO}^0 \mathbf{L} \cdot \mathbf{S} \right] \mathcal{P}.
\end{aligned} \tag{4.23}$$

The extra contribution to the potentials coming from the zero in the axial-vector meson form factor are obtained from the expression (4.23) by making substitutions as follows

$$\Delta V_A^{(1)}(r) = V_A^{(1)}(\phi_C^0 \rightarrow \phi_C^1, \phi_T^0 \rightarrow \phi_T^1, \phi_{SO}^0 \rightarrow \phi_{SO}^1) \cdot \frac{m^2}{U^2}. \tag{4.24}$$

Note that we do not include the similar $\Delta V_A^{(2)}(r)$ since they involve \mathbf{k}^4 -terms in momentum-space.

E. PS-PS-exchange Interactions in Configuration Space

sions for $K^{irr}(BW)$ and $K^{irr}(TMO)$ were derived [30],

In Fig.'s 2 and 3 of paper I, the included two-meson exchange graphs are shown schematically. Explicit expres-

where also the terminology BW and TMO is explained. The TPS-potentials for nucleon-nucleon have been given in detail in [31]. The generalization to baryon-baryon is similar to that for the OBE-potentials. So, we substitute $M \rightarrow \sqrt{M_Y M_N}$, and include all PS-PS possibilities with coupling constants as in the OBE-potentials. As compared to nucleon-nucleon in [31] we have here in addition the potentials with double K-exchange. The masses are the physical pseudo-scalar meson masses. For the intermediate two-baryon states we take into account the effects of the different thresholds. We have not included uncorrelated PS-vector, PS-scalar, or PS-diffractive exchange. This because the range of these potentials is similar to that of the vector-, scalar-, and axial-vector-potentials. Moreover, for potentially large potentials, in particularly those with scalar mesons involved, there will be very strong cancellations between the planar- and crossed-box contributions.

F. MPE-exchange Interactions

In Fig. 4 of paper I the pair graphs are shown. In this work we include only the one-pair graphs. The argument for neglecting the two-pair graph is to avoid some 'double-counting'. Viewing the pair-vertex as containing heavy-meson exchange means that the contributions from $\rho(750)$ and $\epsilon = f_0(760)$ to the two-pair graphs is already accounted for by our treatment of the broad ρ and ϵ OBE-potential. The MPE-potentials for nucleon-nucleon have been given in Ref. [31]. The generalization to baryon-baryon is similar to that for the TPS-potentials. For the intermediate two-baryon states we neglect the effects of the different two-baryon thresholds. The inclusion of these, although in principle possible, would complicate the computation of the potentials considerably and the influence is not expected to be significant. The generalization of the pair-couplings to baryon-baryon is described in Ref. [6], section III. Also here in NN , we have in addition to [31] included the pair-potentials with KK -, KK^* -, and $K\kappa$ -exchange. The convention for the MPE coupling constants is the same as in Ref. [31].

G. Meson-Pair Potentials, Axial-Pairs (2^{nd} -kind, $J^{PC} = 1^{+-}$)

Recently we have completed the $1/M, 1/M^2$ -corrections to the adiabatic approximation for the pair-potentials. The main reason is the need for a careful evaluation of the anti-symmetric spin-orbit terms for ΛN , in particular for pair-interactions involving strangeness-exchange like $\pi - K, \pi - K^*$ etc. From this evaluation new contributions emerged, in particular for the axial pair-interactions $J^{PC} = 1^{++}, 1^{+-}$, leading to a substantial improvement w.r.t. experimental spin-orbit splittings [15]. In our fitting procedure for the YN -data

the spin-orbit plays no role, therefore we will report on the details of the new spin-orbit terms in a separate paper [32]. However, also new $1/M$ -corrections for the spin-spin and tensor potentials were obtained for the axial-pair interaction of the 2nd kind, i.e. $J^{PC} = 1^{+-}$. These are relevant for the fits presented in this paper, and will be given in this section. Below we give the full one-pair exchange potential as used at present, because it has not been published before. In the ESC04-models only the leading, i.e. the $(1/M)^0$ -terms, were used. For the derivation of the soft-core pair-interactions we refer the reader to [31]. Below we report on this derivation for the axial-pair terms of the 2nd kind. The used pair-interaction Hamiltonian for e.g. the $(\pi\omega)$ -pair is

$$\mathcal{H}_B = g_{(\pi\omega)} \bar{\psi} \gamma_5 \sigma_{\mu\nu} \tau \psi \cdot \partial^\nu (\pi \phi_\omega^\mu) / (m_\pi \mathcal{M}), \quad (4.25)$$

which gives the BBm_1m_2 -vertex

$$\bar{u}(\mathbf{p}') \Gamma_B^{(2)} u(\mathbf{p}) = i \frac{g_{(\pi\omega)_1}}{m_\pi \mathcal{M}} \left[(\pm\omega_1 \pm \omega_2) \boldsymbol{\sigma} \cdot \boldsymbol{\omega} + \boldsymbol{\sigma} \cdot \mathbf{k} \omega^0 \right]. \quad (4.26)$$

The full $SU(3)$ -structure is given in [6], section IIIA. It is assumed that this pair-coupling is dominated by the $SU(3)$ -octet symmetric coupling, and is given by the $SU(3)$ -octet symmetric couplings Hamiltonian in terms of $SU(2)$ -isospin invariants and $SU(3)$ isoscalar-factors:

$$\begin{aligned} \mathcal{H}_{B_8VP} = \frac{g_{B_8VP}}{\sqrt{6}} \left\{ \frac{1}{2} [(\mathbf{B}_1^\mu \cdot \boldsymbol{\rho}_\mu) \eta_8 + (\mathbf{B}_1^\mu \cdot \boldsymbol{\pi}_\mu) \phi_8] \right. \\ + \frac{\sqrt{3}}{4} [\mathbf{B}_1 \cdot (K^{*\dagger} \boldsymbol{\tau} K) + h.c.] \\ + \frac{\sqrt{3}}{4} [(K_1^\dagger \boldsymbol{\tau} K^*) \cdot \boldsymbol{\pi} + (K_1^\dagger \boldsymbol{\tau} K) \cdot \boldsymbol{\rho} + h.c.] \\ - \frac{1}{4} [(K_1^\dagger \cdot K^*) \eta_8 + (K_1^\dagger \cdot K) \phi_8 + h.c.] \\ \left. + \frac{1}{2} H^0 \left[\boldsymbol{\rho} \cdot \boldsymbol{\pi} - \frac{1}{2} (K^{*\dagger} \cdot K + K^\dagger \cdot K^*) - \phi_8 \eta_8 \right] \right\} \quad (4.27) \end{aligned}$$

Here, $\mathbf{B}_1 \sim [\bar{\psi} \gamma_5 \boldsymbol{\tau} \sigma_{\mu\nu} \psi]$ etc. See for a definition of the octet-fields η_8, ϕ_8 in terms of the physical mesons [6]. From the pair-interaction Hamiltonian (4.27) one can easily read off the different meson-pairs that occur from the $J^{PC} = 1^{+-}$ -vertex. In Appendix B we give the explicit potentials generated by the pair-interaction (4.27).

V. SHORT-RANGE PHENOMENOLOGY

It is well known that the most extensive study of the baryon-baryon interactions using meson-exchange has difficulties to achieve sufficiently repulsive short-range interactions in two channels. Namely, (i) the $\Sigma^+ p (I = 3/2, {}^3S_1)$ - and (ii) the $\Sigma N (I = 1/2, {}^1S_0)$ -channel. The

short-range repulsion in baryon-baryon comes in principle from two sources: (a) meson- and multi-gluon-exchange, and (b) the occurrence of forbidden states by the Pauli-principle, henceforth referred to as Pauli-repulsion or Quark-core. As for (a) in the ESC-model [5, 6] the short-range repulsion comes from vector-meson exchange and Pomeron/Odderon-exchange (i.e. multi-gluon). The possibility of mechanism (b) has been explored in the Quark-Cluster model. See the reviews [20, 21].

Analyzing the Pauli-repulsion in terms of the $SU_f(3)$ -irreps we find that the "forbidden" $L = 0$ BB-states, which are classified in $SU_{fs}(6)$ by the [51]-irrep, indeed occur dominantly in the $SU_f(3)$ -irreps $\{10\}$ and $\{8_s\}$. These $SU(3)$ -irreps dominate the $\Sigma^+p(I = 3/2, {}^3S_1)$ - and the $\Sigma N(I = 1/2, {}^1S_0)$ -states respectively. These facts open the possibility to incorporate the exceptionally strong Pauli-repulsion for these states by enhancing the Pomeron coupling in the ESC-approach to baryon-baryon. For the other BB-states the [51]-irrep is present also, but roughly with an equal weight as the [33]-irrep. Only in a few $S=-2$ channels, e.g. $\Xi N(I = 1, S = 0)$ there is a stronger presence of the irrep [51]. Therefore a slightly moderated $SU_f(3)$ -singlet Pomeron-exchange can effectively take care of this Quark-core phenomenologically, together with multi-gluon-exchange effects.

A. Relation $SU_f(3)$ -irreps and $SU_{fs}(6)$ -irreps Classification YN-states

In Table V A the $SU_f(3)$ -contents of the NN and YN states are shown. In Table V A we show the the weights of the $SU(6)_{fs}$ -irreps. These are taken from [20] Table I, where the $SU(6)_{fs}$ -classifications are given. Analyzing now the $(\Lambda N, \Sigma N)$ -system for $(S = 0, I = 1/2)$ we find from these tables

$$\begin{pmatrix} V_{\Lambda N, \Lambda N} \\ V_{\Sigma N, \Sigma N} \end{pmatrix} = \begin{pmatrix} \frac{1}{2} & \frac{1}{2} \\ \frac{17}{18} & \frac{1}{18} \end{pmatrix} \begin{pmatrix} V_{[51]} \\ V_{[33]} \end{pmatrix} \\ = \begin{pmatrix} \frac{9}{10} & \frac{1}{10} \\ \frac{1}{10} & \frac{9}{10} \end{pmatrix} \begin{pmatrix} V_{\{27\}} \\ V_{\{8_s\}} \end{pmatrix}. \quad (5.1)$$

1. From (5.1) we obtain by simple matrix operations the relation between the $SU(6)_{fs}$ -irreps and the $SU(3)_f$ -irreps, which read

$$\begin{pmatrix} V_{\{27\}} \\ V_{\{8_s\}} \end{pmatrix} = \begin{pmatrix} \frac{4}{9} & \frac{5}{9} \\ 1 & 0 \end{pmatrix} \begin{pmatrix} V_{[51]} \\ V_{[33]} \end{pmatrix}. \quad (5.2)$$

2. Also, we can read off from the tables the following relations

$$V_{NN}(I = 1, S = 0) = \frac{4}{9}V_{[51]} + \frac{5}{9}V_{[33]} = V_{\{27\}}, \quad (5.3a)$$

$$V_{NN}(I = 0, S = 1) = \frac{4}{9}V_{[51]} + \frac{5}{9}V_{[33]} = V_{\{10^*\}}, \quad (5.3b)$$

$$\begin{aligned} V_{\Lambda N}(I = \frac{1}{2}, S = 1) &= \frac{1}{2}V_{[51]} + \frac{1}{2}V_{[33]} \\ &= \frac{1}{2}V_{\{10^*\}} + \frac{1}{2}V_{\{8_a\}}. \end{aligned} \quad (5.3c)$$

TABLE I: $SU(3)_f$ -contents of the various potentials on the isospin basis.

Space-spin antisymmetric states ${}^1S_0, {}^3P, {}^1D_2, \dots$	
$NN \rightarrow NN \quad I = 1$	$V_{NN}(I = 1) = V_{27}$
$\Lambda N \rightarrow \Lambda N$	$V_{\Lambda\Lambda}(I = \frac{1}{2}) = (9V_{27} + V_{8_s})/10$
$\Lambda N \rightarrow \Sigma N \quad I = \frac{1}{2}$	$V_{\Lambda\Sigma}(I = \frac{1}{2}) = (-3V_{27} + 3V_{8_s})/10$
$\Sigma N \rightarrow \Sigma N$	$V_{\Sigma\Sigma}(I = \frac{1}{2}) = (V_{27} + 9V_{8_s})/10$
$\Sigma N \rightarrow \Sigma N \quad I = \frac{3}{2}$	$V_{\Sigma\Sigma}(I = \frac{3}{2}) = V_{27}$
Space-spin symmetric states ${}^3S_1, {}^1P_1, {}^3D, \dots$	
$NN \rightarrow NN \quad I = 0$	$V_{NN}(I = 0) = V_{10^*}$
$\Lambda N \rightarrow \Lambda N$	$V_{\Lambda\Lambda}(I = \frac{1}{2}) = (V_{10^*} + V_{8_a})/2$
$\Lambda N \rightarrow \Sigma N \quad I = \frac{1}{2}$	$V_{\Lambda\Sigma}(I = \frac{1}{2}) = (V_{10^*} - V_{8_a})/2$
$\Sigma N \rightarrow \Sigma N$	$V_{\Sigma\Sigma}(I = \frac{1}{2}) = (V_{10^*} + V_{8_a})/2$
$\Sigma N \rightarrow \Sigma N \quad I = \frac{3}{2}$	$V_{\Sigma\Sigma}(I = \frac{3}{2}) = V_{10}$

TABLE II: $SU(6)_{fs}$ -contents of the various potentials on the spin, isospin basis.

(S, I)	$V = aV_{[51]} + bV_{[33]}$
$NN \rightarrow NN \quad (0, 1)$	$V_{NN} = \frac{4}{9}V_{[51]} + \frac{5}{9}V_{[33]}$
$NN \rightarrow NN \quad (1, 0)$	$V_{NN} = \frac{4}{9}V_{[51]} + \frac{5}{9}V_{[33]}$
$\Lambda N \rightarrow \Lambda N \quad (0, 1/2)$	$V_{\Lambda\Lambda} = \frac{1}{2}V_{[51]} + \frac{1}{2}V_{[33]}$
$\Lambda N \rightarrow \Lambda N \quad (1, 1/2)$	$V_{\Lambda\Lambda} = \frac{1}{2}V_{[51]} + \frac{1}{2}V_{[33]}$
$\Sigma N \rightarrow \Sigma N \quad (0, 1/2)$	$V_{\Sigma\Sigma} = \frac{17}{18}V_{[51]} + \frac{1}{18}V_{[33]}$
$\Sigma N \rightarrow \Sigma N \quad (1, 1/2)$	$V_{\Sigma\Sigma} = \frac{1}{2}V_{[51]} + \frac{1}{2}V_{[33]}$
$\Sigma N \rightarrow \Sigma N \quad (0, 3/2)$	$V_{\Sigma\Sigma} = \frac{4}{9}V_{[51]} + \frac{5}{9}V_{[33]}$
$\Sigma N \rightarrow \Sigma N \quad (1, 3/2)$	$V_{\Sigma\Sigma} = \frac{8}{9}V_{[51]} + \frac{1}{9}V_{[33]}$

From these equations we can solve the $SU(3)_f$ -irreps $\{27\}$, $\{10^*\}$, and $\{8_a\}$ in terms of the $SU(6)_{fs}$ -irreps.

Listing the results we now have

$$V_{\{27\}} = \frac{4}{9}V_{[51]} + \frac{5}{9}V_{[33]} , \quad (5.4a)$$

$$V_{\{10^*\}} = \frac{4}{9}V_{[51]} + \frac{5}{9}V_{[33]} , \quad (5.4b)$$

$$V_{\{10\}} = \frac{8}{9}V_{[51]} + \frac{1}{9}V_{[33]} , \quad (5.4c)$$

$$V_{\{8_a\}} = \frac{5}{9}V_{[51]} + \frac{4}{9}V_{[33]} , \quad (5.4d)$$

$$V_{\{8_s\}} = V_{[51]} . \quad (5.4e)$$

We see from these results that the $[51]$ -irrep has a large weight in the $\{10\}$ - and $\{8_s\}$ -irrep, which gives an argument for the presence of a strong Pauli-repulsion in these $SU(3)_f$ -irreps.

According to the study of the wide range of meson-exchange models in the last decade using the ESC-approach, as a working hypothesis, we assume that the apparent lack of an exceptionally strong repulsion in the ESC-model for the states in the $SU(3)_f$ -irreps $\{10\}$ and $\{8_s\}$ cannot be cured by meson-exchange. The inclusion of this possible "forbidden state" effect can be done phenomenologically in the ESC-approach by making an effective Pomeron potential as the sum of 'pure' Pomeron exchange and of a Pomeron-like representation of the Pauli-repulsion. As a consequence the effective Pomeron potential gets quite stronger in the $SU(3)_f$ -irreps $\{10\}$ and $\{8_s\}$. This way we incorporate the Pauli repulsion effect in the ESC-approach in this paper.

B. Parametrization Quark-core effects

1. Linear method: we split the repulsive short-range Pomeron-like NN potential as follows:

$$\begin{aligned} V_{PNN} &= (1 - a_{PB})V_{PNN} + a_{PB}V_{PNN} \\ &\equiv V_{NN}(POM) + V_{NN}(PB) \end{aligned} \quad (5.5)$$

where $V_{NN}(POM)$ represents the genuine Pomeron and $V_{NN}(PB)$ the structural effects of the Quark-core forbidden $[51]$ -configuration, i.e. a Pauli-blocking (PB) effect. So a_{PB} denotes the Quark-core fraction of the total Pomeron-like potential. A similar relation holds for all BB channels.

$$\begin{aligned} V_{PBB} &= (1 - a_{PB})V_{PBB} + a_{PB}V_{PBB} \\ &\equiv V_{BB}(POM) + V_{BB}(PB) \end{aligned} \quad (5.6)$$

Since the Pomeron is a unitary-singlet its contribution is the same for all BB-channels (apart from some small baryon mass breaking effects). The PB-effect for the BB-channels is assumed to be proportional to the relative weight of the forbidden $[51]$ -configuration compared to its weight in NN

$$V_{BB}(PB) = (w_{BB}[51]/w_{NN}[51]) \cdot V_{NN}(PB) \quad (5.7)$$

TABLE III: Effective Pomeron+PB contribution on the spin, isospin basis.

	(S, I)	V_{PBB}/V_{PNN}	ESC08c
$NN \rightarrow NN$	$(0, 1)$	1	1.000
$NN \rightarrow NN$	$(1, 0)$	1	1.000
$\Lambda N \rightarrow \Lambda N$	$(0, 1/2)$	$1 + \frac{1}{8}a_{PB}$	1.022
$\Lambda N \rightarrow \Lambda N$	$(1, 1/2)$	$1 + \frac{1}{8}a_{PB}$	1.022
$\Sigma N \rightarrow \Sigma N$	$(0, 1/2)$	$1 + \frac{9}{8}a_{PB}$	1.200
$\Sigma N \rightarrow \Sigma N$	$(1, 1/2)$	$1 + \frac{1}{8}a_{PB}$	1.022
$\Sigma N \rightarrow \Sigma N$	$(0, 3/2)$	1	1.000
$\Sigma N \rightarrow \Sigma N$	$(1, 3/2)$	$1 + a_{PB}$	1.178

Then we have

$$V_{PBB} = (1 - a_{PB})V_{PNN} + a_{PB} \left(\frac{w_{BB}[51]}{w_{NN}[51]} \right) \cdot V_{PNN} \quad (5.8)$$

For example, in the $SU(3)$ -irrep $\{10\}$, e.g. the $\Sigma^+ p(^3S_1, T = 3/2)$ -channel, one has $w_{BB}[51] = 8/9 = 2w_{NN}[51]$ and therefore $V_{10}(PB) = 2V_{NN}(PB)$. Consequently, the total short-range repulsive potential, i.e. the 'effective pomeron', becomes $V_{10} = (1 - a_{PB})V_{PNN} + 2a_{PB}V_{PNN} = (1 + a_{PB})V_{PNN}$. In Table V B we give the factors for the various $S=0$ and $S=-1$ BB channels as well as the results in the ESC08c model.

In principle one might choose a different mass for the Quark-core repulsive potential. However, this extra parameter does not lead to better fits to NN and/or YN. Therefore we keep for the Pauli-blocking the same mass as the Pomeron mass. The value of the PB factor a_{PB} is searched in the fit to the YN-data. The $S=-2$ PB effects are then also entirely determined. In the case of the models ESC08a' and ESC08b' only the channels where $w_{BB}[51]$ is conspicuously large are treated approximately this way, but with equal weights. These channels are: $\Sigma^+ p(^3S_1, T = 3/2)$, $\Sigma N(^1S_0, T = 1/2)$, and $\Xi N(^1S_0, T = 1)$. A subtle treatment of *all* BB channels according to this linear scheme is characteristic for the ESC08c-model. The parameter a_{PB} turns out to be about 27.5%. This means that the Quark-core repulsion is roughly 34% of the genuine Pomeron repulsion. Around $r=0$ the Quark-core repulsion comes out at 115 MeV, whereas the pure Pomeron repulsion is 304 MeV.

2. Non-linear method: we introduce next to the fraction parameter a_{PB} a nonlinear function $f(w_{BB}[51])$ in (5.6) by writing

$$V_{BB} = (1 - a_{PB})V_{PNN} + a_{PB}f(w_{BB}[51])V_{PNN} \quad (5.9)$$

with the requirement that $f(w_{NN}[51]) = 1$. Such a scheme is more flexible than the linear method. For example, by taking a steeper function than the linear function for arguments larger than $w_{NN}[51]$ one could reduce the PB-effects for small $w_{BB}[51]$ values like in ΛN or ΞN and at the same time one could preserve a strong PB-effect in the $\{10\}$ -irrep having $f(w_{10}[51])$ around 2. Therefore starting from the ESC08c solutions alternative YN/YY solutions can be obtained easily. As an example one could take the function $f(w_{BB}[51]) = \tan(\varphi_{BB})$ with $\varphi_{NN} = 45^\circ$. Taking for $\arctan(\varphi_{10}) = 2$ one recovers the same $V_{10}(PB)$ as in the linear scheme above. Exploiting the weights $w_{BB}[51]$ by parametrizing φ_{BB} in the following way

$$\varphi_{BB} = \left(\frac{w_{BB}[51] - w_{NN}[51]}{w_{10}[51] - w_{NN}[51]} \right) \cdot (\varphi_{10} - \varphi_{NN}) + \varphi_{NN}. \quad (5.10)$$

one gets the same PB-repulsion for $\Sigma^+ p(^3S_1, T = 3/2)$ as in the linear method, but smaller PB-repulsions in the ΛN and ΞN channels.

VI. ESC08: FITTING $NN \oplus YN \oplus YY$ -DATA

In this section we describe mainly the recent changes in the fitting process. For details on the standard $NN \oplus YN$ -fitting we refer to [13].

(i) As usual we fit to the 1993 Nijmegen representation of the χ^2 -hypersurface of the NN scattering data below $T_{lab} = 350$ MeV [33, 34]. The NN low-energy parameters are fitted along with the scattering data. In order to accomodate the differences between the 1S_0 -waves for pp, np, and nn in the model, we introduce some charge independence breaking by taking different electric ρ -couplings $g_{pp\rho} \neq g_{np\rho} \neq g_{nn\rho}$, where $g_{nn\rho}$ is considered to be the $SU(3)$ -octet coupling. With this phenomenological device we fit the difference between the $^1S_0(pp)$ and $^1S_0(np)$ phases, and the different NN scattering lengths and effective ranges very well. We have found $g_{pp\rho} = 0.6389$, $g_{np\rho} = 0.5889$, which are not far from $g_{nn\rho} = 0.6446$ (cfr. Table V).

(ii) Simultaneously we fit to 52 YN scattering data. These data consist of the usual set of 35 low-energy YN-data, as used in [12, 13] and [6] plus 3 total $\Sigma^+ p$ X-sections from the recent KEK-experiment E289 [35] and some Λp elastic and inelastic data Ref. [36] and $\Sigma^- p$ elastic data at higher energies Ref. [37]. For the total $\Sigma^+ p$ and $\Sigma^- p$ elastic X-sections we have performed the same redefinition as eq. (6.3) of [13]. (iii) A novel feature in the simultaneous fitting procedure is the inclusion of constraints from information derived from hypernuclei and hypernuclear matter. For the ΛN -interaction this means not only a) the usual absence of bound states but also b) the requirement of a sizable spin-splitting leading to $U_{\sigma\sigma} > 1$ (cfr. section VII A). c) Because of the experimental absence of Σ -hypernuclei we require the total single particle Σ -potential in nuclear matter U_Σ to be overall

repulsive. In the $S=-2$ channels there are two clear experimental indications: d) from the analysis of the Nagara event [38] of the double- Λ hypernucleus $^6_{\Lambda\Lambda}\text{He}$ it appears that the forces in the $\Lambda\Lambda(^1S_0)$ -channel are weakly attractive, indicated by a scattering length $a_{\Lambda\Lambda}(^1S_0) > -1$ fm [39]. This evidence has been incorporated in the fit in the form of 'pseudo-data' for the $(^1S_0)\Lambda\Lambda$ scattering length $a_{\Lambda\Lambda} = -0.8 \pm (0.2 - 0.4)$. the error depending on the desired impact in the fitting process. e) Experimentally the Ξ -nucleus interaction seems to be attractive from analyses of events with twin- Λ hypernuclei in emulsion data, where the initial Ξ^- energies were determined after $\Xi^- p - \Lambda\Lambda$ conversion in nuclei. The Ξ -nucleus interaction can be described well with a Wood-Saxon potential with a depth of $\approx 14 \text{ MeV}$ [40]. As a consequence we require the total single particle Ξ -potential in nuclear matter U_Ξ to be overall attractive. We calculate U_Ξ with the G-matrix formalism (cfr. section X). It appears that in the ESC08 model the $\Xi N(^3S_1, T = 1)$ channel is quite sensitive to variation of the coupling constants, whereas the other s- and p-wave contributions have rather shallow dependencies. The total sum of the contributions of the other $T = 0$ and $T = 1$ s- and p-waves to U_Ξ is $\approx +4$ MeV. In order to ensure a clearly total attractive U_Ξ we add 'pseudo-data' for the $\Xi N(^3S_1, T = 1)$ contribution $U_\Xi(^3S_1, T = 1) = -12 \pm (2 - 4)$, the error depending on the desired impact in the fitting process. In practice this particular partial wave channel plays a very important role in the simultaneous fitting of the total BB-description. The fit has resulted in an excellent simultaneous $NN \oplus YN \oplus YY$ -fit. We obtained for the NN-data $\chi^2/N_{data} = 1.081$ with also very good results for the NN low energy parameters: the deuteron binding energy and the pp, np and nn scattering lengths and effective ranges. For the YN-data $\chi^2/YN_{data} = 1.08$. The ESC08 fits were achieved with only physical meson-coupling parameters, which are partial-wave independent. The quality of the NN-fit is at par with models of Reid-like potentials like the Nijm93, Nijm I, and II, which are effective NN-potentials with some meson parameters adjusted per partial wave [41, 42]. Since the ESC08-model is an extension of the ESC04-model, it is not surprising that in the simultaneous NN -, YN and YY fit the OBE-couplings could be kept in line with the 'naive' predictions of the QPC-model [5, 9]. Just as in ESC04 most of the $F/(F + D)$ -ratios are fixed by QPC, both for the OBE and MPE couplings. Once more we stress the fact that the in the simultaneous fit of the NN -, YN - and YY -data, a *single set of parameters* was used. Of course, the accurate and very numerous NN -data put strong constraints on the parameters. However, the YN-data, plus the constraints for the YN- and YY- channels, are also quite relevant for the set of parameters finally obtained. In particular, certain fitted $F/(F + D)$ -ratios, are obviously influenced by the YN-data. The requirement of an overall attractive U_Ξ results in the model always in the occurrence of a bound state in $\Xi N(^3S_1, T = 1)$ -channel with a binding energy of ≈ 2 MeV.

A. Coupling Parameters and $NN \oplus YN \oplus YY$ Fit

The treatment of the broad mesons ρ and ϵ is as usual in the Nijmegen models. For the ρ -meson the same parameters are used in the OBE-models [11, 12]. For the $\epsilon = f_0(760)$ assuming $m_\epsilon = 760$ MeV and $\Gamma_\epsilon = 640$ MeV we use the Bryan-Gersten parametrization [43]. For the chosen mass and width they are: $m_1 = 496.39796$ MeV, $m_2 = 1365.59411$ MeV, and $\beta_1 = 0.21781, \beta_2 = 0.78219$. For the 'diffractive' 0^{++} -exchanges we restrict ourselves to the SU(3)-singlet part, henceforth referred to as 'pomeron'. The possible $J=0$ part of the tensor-meson exchange [11, 12] is not considered. The 'mass' parameter of the pomeron is fitted to be $m_P = 227.05$ MeV. The 'diffractive' 0^{--} -exchange 'odderon' is also an SU(3)-singlet with a fitted mass $m_O = 273.35$ MeV.

Summarizing the fitted parameters in ESC08c we have:

1. Meson-couplings: $f_{NN\pi}, f_{NN\eta'}, g_{NN\rho}, g_{NN\omega}, f_{NN\rho}, f_{NN\omega}, g_{NNa_0}, g_{NN\epsilon}, g_{NNa_1}, f_{NNa_1}, g_{NNf'_1}, f_{NNf'_1}, f_{NNb_1}, f_{NNh'_1}$
2. Pair couplings: $g_{NN(\pi\pi)_1}, f_{NN(\pi\pi)_1}, g_{NN(\pi\rho)_1}, g_{NN\pi\omega}, g_{NN\pi\eta}, g_{NN\pi\epsilon}$
3. Diffractive-couplings/masses: $g_{NNP}, g_{NNO}, f_{NNO}, a_{PB}, m_P, m_O$
4. $F/(F+D)$ -ratio's: α_V^m, α_A
5. Cut-off masses: $\Lambda_8^P = \Lambda_1^P, \Lambda_8^V, \Lambda_1^V, \Lambda_8^S, \Lambda_1^S, \Lambda_8^A = \Lambda_1^A$

These are in total 34 physical parameters, of which are (i) 14 meson-couplings, (ii) 2 $F/(F+D)$ -ratio's, (iii) 4 'diffractive' couplings and 2 mass parameters, (iv) 6 meson-pair couplings, and (v) 6 cut-off mass parameters. As compared to the ESC04-model, we have added in ESC08 the following fitting parameters: (i) the derivative axial-couplings $f_{NNa_1}, f_{NNf'_1}$, (ii) the 1^{+-} axial-couplings $f_{NNb_1}, f_{NNh'_1}$, (iii) the odderon-couplings g_{NNO}, f_{NNO} , and mass m_O (iv) the pomeron Pauli-blocking parameter a_{PB} , i.e. 8 new physical parameters. All new parameters have been explained above. They introduce new dynamical refinements/effects into the model, which have resulted in a quality of the combined NN+YN+YY fit for the NN-phases equal to those of a purely NN-fit. Some other parameters have been set, like e.g. many $F/(F+D)$ -ratio's, see below, and a few cut-off parameters.

VII. COUPLING CONSTANTS, $F/(F+D)$ RATIOS, AND MIXING ANGLES

Like in ESC04, we constrained the OBE-couplings by the 'naive' predictions of the QPC-model [8]. We kept during the searches all OBE-couplings in the neighborhood of these predictions, but less tight than in ESC04. The same holds for the searched $\alpha = F/(F+D)$ -ratios, i.e. for the BBM -couplings and the BB -Pair-couplings. In fact only two meson-coupling $F/(F+D)$ -ratio's were allowed to vary during the searches: α_V^m for the vector mesons, and α_A for the axial-vector mesons. As mentioned above α_P was kept at the fixed value $\alpha_P = 0.365$. Furthermore we kept $\alpha_V^E = 1$ and $\alpha_S = 1$ at their QPC values. The input and fitted values are displayed in Table V.

The pair coupling $g_{NN(\pi\pi)_0}$ is set to be zero, which is motivated in the Nijmegen soft-core models in view of the fact that in πN it is constrained by chiral-symmetry. In the fitting process we look for solutions which have meson-couplings which are reasonably close to the 'naive' predictions of the QPC-model. This is also the case for the $F/(F+D)$ -ratio's, both for meson- and for pair-couplings. During the fitting we experienced a rather shallow dependence on the $F/(F+D)$ -ratio α^P for the pseudoscalar octet. In fact we could obtain a very good YN fit in a values range 0.33-0.40. Therefore we have fixed it on the value $\alpha^P = 0.365$ obtained from the Cabibbo theory of semileptonic decay of baryons [48]. Furthermore, the meson-pair couplings turn out to come out rather close to predictions based on the 'heavy-meson-saturation'-model. So, the fit-parameters are (i) physical parameters, i.e. they can be checked in other reactions, and (ii) many are 'constraint' by the QPC-model.

In this work like in the ESC04-models [5, 6], the form factors depend on the SU(3) assignment of the mesons. In principle, we introduce form factor masses Λ_8 and Λ_1 for the $\{8\}$ and $\{1\}$ members of each meson nonet, respectively. Moreover, for the $I=0$ -mesons we assign the $\{1\}$ cut-off to the dominant singlet meson and the $\{8\}$ cut-off to the dominant octet meson, as if there were no meson-mixing. For example we assign Λ_1 to η', ω, ϵ , and Λ_8 to η, ϕ, S^* , etc. Notice that the strange octet-mesons K etc. are given the same $\{8\}$ form factors as their non-strange companions. For the cut-off masses Λ we used as free search parameters $\Lambda_8^P = \Lambda_1^P$ for the pseudoscalar mesons, Λ_8^V and Λ_1^V for the vector mesons and Λ_8^S and Λ_1^S for the scalar mesons. Furthermore, we finally used $\Lambda_8^A = \Lambda_1^A$ for the axial-mesons with $J^{PC} = 1^{++}$. For the axial-mesons with $J^{PC} = 1^{+-}$ (B-mesons) the cut-off masses have been set equal to those of the pseudoscalar mesons $\Lambda_8^B = \Lambda_8^P$ and $\Lambda_1^B = \Lambda_1^P$. Some of the previous $\{8\}$ and $\{1\}$ form factors have been chosen to be equal as a consequence of the impossibility to distinguish them in the fitting process.

Similar to ESC04 we introduce a zero in the form factors of mesons, which are P-wave bound states in a $q\bar{q}$ -picture. These are the scalar mesons (3P_0) and the axial-vector ($^3P_1, ^1P_1$) mesons. Like in ESC04, we use a fixed zero by taking $U = 750$ MeV in (4.22) and (4.24).

TABLE IV: Meson couplings and parameters employed in the ESC08c-potentials. Coupling constants are at $\mathbf{k}^2 = 0$. An asterisk denotes that the coupling constant is constrained via $SU(3)$. The masses and Λ 's are given in MeV. Note that the B-meson couplings are scaled with m_{B_1} . The mesons with strangeness are the (i) pseudoscalar $K(495.8)$, (ii) vector $K^*(892.6)$, (iii) scalar $\kappa(841.0)$, (iv) axial $K_A(1273.0)$ and $K_B(1400.0)$, with masses as indicated in the parentheses.

meson	mass	$g/\sqrt{4\pi}$	$f/\sqrt{4\pi}$	Λ
π	138.04		0.2687	1056.13
η	547.45		0.1265*	„
η'	957.75		0.2309	„
ρ	768.10	0.6446	3.7743	695.67
ϕ	1019.41	-1.3390*	3.1678*	„
ω	781.95	3.4570	-0.8575	758.58
a_1	1270.00	-0.7895	-0.8192	1051.80
f_1	1420.00	0.7311*	0.3495*	„
f'_1	1285.00	-0.7613	-0.4467	„
b_1	1235.00		-1.8088	1056.13
h_1	1380.00		-0.5553*	„
h'_1	1170.00		-0.3000	„
a_0	962.00	0.5853		994.89
f_0	993.00	-1.6898*		„
ε	760.00	4.1461		1113.57
Pomeron	220.50	3.5815		
Odderon	273.35	4.6362	-4.7602	

The mixing angles for the various meson nonets are discussed in paper I. The used values can be found in Table V. For completeness we reproduce in Table IV the fitted ESC08c NN meson couplings and cut-off masses from paper I. Here we discuss only aspects specific for the YN-channels. In Table V the ESC08 $SU(3)$ singlet and octet couplings $g/\sqrt{4\pi}$ are listed, the $F/(F + D)$ -ratios and the used mixing angles.

TABLE V: ESC08c $SU(3)$ coupling constants, $F/(F + D)$ -ratio's, mixing angles etc. The values with *) have are theoretical input or determined by the fitting and the constraint from the YN-analysis.

mesons		$\{1\}$	$\{8\}$	$F/(F + D)$	angles
ps-scalar	f	0.2534	0.2687	$\alpha_P = 0.365^{*)}$	$\theta_P = -13.00^0 \text{ } ^{*)}$
vector	g	3.5351	0.6446	$\alpha_V^e = 1.0^{*)}$	$\theta_V = 38.70^0 \text{ } ^{*)}$
	f	-2.6499	3.7743	$\alpha_V^m = 0.4721^{*)}$	
axial(A)	g	-1.0494	-0.7895	$\alpha_A = 0.3121$	$\theta_A = +50.00^0 \text{ } ^{*)}$
	f	-0.5548	-0.8192	$\alpha_A^p = 0.3121^{*)}$	
axial(B)	f	0.0760	-1.8088	$\alpha_B = 0.40^{*)}$	$\theta_B = 35.26^0 \text{ } ^{*)}$
scalar	g	4.3610	0.5853	$\alpha_S = 1.00^{*)}$	$\theta_S = 35.26^0 \text{ } ^{*)}$
diffractive	g_P	3.5815			$a_{PB} = 0.275^{*)}$
	g_O	4.6362			
	f_O	-4.7602			

In Table VI we list the couplings of the physical mesons to the nucleons ($Y = 1$), and to the hyperons with $Y = 0$ or

$Y = -1$. These were calculated using unbroken $SU(3)$ -symmetry. Next to the values in the table we have incorporated, like in the ESC04 model [6], Charge Symmetry Breaking (CSB) between Λp and Λn with nonzero Λ -couplings of the $I=1$ mesons and $I=1$ pairs due to $\Lambda - \Sigma^0$ mixing.

TABLE VI: Coupling constants for model ESC08c, divided by $\sqrt{4\pi}$. M refers to the meson. The coupling constants are listed in the order pseudoscalar, vector (g and f), axial vector A (g and f), scalar, axial vector B, and diffractive.

	M	NNM	$\Sigma\Sigma M$	$\Sigma\Lambda M$	$\Xi\Xi M$	M	ΛNM	$\Lambda\Xi M$	ΣNM	$\Xi\Xi M$
f	π	0.2687	0.1961	0.1970	-0.0725	K	-0.2683	0.0714	0.0725	-0.2687
g	ρ	0.6446	1.2892	0.0000	0.6446	K^*	-1.1165	1.1165	-0.6446	-0.6446
f		3.7743	3.5639	2.3006	-0.2104		-4.2367	1.9362	0.2104	-3.7743
g	a_1	-0.7895	-0.4929	-0.6271	0.2967	K_{1A}	0.7404	-0.1133	-0.2967	0.7895
f		-0.8192	-0.5114	-0.6507	0.3078		0.7683	-0.1175	-0.3078	0.8192
g	a_0	0.5853	1.1705	0.0000	0.5853	κ	-1.0137	1.0137	-0.5852	-0.5852
f	b_1	-1.8088	-1.4470	-1.2532	0.3618	K_{1B}	1.8798	-0.6266	-0.3618	1.8088
g	a_2	0.00000	0.00000	0.00000	0.00000	K^{**}	0.00000	0.00000	0.00000	0.00000
	M	NNM	$\Lambda\Lambda M$	$\Sigma\Sigma M$	$\Xi\Xi M$	M	NNM	$\Lambda\Lambda M$	$\Sigma\Sigma M$	$\Xi\Xi M$
f	η	0.1265	-0.1349	0.2490	-0.2045	η'	0.2309	0.2912	0.2026	0.3073
g	ω	3.4570	2.7589	2.7589	2.0608	ϕ	-1.3390	-2.2103	-2.2103	-3.0816
f		-0.8574	-3.5064	-0.6296	-4.7170		3.1678	-0.1386	3.4522	-1.6497
g	f'_1	-0.7613	-0.1942	-1.1549	-0.1074	f_1	0.7311	1.2070	0.4008	1.2798
f		-0.4467	0.1418	-0.8551	0.2319		0.3495	0.8433	0.4008	1.2798
g	ε	4.1461	3.5609	3.5609	2.9758	f_0	-1.6898	-2.5176	-2.5176	-3.3453
f	h'_1	-0.3000	0.7852	-0.6617	1.1469	h_1	-0.5553	0.9796	-1.0669	1.4913
g	P	3.5815	3.5815	3.5815	3.5815	f_2	0.0000	0.0000	0.0000	0.0000
g	O	3.6362	3.6362	3.6362	3.6362					
f		-4.7602	-4.7602	-4.7602	-4.7602					

In Table VII we present the fitted Pair-couplings for the MPE-potentials. We recall that only One-pair graphs are included, in order to avoid double counting, see paper I. The $F/(F + D)$ -ratios are all fixed, assuming heavy-boson domination of the pair-vertices. The ratios are taken from the QPC-model for $Q\bar{Q}$ -systems with the same quantum numbers as the dominating boson. Only the ratio in the system with the pseudoscalar quantum numbers deviates slightly from QPC, since it has been set equal to the value of $\alpha_P = 0.365$. The BB -Pair couplings are calculated, assuming unbroken $SU(3)$ -symmetry, from the NN -Pair coupling and the $F/(F + D)$ -ratio using $SU(3)$.

TABLE VII: Pair-meson coupling constants employed in the ESC08c MPE-potentials. Coupling constants are at $\mathbf{k}^2 = 0$. The $F/(F+D)$ -ratio are QPC-predictions, except that $\alpha_{(\pi\omega)} = \alpha_{pv}$, which is very close to QPC.

J^{PC}	$SU(3)$ -irrep	$(\alpha\beta)$	$g/4\pi$	$F/(F + D)$
0^{++}	$\{1\}$	$g(\pi\pi)_0$	—	—
0^{++}	„	$g(\sigma\sigma)$	—	—
0^{++}	$\{8\}_s$	$g(\pi\eta)$	-1.2371	1.000
1^{--}	$\{8\}_a$	$g(\pi\pi)_1$	0.2703	1.000
		$f(\pi\pi)_1$	-1.6592	0.400
1^{++}	„	$g(\pi\rho)_1$	5.1287	0.400
1^{++}	„	$g(\pi\sigma)$	-0.2989	0.400
1^{++}	„	$g(\pi P)$	—	—
1^{+-}	$\{8\}_s$	$g(\pi\omega)$	-0.2059	0.365

Unlike in [31], we did not fix pair couplings using a theoretical model, based on heavy-meson saturation and chiral-symmetry. So, in addition to the 14 coupling parameters used in [31] we now have 6 pair-coupling fit parameters. In Table VII the fitted pair-couplings are given, and in Appendix A the $SU(3)$ -structure of the pair-couplings. Note

that the $(\pi\pi)_0$ -pair coupling gets contributions from the $\{1\}$ and the $\{8_s\}$ pairs as well, giving in total $g_{(\pi\pi)} = -0.4876/2 = -0.2438$, which has an opposite sign as in [31]. Also the $f_{(\pi\pi)_1}$ -pair coupling has an opposite sign as compared to [31]. In a model with a more complex and realistic meson-dynamics [44] this coupling is predicted as found in the present ESC-fit. The $(\pi\rho)_1$ -coupling agrees nicely with A_1 -saturation, see [31]. The pair-couplings are used in a phenomenological way in the ESC-approach. They are in general not yet quantitatively understood, and certainly deserve more study in the future.

The ESC-model described here, is fully consistent with $SU(3)$ -symmetry using a straightforward extension of the NN-model to YN and YY. For example $g_{(\pi\rho)_1} = g_{A_8VP}$, and besides $(\pi\rho)$ -pairs one sees also that $KK^*(I=1)$ - and $KK^*(I=0)$ -pairs contribute to the NN potentials. All $F/(F+D)$ -ratio's are taken fixed with heavy-meson saturation in mind. The approximation we have made in this paper is to neglect the baryon mass differences, i.e. we put $m_\Lambda = m_\Sigma = m_N$. This because we have not yet worked out the formulas for the inclusion of these mass differences, which is straightforward in principle.

A. Parameters and Hyperon-nucleon Fit

All 'best' low-energy YN-data are included in the fitting, This is a selected set of 35 low-energy YN-data, the same set has been used in [12] and [13]. We added (i) 3 total Σ^+p X-sections from the KEK-experiment E289 [35], (ii) 7 elastic and 4 inelastic Λp X-sections from Berkeley [36], and (iii) 3 elastic Σ^-p X-sections [37]. In section VIII these are given together with the results. Next to these we added 'pseudo-data' for the Λp and Σ^+p scattering length's in order to ensure that the $\Lambda p(^1S_0)$ forces are sufficiently stronger than the $\Lambda p(^3S_1)$. In the construction of the ESC04-models, the experience with the NSC97 models was used in hypernuclear calculations. Technically 'favored' values of the s-wave scattering lengths for ΛN were imposed as pseudo-data during the fitting procedures, in order to get the right spin-splitting for the ΛN -interaction in hypernuclei. In nuclear matter this implies $U_{\sigma\sigma} > 1$. In this succeeding model ESC08, however, the ΛN behavior is slightly different leading to smaller values of $U_{\sigma\sigma}$. This time, we impose instead a larger difference between the s-wave scattering lengths with, of course, $|a_s| > |a_t|$ in order to fulfill the constraint $U_{\sigma\sigma} > 1$. Furthermore we added 'pseudo-data' for the $\Sigma^+p(^3S_1)$ scattering length with the goal to get enough repulsion in this wave in order to reach a total repulsive U_Σ . For the pseudo-data in the S=-2 channels we refer to section VI. In the final stages of the fitting process all pseudo-data were turned off. in fm:

$$\begin{aligned}\hat{a}_{\Lambda p}(^1S_0) &= -2.60 \pm (0.10 - 0.20) , \\ \hat{a}_{\Lambda p}(^3S_1) &= -1.60 \pm (0.10 - 0.20) , \\ \hat{a}_{\Sigma^+p}(^3S_1) &= +0.65 \pm (0.10 - 0.20) ,\end{aligned}\tag{7.1}$$

Also, during the fitting process checks were done to prevent the occurrence of bound Λp states. Parameters, typically strongly influenced by the YN-data, are

1. $F/(F+D)$ -parameters: α_V^m and to a less extent α_A , For the sensitivity of α^P see section VII.
2. Pauli-blocking fraction parameter a_{PB} .

The dependence of a_{PB} in the fit to YN and YY is rather shallow in a range 0.20 – 0.30. The final value has been determined by a minimal value of χ^2 of the set of the 52 YN data, while simultaneously providing a repulsive U_Σ . This implies that the S=-2 (and -3, -4) results are completely determined. Finally we want to mention that in the fitting process we have, if necessary, accounted for the vast difference in quality of the data. The abundance of the 4313 precise NN data is to be contrasted to the 52 less precise YN data. In the simultaneous fit we require for both the NN and for the YN that the quality of the partial fit is comparable, i.e. $\chi^2/NN_{data} \approx \chi^2/YN_{data}$. If necessary we add weight factors to the partial sums in the total χ^2 . It turned out that in the last stages of the fitting process the weight factors are equal.

VIII. ESC08-MODEL , YN-RESULTS

A. Hyperon-nucleon (S=-1) X-sections, phases, etc.

The used YN scattering data from Refs. [45]-[51] in the combined NN and YN fit are shown in Table VIII. The NN interaction puts very strong constraints on most of the parameters, and so we are left with only a limited set of parameters which have some freedom to steer the YN channels as compared to the NN-channels. The fitted parameters are given in paper I, Table's III-VI and X.

The aim of the present study was to construct a realistic potential model for baryon-baryon systems with parameters that are optimal theoretically, but at the same time describes the baryon-baryon scattering data very satisfactory.

This model can then be used with a great deal of confidence in calculations of hypernuclei and in their predictions for the $S = -2, -3$, and -4 sectors. Especially for the latter application, these models will be the first models for the $S = -2, -3, -4$ sectors to have their theoretical foundation in the NN and YN sectors.

$\Lambda p \rightarrow \Lambda p$			$\chi^2 = 3.6$	$\Lambda p \rightarrow \Lambda p$			$\chi^2 = 3.8$
p_Λ	σ_{exp}^{RH}		σ_{th}	p_Λ	σ_{exp}^M		σ_{th}
145	180±22		197.0	135	187.7±58		215.6
185	130±17		136.3	165	130.9±38		164.1
210	118±16		107.8	195	104.1±27		124.1
230	101±12		89.3	225	86.6±18		93.6
250	83± 9		73.9	255	72.0±13		70.5
290	57± 9		50.6	300	49.9±11		46.0
$\Lambda p \rightarrow \Lambda p$			$\chi^2 = 12.1$				
350	17.2±8.6		28.7	750	13.6±4.5		10.2
450	26.9±7.8		11.9	850	11.3±3.6		11.4
550	7.0±4.0		8.6	950	11.3±3.8		12.9
650	9.0±4.0		18.5				
$\Lambda p \rightarrow \Sigma^0 p$			$\chi^2 = 6.9$				
667	2.8 ±2.0		3.3	850	10.6±3.0		4.1
750	7.5±2.5		4.0	950	5.6±5.0		3.9
$\Sigma^+ p \rightarrow \Sigma^+ p$			$\chi^2 = 12.4$	$\Sigma^- p \rightarrow \Sigma^- p$			$\chi^2 = 5.2$
p_{Σ^+}	σ_{exp}		σ_{th}	p_{Σ^-}	σ_{exp}		σ_{th}
145	123.0±62		136.1	142.5	152±38		152.8
155	104.0±30		125.1	147.5	146±30		146.9
165	92.0±18		115.2	152.5	142±25		141.4
175	81.0±12		106.4	157.5	164±32		136.1
				162.5	138±19		131.1
				167.5	113±16		126.3
400	93.5±28.1		35.1	450.0	31.7±8.3		28.5
500	32.5±30.4		30.9	550.0	48.3±16.7		19.8
650	64.6±33.0		28.2	650.0	25.0±13.3		15.1
$\Sigma^- p \rightarrow \Sigma^0 n$			$\chi^2 = 5.7$	$\Sigma^- p \rightarrow \Lambda n$			$\chi^2 = 4.8$
p_{Σ^-}	σ_{exp}		σ_{th}	p_{Σ^-}	σ_{exp}		σ_{th}
110	396±91		200.6	110	174±47		241.3
120	159±43		175.8	120	178±39		207.2
130	157±34		155.9	130	140±28		180.1
140	125±25		139.7	140	164±25		158.1
150	111±19		126.2	150	147±19		140.0
160	115±16		114.9	160	124±14		125.0
$r_R^{exp} = 0.468 \pm 0.010$				$r_R^{th} = 0.455$			$\chi^2 = 1.7$

TABLE VIII: Comparison of the calculated ESC08 and experimental values for the 52 YN -data that were included in the fit. The superscripts RH and M denote, respectively, the Rehovoth-Heidelberg Ref. [45] and Maryland data Ref. [46]. Also included are (i) 3 $\Sigma^+ p$ X-sections at $p_{lab} = 400, 500, 650$ MeV from Ref. [35], (ii) Λp X-sections from Ref. [36]: 7 elastic between $350 \leq p_{lab} \leq 950$, and 4 inelastic with $p_{lab} = 667, 750, 850, 950$ MeV, and (iii) 3 elastic $\Sigma^- p$ X-sections at $p_{lab} = 450, 550, 650$ MeV from Ref. [37]. The laboratory momenta are in MeV/c, and the total cross sections in mb.

The χ^2 on the 52 YN scattering data for the ESC08 model is given in Table VIII. The ΛN total cross sections have been calculated with $L \leq 2$, and the ΣN total cross sections with $L \leq 1$. The capture ratio at rest, given in the last

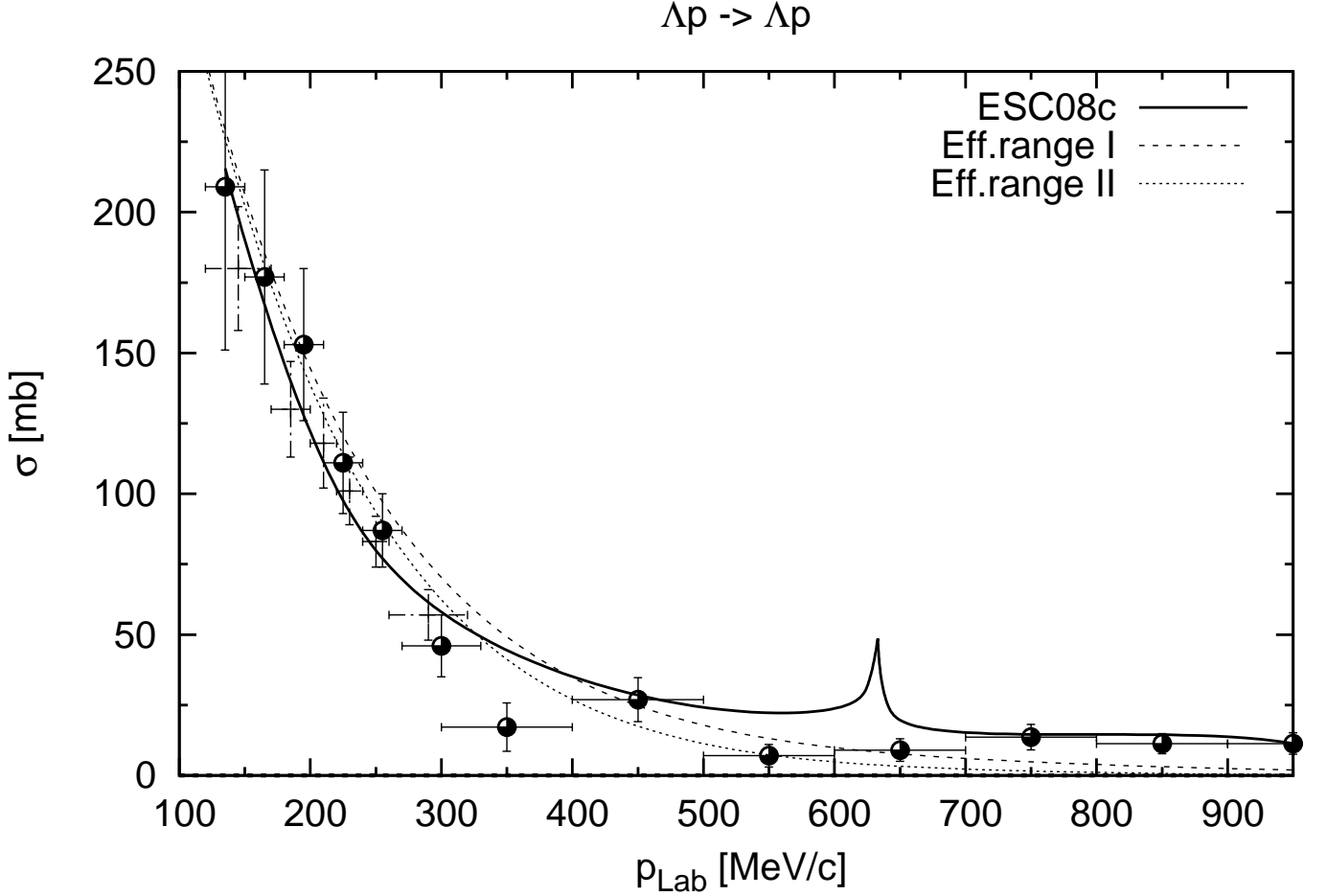


FIG. 1: Model fits total X-sections Λp . Rehovoth-Heidelberg-, Maryland-, and Berkeley-data

row of the table, for its definition see e.g. [13]. This capture ratio turns out to be rather constant in the momentum range from 100 to 170 MeV/c. Obviously, for very low momenta the cross sections are almost completely dominated by s waves, and so the capture ratio in flight converges to the capture ratio at rest. For more details on the evaluation of these observables, we refer to earlier Nijmegen work on this subject.

The Σ^+p nuclear-bar phase shifts as a function of energy are given in Table IX. Notice that the 3S_1 -phase shows repulsion.

The ΛN nuclear-bar phase shifts as a function of energy are given in Table X. In Fig. 1 the Λp total X-sections are shown for ESC08c together with the data. At the ΣN -threshold the cross section shows a large cusp with a large D-wave nuclear-bar phaseshift $\delta(^3D_1) = 73.2^\circ$. This signals the fact that in the $\Sigma N(^3S_1, I = 1/2)$ -state there is a strong attraction, with a deuteron-like virtual bound-state on the unphysical sheet. Also, in Fig. 1 we show the cross sections in the effective range approximation, dashed lines I and II. Line II is including the shape parameter in the effective range expansion. the two-term effective range expansion with the a and r parameters describes the s -wave phases well up to $p_\Lambda \approx 400$ MeV/c.

In Table XI the low-energy parameters for Λp and Λn are shown. The singlet and triplet parameters are displayed with the $\Lambda\Sigma^0$ -mixing turned on for pseudoscalar-, vector-, scalar-, meson-pairs-, and ps-ps- exchanges. Notice that the effect for the scalar mesons of the $\Lambda\Sigma^0$ -mixing is zero because $\alpha_s = 1.00$. It is clear from these tables that the total effect of the $\Lambda\Sigma^0$ -mixing is about given by pseudoscalar and vector exchanges. The differences in the scattering

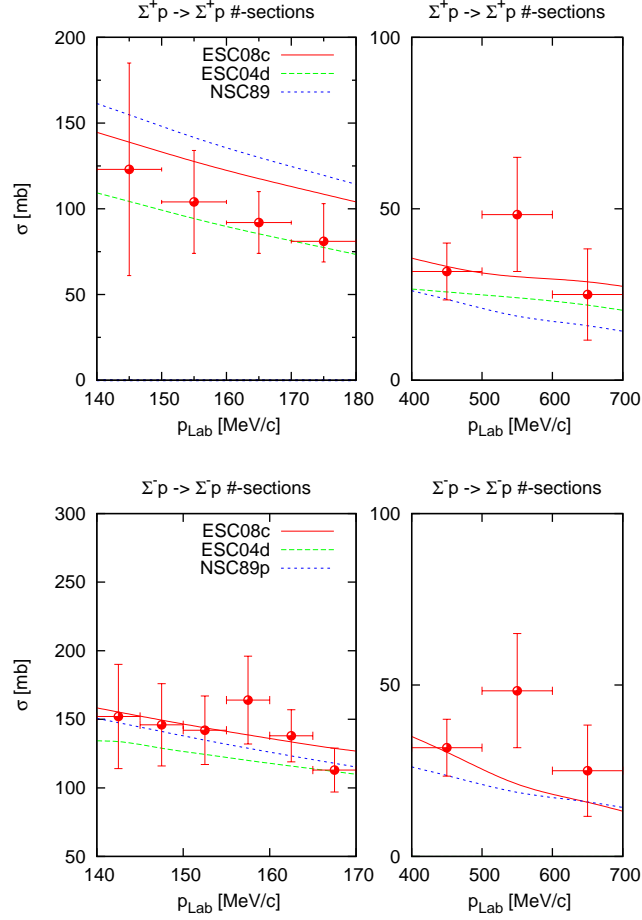


FIG. 2: Model fits total elastic X-sections $\Sigma^\pm p$. Rehovoth-Heidelberg-, KEK-data

lengths are

$$\Delta a_s = a_s(\Lambda p) - a_s(\Lambda n) = +0.164 fm, \quad (8.1a)$$

$$\Delta a_t = a_t(\Lambda p) - a_t(\Lambda n) = -0.010 fm. \quad (8.1b)$$

These differences are comparable to those for the soft-core OBE models [12, 13], and therefore predict a too small binding energy difference in the $A=4$ hypernuclei, which is $\Delta B_\Lambda(exp) = B_\Lambda(^4_\Lambda He) - B_\Lambda(^4_\Lambda H) = (0.29 \pm 0.06)$ MeV. This in contrast to the HC-model D, which has a much larger Δa_t [25]. It appeared that CSB via meson-mixing, like $\pi^0 - \eta, \rho^0 - \omega$ etc., is small and does not improve the CSB for ESC08, which is understandable in view of the large cancellations. However, as a consequence of the ESC-models there is a three-body force produced by the MPE-interactions, which are fixed by the BB-fit. Therefore, the CSB in the ΛNN -potential may improve the CSB predictions significantly.

In Table XII we list the $\Sigma^+ p$ and $\Lambda\Lambda$ scattering lengths and effective ranges. Here, (a_s, r_s) are these quantities for $\Sigma^+ p(^1S_0)$ and (a_t, r_t) for $\Sigma^+ p(^3S_1)$. Notice that the difference between ESC08a'' and ESC08c is small. This is because with SU(3) the 1S_0 -wave is constrained by NN, because the 1S_0 -states in NN and $\Sigma^+ p$ are both in the $\{27\}$ -irrep, and so there is little room for variations in the 3S_1 -wave because of the X-section fit. Therefore, much extra repulsion in the triplet wave is impossible.

In Fig. 4 we plot the total potentials for the S-wave channels $\Lambda N \rightarrow \Lambda N$, $\Lambda N \rightarrow \Sigma N$, and $\Sigma N \rightarrow \Sigma N$. Note the

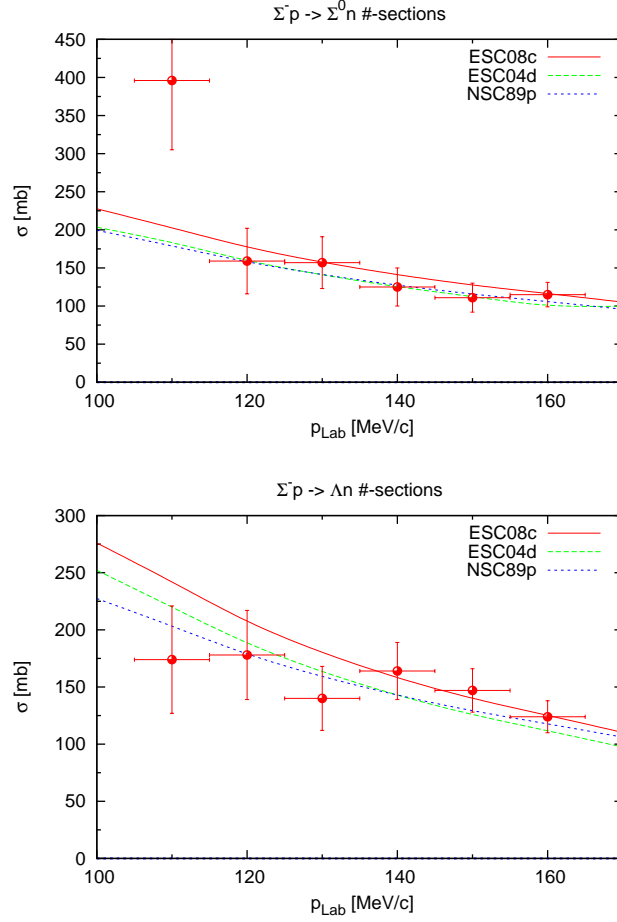


FIG. 3: Model fits total inelastic X-sections $\Sigma^- p \rightarrow \Sigma^0 n, \Lambda n$. Rehovoth-Heidelberg-data

for the soft-core model typical structure of the $\Sigma^+ p(^3S_1)$ -potential. Most contributions to the spin-spin potentials are proportional to \mathbf{k}^2 , and hence have zero volume integral. This causes the attraction in the inner region.

Figures for the OBE-, TME-, and MPE-contributions are similar to those for the ESC04-model and have been displayed in Ref. [6] and we refer the interested reader to this reference. Likewise for the contributions of the various types of mesons to the OBE-potentials, and also for the contributions of the different kind of pair-potentials to MPE.

B. Potentials in SU(3)-irreps

In Fig. 5 the potentials $V_{\{\mu\}}[\text{GeV}]$ in the SU(3) representations for BB-channels are shown. The solid/red curves include SU(3)-breaking and the dashed/green ones are the SU(3)-symmetric curves. In the latter average masses are used for the SU(3)-nonets. The curves resemble strongly (qualitatively) those obtained in lattice QCD, except for the $\{1\}$ -irrep [52]. In the ESC-model the behavior is typical for potentials with a strong spin-spin part, because the spin-spin potentials from pseudoscalar- and vector-exchange have zero volume integral forcing them to change sign for $r \sim 0.5$ fm.

The similarity between the meson-exchange and QCD-lattice potentials shows that with the ESC realization of the program starting from the nuclear force, using SU_f(3)-symmetry and the QM, a realistic generalization to the

TABLE IX: ESC08c nuclear-bar Σ^+p phases in degrees.

p_{Σ^+}	100	200	300	400	500	600	700	800	900	1000
T_{lab}	4.2	16.7	37.3	65.5	100.8	142.8	190.7	244.0	302.1	364.5
1S_0	32.21	38.49	33.16	25.30	16.89	8.57	0.55	-7.10	-14.38	-21.29
3S_1	-5.44	-11.95	-18.40	-24.84	-30.98	-36.54	-41.38	-45.51	-49.04	-52.11
ϵ_1	-0.36	-1.74	-3.22	-4.32	-4.96	-5.23	-5.23	-5.09	-4.86	-4.60
3P_0	0.93	4.86	8.49	9.37	7.61	4.12	-0.25	-4.96	-9.70	-14.27
1P_1	0.42	2.27	4.68	6.64	7.53	7.20	5.79	3.59	0.81	-2.33
3P_1	-0.56	-2.88	-5.91	-9.20	-12.76	-16.57	-20.54	-24.55	-28.50	-32.33
3P_2	0.11	0.92	2.65	4.76	6.71	8.25	9.37	10.09	10.41	10.31
ϵ_2	-0.03	-0.35	-1.02	-1.77	-2.38	-2.78	-2.95	-2.91	-2.73	-2.46
3D_1	0.02	0.29	0.83	1.33	1.40	0.76	-0.68	-2.85	-5.60	-8.76
1D_2	0.02	0.30	0.97	2.01	3.38	4.93	6.40	7.57	8.24	8.33
3D_2	-0.03	-0.42	-1.25	-2.27	-3.41	-4.74	-6.34	-8.21	-10.33	-12.65
3D_3	0.00	0.05	0.25	0.63	1.05	1.32	1.34	1.09	0.64	0.08

TABLE X: ESC08c nuclear-bar Λp phases in degrees.

p_Λ	100	200	300	400	500	600	633.4
T_{lab}	4.5	17.8	39.6	69.5	106.9	151.1	167.3
1S_0	25.14	30.86	27.49	21.11	13.88	6.72	4.72
3S_1	18.89	25.04	23.33	18.55	12.80	7.27	6.14
ϵ_1	0.04	0.12	0.12	-0.01	-0.09	1.73	9.29
3P_0	0.04	0.22	0.21	-0.58	-2.37	-4.89	-5.74
1P_1	-0.08	-0.63	-2.02	-4.40	-7.61	-11.27	-12.50
3P_1	0.02	0.00	-0.34	-1.22	-2.59	-3.88	-3.89
3P_2	0.12	0.77	1.98	3.33	4.48	5.31	5.52
ϵ_2	0.00	-0.00	-0.04	-0.15	-0.32	-0.53	-0.63
3D_1	0.00	0.08	0.57	2.21	6.74	24.38	73.17
1D_2	0.00	0.06	0.38	1.17	2.48	4.19	4.81
3D_2	0.00	0.08	0.44	1.25	2.53	4.10	4.66
3D_3	0.00	0.05	0.25	0.71	1.38	2.10	2.32

BB-force is achieved.

IX. ANALYSES WITH G-MATRIX INTERACTIONS

A. Λ and Σ in nuclear matter

The G-matrix theory gives a good starting point for studies of hyperonic many-body systems on the basis of free-space YN interaction models [53–55]. Here, the correlations induced by hyperonic coupling interactions such as ΛN - ΣN ones are renormalized into single-channel G-matrices. These G-matrix interactions are considered as effective interactions used in models of hypernuclei. Thus, the hypernuclear phenomena and the underlying YN interaction models are linked through the YN G-matrix interactions, and the hypernuclear information gives a feedback to the interaction models. Here, the properties of ΛN and ΣN sectors of ESC08c in nuclear medium are studied on the basis of the G-matrix theory.

TABLE XI: Comparison Λp and Λn scattering lengths and effective ranges in fm for different Nijmegen models.

Model	Λp		Λn	
	a_s	a_t	a_s	a_t
ESC08c	-2.46	-1.73	-2.62	-1.72
NSC97e	-2.10	-1.86	-2.24	-1.83
NSC97f	-2.51	-1.75	-2.68	-1.67
NSC89	-2.73	-1.48	-2.86	-1.24
HC-D	-1.77	-2.06	-2.03	-1.84
Model	r_s	r_t	r_s	r_t
ESC08c	3.14	3.55	3.17	3.50
NSC97e	3.19	3.19	3.24	3.14
NSC97f	3.03	3.32	3.07	3.34
NSC89	2.87	3.04	2.91	3.33
HC-D	3.78	3.18	3.66	3.32

TABLE XII: $\Sigma^+ p$ scattering lengths and effective ranges in fm.

Model	a_s	a_t	r_s	r_t
ESC04d	-3.43	+0.217	3.98	-28.94
ESC08a''	-3.85	+0.62	3.40	-2.13
ESC08c	-3.91	+0.61	3.41	-2.35

In Refs.[56, 57], the three-body interaction is added on ESC08c, being composed of the multi-pomeron exchange repulsive potential (MPP) and the phenomenological three-baryon attraction (TBA). The effective two-body potential derived from MPP is given as

$$V_{MPP}(r; \rho) = g_P^{(3)}(g_P)^3 \frac{\rho}{\mathcal{M}} \cdot \frac{1}{4\pi} \frac{4}{\sqrt{\pi}} \left(\frac{m_P}{\sqrt{2}} \right)^3 \exp \left(-\frac{1}{2} m_P^2 r^2 \right), \quad (9.1)$$

where the pomeron mass m_P and the pair pomeron coupling g_P are fitted to the NN-data etc. In a similar way, one can obtain an effective two-body potential with a quartic pomeron coupling $g_P^{(4)}$. TBA also is given by a density-dependent two-body potential

$$V_{TBA}(r; \rho) = V_{TBA}^0 \exp(-(r/2.0)^2) \rho \exp(-\eta \rho) (1 + P_r)/2,$$

P_r being a space-exchange operator. The values of $g_P^{(3)}$, $g_P^{(4)}$ and V_{TBA}^0 are adjusted to reproduce the angular distribution of $^{16}\text{O}+^{16}\text{O}$ elastic scattering at $E/A = 70$ MeV with use of the G-matrix folding potential and the value $E \sim -16$ MeV of the energy per nucleon in normal-density nuclear matter. Among three sets given in Refs.[56, 57], we adopt here the set MPa ($g_P^{(3)} = 2.34$, $g_P^{(4)} = 30.0$, $V_{TBA}^0 = -32.8$ MeV, $\eta = 3.5 \text{ fm}^3$), which gives rise to the stiff EoS of neutron matter to reproduce a maximum mass $2M_\odot$ of a neutron star.

MPP works universally in all baryon-baryon channels according to its definition. The above values of $g_P^{(3)}$ and $g_P^{(4)}$ are adopted in this work. Assuming here that TBA works also in YN channels, its strength is adjusted to reproduce well energy spectra of Λ hypernuclei. As explained later, we take $V_{TBA}^0 = -21.0$ MeV differently from the above value. Hereafter, the interaction ESC08c+MPP+TBA is denoted as ESC08c⁺.

We start from the channel-coupled G-matrix equation for the baryon pair $B_1 B_2$ in nuclear matter [53], where $B_1 B_2 = \Lambda N$ and ΣN :

$$G_{cc_0} = v_{cc_0} + \sum_{c'} v_{cc'} \frac{Q_{y'}}{\omega - \epsilon_{B'_1} - \epsilon_{B'_2} + \Delta_{yy'}} G_{c'c_0}, \quad (9.2)$$

where c denotes a YN relative state (y, T, L, S, J) with $y = (B_1, B_2)$. S and T are spin and isospin quantum numbers, respectively. Orbital and total angular momenta are denoted by L and J , respectively, with $\mathbf{J} = \mathbf{L} + \mathbf{S}$. Then, a two-particle state is represented as $^{2S+1}L_J$. In Eq. (9.2), ω gives the starting energy in the starting channel c_0 .

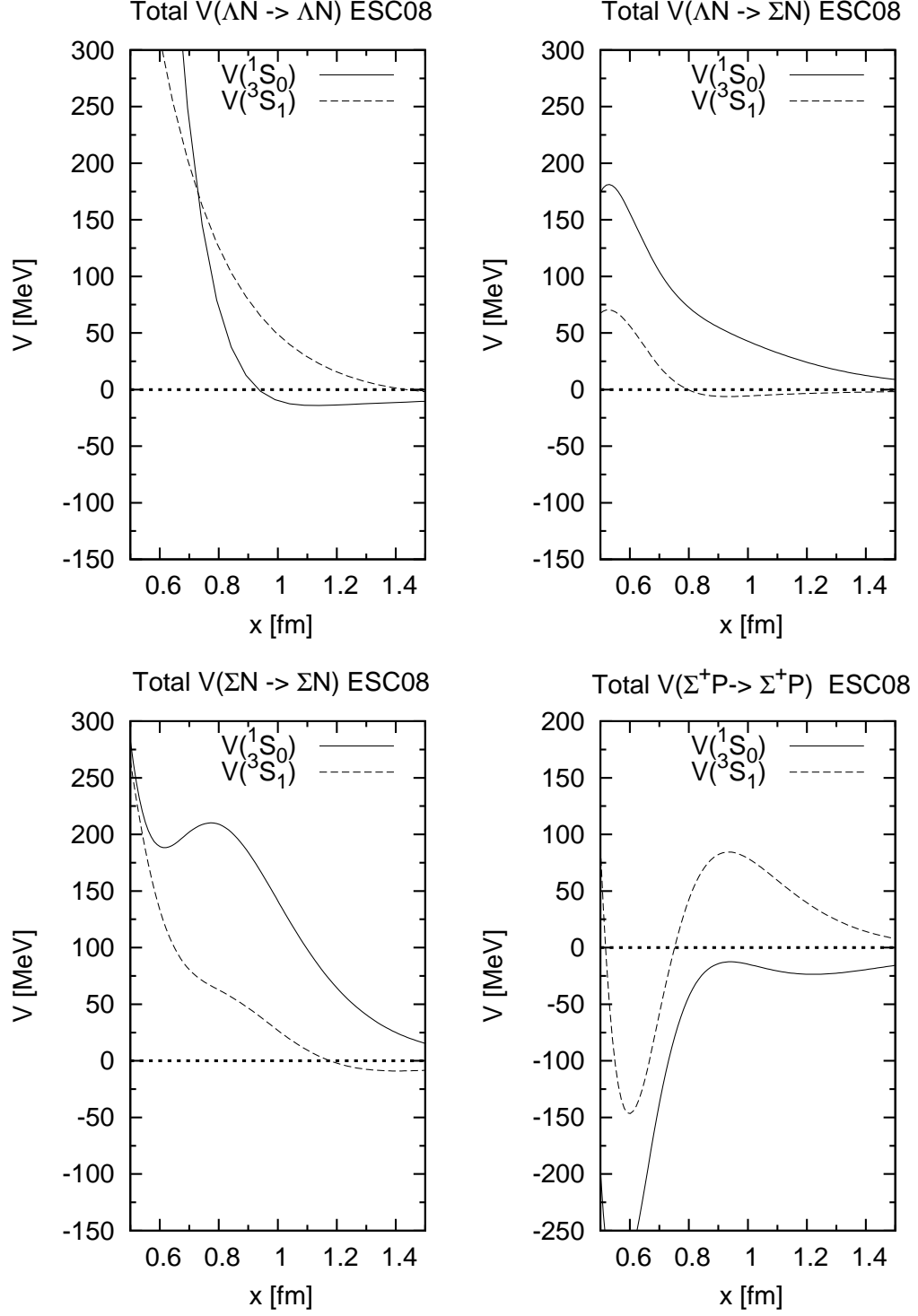


FIG. 4: Total potentials in the partial waves 1S_0 and 3S_1 , for $I = 1/2$ - and $I = 3/2$ -states.

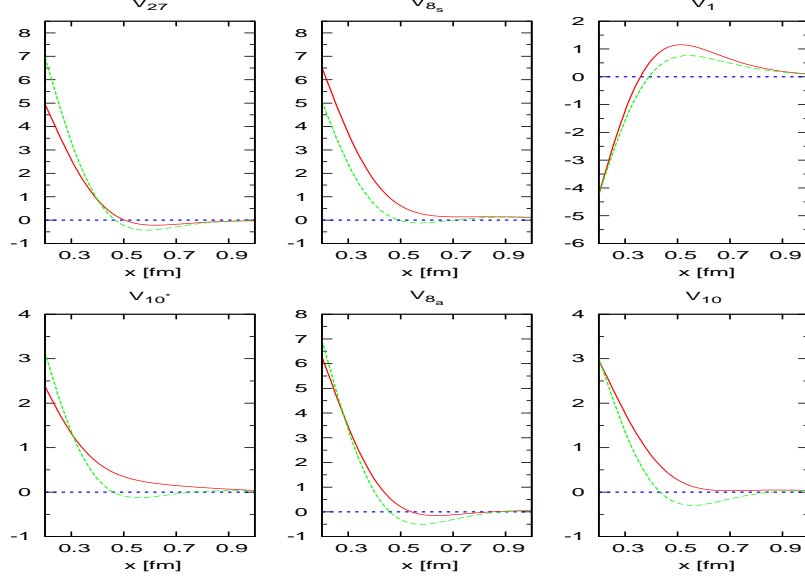


FIG. 5: Exact flavor SU(3)-symmetry: $m_\pi = m_K = m_\eta = 450$ MeV

$\Delta_{yy'} = M_{B_1} + M_{B_2} - M_{B'_1} - M_{B'_2}$ denotes the mass difference between two baryon channels. The Pauli operator Q_y acts on intermediate nucleon states in a channel $y = (B_1, B_2) = (\Lambda N, \Sigma N)$. We adopt here the continuous (CON) choice for intermediate single particle potentials in the G-matrix equation. The G-matrix equation (9.2) is represented in the coordinate space, whose solutions give rise to G-matrix elements. The hyperon single particle (s.p.) energy ϵ_Y in nuclear matter is given by

$$\epsilon_Y(k_Y) = \frac{\hbar^2 k_Y^2}{2M_Y} + U_Y(k_Y) , \quad (9.3)$$

where k_Y is the hyperon momentum. The potential energy U_Y is obtained self-consistently in terms of the G-matrix as

$$U_Y(k_Y) = \sum_{|\mathbf{k}_N|} \langle \mathbf{k}_Y \mathbf{k}_N | G_{YN}(\omega = \epsilon_Y(k_Y) + \epsilon_N(k_N)) | \mathbf{k}_Y \mathbf{k}_N \rangle . \quad (9.4)$$

Here, we need not only on-shell single particle potentials but also off-shell ones because of adopting the CON choice.

First, let us calculate Λ binding energies in nuclear matter. In Table XIII we show the potential energies $U_\Lambda(\rho_0)$ for a zero-momentum Λ and their partial-wave contributions in $^{2S+1}L_J$ states at normal density ρ_0 ($k_F=1.35$ fm $^{-1}$), where a statistical factor $(2J+1)$ is included in each contribution in $^{2S+1}L_J$ state. The value specified by D gives the sum of $^{2S+1}L_J$ contributions. Results for ESC08c and ESC08c $^+$ are found to be not so different from each other, because repulsive contributions of MPP are rather cancelled by attractive TBA contributions in normal and lower density regions. It should be noted here that the important role of MPP is to stiffen the EOS remarkably by strongly repulsive contributions in high density regions.

The contributions to U_Λ from S -state spin-spin components can be seen qualitatively in values of $U_{\sigma\sigma} = (U_\Lambda(^3S_1) - 3U_\Lambda(^1S_0))/12$. These values of $U_{\sigma\sigma}$ also are given in Table XIII. In the same treatment, we obtain $U_{\sigma\sigma}=1.54$ and 0.92 MeV for NSC97f and NSC97e, respectively. Various analyses suggest that the reasonable value of $U_{\sigma\sigma}$ is between these values [55]. Then, one should note that the $U_{\sigma\sigma}$ values for ESC08c/ c^+ are reasonable.

Next, Σ binding energies in nuclear matter are obtained by solving the ΣN starting channel G-matrix equation for ESC08c/ c^+ . In Table XIV we show the potential energies $U_\Sigma(\rho_0)$ for a zero-momentum Σ and their partial-wave contributions in $(^{2S+1}L_J, T)$ states for ESC08c/ c^+ . It should be noted here that the strongly repulsive contributions in 3S_1 $T=3/2$ and 1S_0 $T=1/2$ states are due to the Pauli-forbidden effects in these states, being taken into account by strengthening the pomeron coupling in the ESC08 modeling. Experimentally, the repulsive Σ -nucleus potentials are suggested in the observed (π^-, K^-) spectra. [24, 58, 59] It is a future problem to calculate (π^-, K^-) spectra with use of G-matrix folding potentials, and to select out a reasonable ΣN interaction model.

TABLE XIII: Values of $U_\Lambda(\rho_0)$ and partial wave contributions in $^{2S+1}L_J$ states from the G-matrix calculations (in MeV). The value specified by D gives the sum of $^{2S+1}D_J$ contributions. Contributions from S -state spin-spin interactions are given by $U_{\sigma\sigma} = (U_\Lambda(^3S_1) - 3U_\Lambda(^1S_0))/12$.

	1S_0	3S_1	1P_1	3P_0	3P_1	3P_2	D	U_Λ	$U_{\sigma\sigma}$
ESC08c	-13.1	-26.5	2.4	0.1	1.1	-3.1	-1.6	-40.8	1.07
ESC08c ⁺	-12.6	-25.4	2.9	0.3	1.6	-2.1	-2.3	-37.6	1.03

TABLE XIV: Values of $U_\Sigma(\rho_0)$ at normal density and partial wave contributions in $(^{2S+1}L_J, T)$ states for ESC08c/ c^+ (in MeV).

model	T	1S_0	3S_1	1P_1	3P_0	3P_1	3P_2	D	U_Σ
ESC08c	1/2	11.1	-22.0	2.4	2.1	-6.1	-1.0	-0.7	+1.4
	3/2	-12.8	30.7	-4.8	-1.8	6.0	-1.4	-0.2	
ESC08c ⁺	1/2	11.1	-20.4	2.6	2.1	-5.8	-0.6	-0.8	+7.9
	3/2	-11.9	31.8	-4.2	-1.6	6.4	-0.4	-0.6	

In the left (right) panel of Fig. 6, U_Σ values (their S -state contributions) are drawn as a function of k_F for ESC08c⁺ and ESC08c by solid and dashed curves, respectively. It is demonstrated that the repulsive U_Σ values are due to $T = 3/2$ 3S_1 and $T = 1/2$ 1S_0 contributions, and the repulsions are enhanced by the MPP contributions.

B. ΛN G-matrix interactions

For applications to various hypernuclear problems, it is convenient to construct k_F -dependent effective local potentials $\mathcal{G}(k_F; r)$ which simulate the G-matrices. Here we parameterize them in a three-range Gaussian form

$$\mathcal{G}(k_F, r) = \sum_{i=1}^3 (a_i + b_i k_F + c_i k_F^2) \exp(-r^2/\beta_i^2). \quad (9.5)$$

The parameters (a_i, b_i, c_i) are determined so as to simulate the calculated G-matrix for each $^{2S+1}L_J$ state. The procedures to fit the parameters are given in Ref. [55]. The obtained parameters for ESC08c are shown in Table XV. For ESC08c⁺, contributions from MPP+TBA are represented by modifying the second-range parts of $\mathcal{G}(k_F, r)$ for ESC08c by $\Delta\mathcal{G}(k_F, r) = (a + bk_F + ck_F^2) \exp(-(r/0.9)^2)$. The parameters for $\Delta\mathcal{G}(k_F, r)$ are given in Table XVI.

Here, it is worthwhile to comment about a qualitative feature of $\Delta\mathcal{G}(k_F, r)$. The MPP contributions increase rapidly with matter density: In high (low) density region, they are very large (small), and rather cancelled by TBA at normal-density region. Then, net contributions of MPP+TBA given by $\Delta\mathcal{G}(k_F, r)$ are attractive for smaller values of k_F than 1.35 fm^{-1} .

The solved G-matrices include not only ΛN - ΛN diagonal parts but also ΛN - ΣN coupling parts, and it is possible to extract such coupling parts to treat ΛN - ΣN mixing problems. The ΛN - ΣN coupling interaction is determined so that its matrix elements in k space simulate the corresponding G-matrix elements and its radial form tend to that of the bare interaction in the outermost region. In Table XVII (Table XVIII), the parameters of the central (tensor) parts of ΛN - ΣN and ΣN - ΣN interactions in S states are given in a three-range Gaussian (r^2 -Gaussian) form. Here, the k_F dependences are represented in the same form as the above diagonal parts. These coupling interactions can be used for ΛN - ΣN mixing problems together with the ΛN - ΛN diagonal interactions in the Table XV.

The SLS interactions $\mathcal{G}_{SLS}(r)$ are derived from G-matrices $\mathcal{G}_{LL'}^{JS}(r)$ with $S = 1$ by the linear transformation. The ALS G-matrix interaction \mathcal{G}_{ALS} between 3P_1 and 1P_1 states is given so that its matrix elements in k space simulate the corresponding G matrix elements $\langle ^3P_1 | G | ^1P_1 \rangle$. Because $\langle ^3P_1 | G | ^1P_1 \rangle$ and $\langle ^1P_1 | G | ^3P_1 \rangle$ are different from each other, we derive \mathcal{G}_{ALS} from their averaged values. The SLS and ALS G-

matrix interactions obtained as a function of k_F are represented in three-range Gaussian forms, the parameters of which are given for ESC08c in Table XIX.

In order to compare clearly the SLS and ALS components, it is convenient to derive the strengths of the Λ l - s potentials in hypernuclei. In the same way as in Refs. [6, 13], the expression can be derived with the Scheerbaum approximation [60] as $U_\Lambda^{ls}(r) = K_\Lambda \frac{1}{r} \frac{d\rho}{dr} \mathbf{l} \cdot \mathbf{s}$.

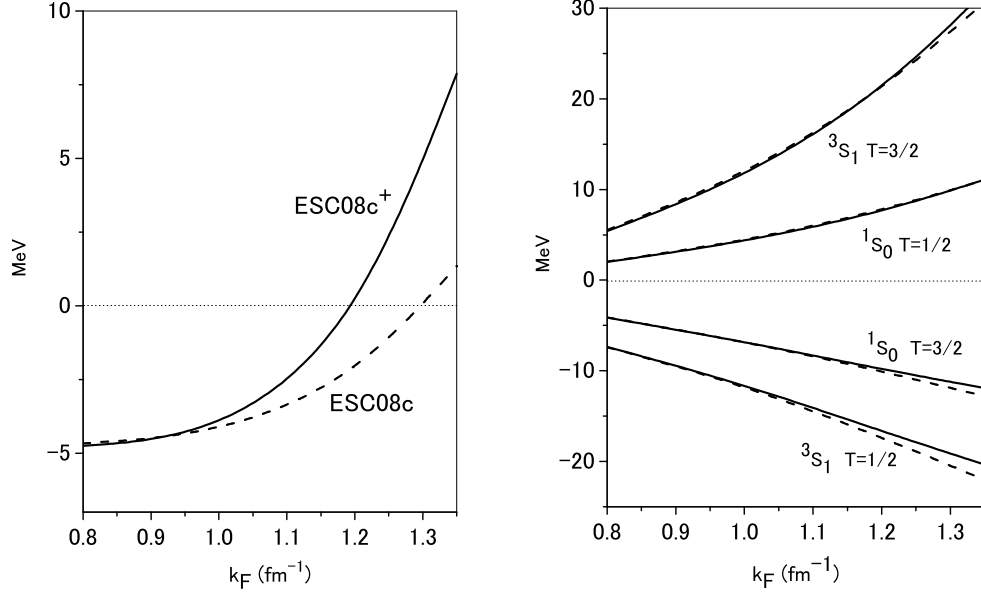


FIG. 6: In the left (right) panel, the values of U_Σ (partial-wave contributions) are drawn as a function of k_F by solid and dashed curves for ESC08c⁺ and ESC08c, respectively.

TABLE XV: Parameters of YNG-ESC08c Continuous choice : $\mathcal{G}(k_F; r) = \sum_{i=1}^3 (a_i + b_i k_F + c_i k_F^2) \exp(-(r/\beta_i)^2)$

	β_i	0.50	0.90	2.00
¹ E	a	-3434.	396.0	-1.708
	b	6937.	-1057.	0.0
	c	-2635.	415.9	0.0
³ E	a	-1933.	195.4	-1.295
	b	4698.	-732.8	0.0
	c	-1974.	330.1	0.0
¹ O	a	206.1	67.89	-8.292
	b	-30.52	34.11	0.0
	c	16.23	2.471	0.0
³ O	a	2327.	-254.1	-9.959
	b	-2361.	202.6	0.0
	c	854.3	-43.71	0.0

TABLE XVII: Central coupling parts of G-matrix interactions for ESC08c, represented in a Gaussian form $\sum_{i=1}^3 (a_i + b_i k_F + c_i k_F^2) \exp(-(r/\beta_i)^2)$.

	β_i	0.50	0.90	2.00
ΛN - ΣN ¹ S ₀	a	4596.	-702.3	8.525
	b	-7150.	1160.	0.0
	c	2760.	-438.4	0.0
ΣN - ΣN ¹ S ₀	a	-311.9	171.0	8.713
	b	861.6	-79.17	0.0
	c	-355.3	70.65	0.0
ΛN - ΣN ³ S ₁	a	-1525.	211.4	-2.749
	b	2775.	-442.0	0.0
	c	-1253.	208.0	0.0
ΣN - ΣN ³ S ₁	a	899.5	-158.0	-4.252
	b	240.3	-31.34	0.0
	c	-199.9	41.30	0.0

TABLE XVI: $\Delta\mathcal{G}(k_F; r) = (a + b k_F + c k_F^2) \exp(-(r/0.9)^2)$

	¹ E	³ E	¹ O	³ O
a	20.71	19.16	26.31	24.95
b	-51.74	-49.31	-73.58	-71.92
c	28.84	27.30	64.01	66.73

The values of K_Λ can be calculated with use of $\mathcal{G}_{SL S}(r)$ and $\mathcal{G}_{AL S}(r)$: The obtained value at $k_F = 1.0 \text{ fm}^{-1}$ is 3.6 MeV fm^5 . This value is far (slightly) smaller than those for NSC97e/f (ESC08a/b) [55].

C. Λ hypernuclei by G-matrix folding potentials

The ΛN G-matrix interaction given by Table XV is expressed as $\mathcal{G}_{(\pm)}^S(r)$, S and (\pm) denoting spin and party quantum numbers, respectively. A Λ -nucleus potential in a finite system is derived from this ΛN interaction by the expression

$$\begin{aligned}
 U_\Lambda(\mathbf{r}, \mathbf{r}') &= U_{dr} + U_{ex}, \\
 U_{dr} &= \delta(\mathbf{r} - \mathbf{r}') \int d\mathbf{r}'' \rho(\mathbf{r}'') V_{dr}(|\mathbf{r} - \mathbf{r}''|; k_F) \\
 U_{ex} &= \rho(\mathbf{r}, \mathbf{r}') V_{ex}(|\mathbf{r} - \mathbf{r}'|; k_F), \quad (9.6)
 \end{aligned}$$

TABLE XVIII: Tensor coupling parts of G-matrix interactions for ESC08c, represented in a r^2 -Gaussian form $\sum_{i=1}^3 (a_i + b_i k_F + c_i k_F^2) r^2 \exp(-(r/\beta_i)^2)$.

β_i		0.50	0.90	2.00
ΛN - ΣN 3S_1	a	-39470.	470.3	-7443
	b	61860.	-901.1	0.0
	c	-23750.	343.3	0.0
ΛN - ΛN 3S_1	a	-209.3	-1.836	-.0218
	b	367.6	8.251	0.0
	c	334.4	-14.09	0.0

TABLE XIX: Parameters of SLS and ALS G-matrix interactions represented by three-range Gaussian forms $\mathcal{G}(r; k_F) = \sum_i (a_i + b_i k_F + c_i k_F^2) \exp(-(r/\beta_i)^2)$ in the cases of ESC08c.

β_i		0.40	0.80	1.20
SLS	a	-12920.	372.4	-2.030
	b	24580.	-840.0	0.0
	c	-10180.	337.1	0.0
ALS	a	1985.	12.73	2.109
	b	-1828.	41.30	0.0
	c	679.8	-17.58	0.0

On the other hand, $V_{TBA}^0 = -21.0$ MeV in ESC08c⁺ is chosen so as to give best fitting to the experimental spectrum of $^{89}\Lambda\text{Y}$. In such an approach, the choice of V_{TBA}^0 depends on the adopted two-body interaction. In [57], the previous version of ESC08c was used, giving $U_\Lambda(\rho_0) = -39.4$ MeV shallower than the value -40.8 MeV in the present work. Then, V_{TBA}^0 was taken as -32.8 MeV in the same as that in NN channels.

In Fig. 7, the calculated values are compared with the experimental values marked by open circles, the horizontal axis being given as $A^{-2/3}$, where solid and dashed curves are for ESC08c⁺ and ESC08c, respectively. Here, the experimental data are shifted by 0.5 MeV from the values given in Ref.[61], which has been recently proposed according to the improved calibration [63]. The difference between ESC08c⁺ and ESC08c is due to the extra terms $\Delta\mathcal{G}(k_F, r)$ originated from MPP+TBA. Especially, MPP plays an essential role to reproduce the nuclear saturation property and the stiffness of the EoS of neutron-star matter [56, 57]. Then, it is very important that ESC08c⁺ gives better fitting than ESC08c: The density-dependent attraction $\Delta\mathcal{G}(k_F, r)$ in low-density region works to reproduce better the energy spectra of heavy systems and B_Λ values of light systems. In high-density region, this extra term leads to the stiff EoS of the hyperon-mixed neutron-star matter [57]. The present result suggests that such an effect of MPP+TBA can be tested in terrestrial data of B_Λ values.

Finally, it is commented that the Λ s.p. energies in finite systems are not related simply to the $U_\Lambda(\rho_0)$ val-

$$\begin{pmatrix} V_{dr} \\ V_{ex} \end{pmatrix} = \frac{1}{4} \sum_{S=0,1} (2S+1) [\mathcal{G}_{(\pm)}^S \pm \mathcal{G}_{(\mp)}^S] . \quad (9.7)$$

Here, densities $\rho(r)$ and mixed densities $\rho(r, r')$ are obtained from spherical Skyrme-HF wave functions.

An important problem is how to treat k_F values included in G-matrix interactions. We use here the following Averaged-Density Approximation (ADA), where an averaged value $\langle \rho \rangle$ is calculated by $\langle \phi_\Lambda(r) | \rho(r) | \phi_\Lambda(r) \rangle$ for each Λ state $\phi_\Lambda(r)$, and $\langle k_F \rangle$ is obtained by $(1.5\pi^2 \langle \rho \rangle)^{1/3}$.

Let us calculate the energy spectra of Λ hypernuclei systematically ($^{13}_\Lambda\text{C}$, $^{28}_\Lambda\text{Si}$, $^{51}_\Lambda\text{V}$, $^{89}_\Lambda\text{Y}$, $^{139}_\Lambda\text{La}$, $^{208}_\Lambda\text{Pb}$). In calculations, since the G-matrix interaction for ESC08c gives rise to larger values of B_Λ systematically compared to experimental data, a factor 1.033 is multiplied on core parts ($\beta = 0.5$ fm).

ues given in Table XV. The $U_\Lambda(\rho_0)$ values of -40.8 MeV (-37.6 MeV) for ESC08c (ESC08c⁺) are very attractive compared to the experimental value of -30 MeV, which is the depth U_{WS} of the Λ Woods-Saxon (WS) potential suitable to the data of Λ hypernuclei. However, it is misleading to compare the $U_\Lambda(\rho_0)$ value directly to the U_{WS} one. The Λ -nucleus folding potential depends not only on the strengths of ΛN G-matrices but also on their k_F dependences. Then, the depth U_{WS} of the phenomenological Woods-Saxon potential of Λ cannot be considered as the Λ potential depth in nuclear matter.

X. DISCUSSION, CONCLUSIONS AND OUTLOOK

We have again shown in this paper that the ESC-approach to the nuclear force problem is able to make a connection between on the one hand the at present available baryon-baryon data and on the other hand the underlying quark structure of the baryons and mesons. Namely, a very successful description of both the NN - and YN -scattering data is obtained with meson-baryon coupling parameters which are almost all explained by the QPC-model. This at the same time in obedience of the strong constraint of no bound states in the $S = -1$ -systems. Therefore, the ESC08c model of this paper are an important further step in the determination of the baryon-baryon interactions for low energy scattering and the description of hypernuclei in the context of bro-

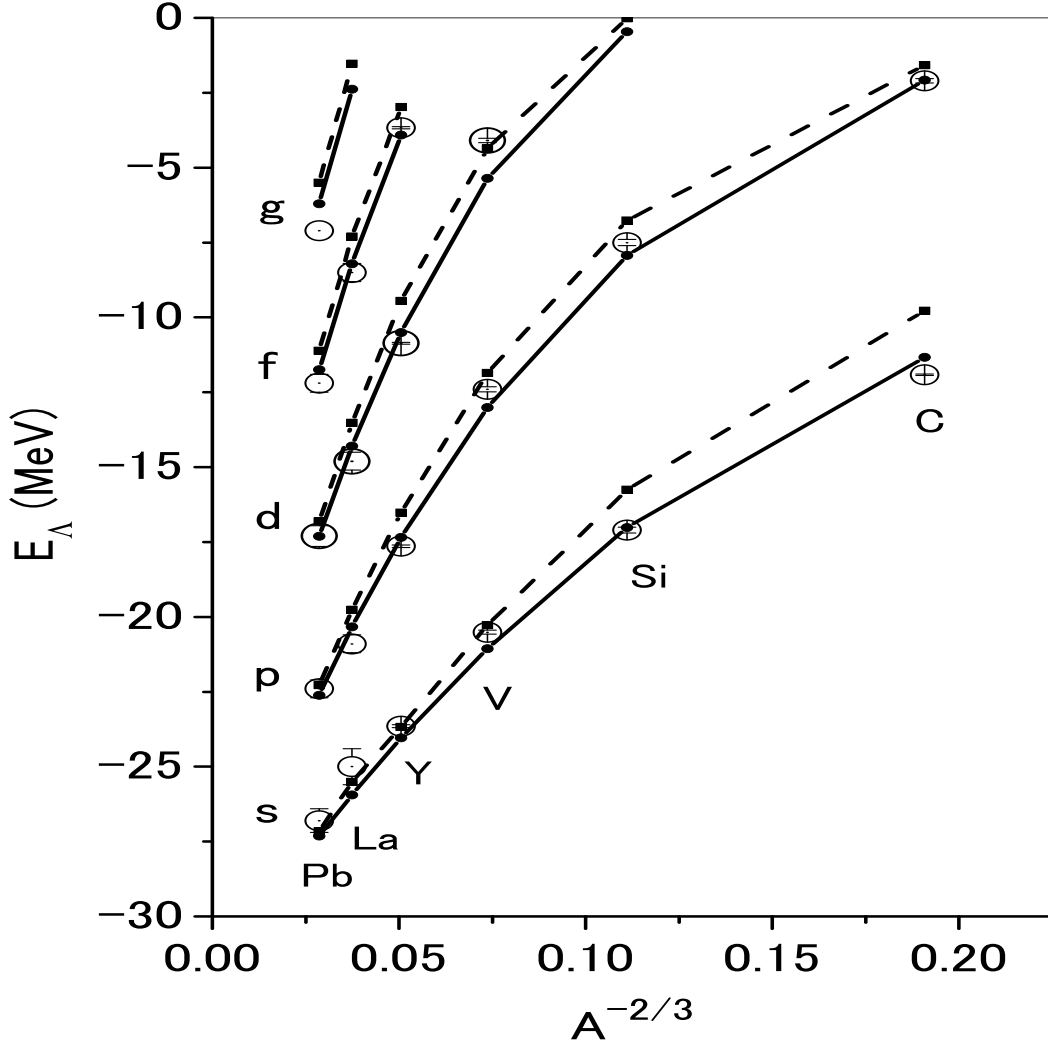


FIG. 7: Energy spectra of $^{13}_{\Lambda}\text{C}$, $^{28}_{\Lambda}\text{Si}$, $^{51}_{\Lambda}\text{V}$, $^{89}_{\Lambda}\text{Y}$, $^{139}_{\Lambda}\text{La}$ and $^{208}_{\Lambda}\text{Pb}$ are given as a function of $A^{-2/3}$, A being mass numbers of core nuclei. Solid (dashed) lines show calculated values by the G-matrix folding model derived from ESC08c⁺ (ESC08c). Open circles denote the experimental values taken from Ref. [61].

ken SU(3)-symmetry. The values for many parameters, which in previous work were considered to be free to a large extend, are now limited strongly, and tried to be made consistent with the present theoretical view on low energy hadron physics. This is in particularly the case for the $F/(F+D)$ -ratios of the MPE-interactions. These ratio's for the vector- and scalar-mesons are rather close to the QPC-model predictions.

In analyzing the effect of the Pauli-blocking repulsion the conclusion is that from the standpoint of the BB scattering-data fitting such a repulsion is not strong. This conclusion is in line with arguments from strong-coupling QCD (SCQCD). Namely, it has been argued in [64] that quark-exchange effects are small.

The G-matrix results show that basic features of hypernuclear data are reproduced nicely by ESC08c, improving the weak points of the soft-core OBE-models NSC89

[12], NSC97 [13], and ESC04-models [5–7]. The ESC08-models are superior for hypernuclear data and many aspects of the effective (two-body) interactions in hypernuclei can be obtained using the ESC08-model. For example, this is the case for the well depth U_{Σ} .

Experience has shown that a good fit to the scattering data not necessarily means success in the G-matrix results. To explain this one can think of two reasons: (i) the G-matrix results are sensitive to the two-body interactions below 1 fm, whereas the present YN-scattering data are not, (ii) other than two-body forces play an important role. However, since the $NN + YN$ -fit is so much superior for ESC04- than for OBE-models, we are inclined to look for solutions to the remaining problems outside the two-body forces. A natural possibility is the presence of three-body forces (3BF) in hypernuclei which can be viewed as generating effective two-body forces,

which could solve the well-depth issues. In the case of the $\Delta B_{\Lambda\Lambda}$ also 3BF could be operating. This calls for an evaluation of the 3BF's NNN , ΛNN , ΣNN , $\Lambda\Lambda N$, etc. for the soft-core ESC-model, consistent with its two-body forces.

The ΛN p-waves seem to be better, which is the result of the truly simultaneous $NN + YN$ -fitting. This is also reflected in the better K_Λ -value, making the well-known small spin-orbit splitting smaller. In the course of the development of the ESC-model for baryon-baryon, up to and including ESC06 [65] it was tried to solve all problems for NN and YN , both for scattering and hypernuclear well-depth's, by keeping the potentials restricted to meson-exchange. For that purpose, in ESC06 a 'super-extended' the ESC-approach was studied by including the second generation of the mesons, i.e. the heavy pseudo-scalar, vector, and scalar meson nonets. In the Quark-Model they would correspond to the first radially excited $Q\bar{Q}$ -states, with masses in the range $1\text{GeV}/c^2 < M < 1.7\text{GeV}/c^2$. With this extension it is possible to produce extra repulsion in the $\Sigma^+ p(^3S_1)$, but correlated with this was an extremely strong attraction in the $\Sigma^+ p(^1P_1)$ partial-wave. Although the ESC06-approach is not ruled out by the data, we think that the solutions presented with ESC08 are much more superior. In the future, such a 'super-extended' ESC08-model may be explored. For example, the axial-vector and heavy pseudoscalar ($\pi(1300)$) meson sectors can be studied more closely. furthermore, for the scalar mesons the inclusion of a finite width for the broad κ -meson can be investigated.

Appendix A: MPE interactions and $SU(3)$

Below, $\sigma, \mathbf{a}_0, \mathbf{A}_1, \dots$ are short-hands for respectively the baryon $SU(3)$ -singlet and -octet densities $\bar{\psi}\psi, \bar{\psi}\boldsymbol{\lambda}\psi, \bar{\psi}\gamma_5\gamma_\mu\boldsymbol{\lambda}\psi, \dots$. Here, $\lambda_i, i = 0, 1, \dots, 8$ are the Gell-Mann $SU(3)$ -matrices.

For the pseudoscalar-, vector-, scalar-, and axial-vector mesons The $SU(3)$ octet and singlet states appearing in the meson-pairs, denoted by the subscript 8 respectively 1, are in terms of the physical ones defined as follows:

(i) Pseudo-scalar-mesons:

$$\begin{aligned}\eta_1 &= \cos\theta_P\eta' - \sin\theta_P\eta \\ \eta_8 &= \sin\theta_P\eta' + \cos\theta_P\eta\end{aligned}$$

Here, η' and η are the physical pseudo-scalar mesons $\eta(957)$ respectively $\eta(548)$.

(ii) Vector-mesons:

$$\begin{aligned}\phi_1 &= \cos\theta_V\omega - \sin\theta_V\phi \\ \phi_8 &= \sin\theta_V\omega + \cos\theta_V\phi\end{aligned}$$

Here, ϕ and ω are the physical vector mesons $\phi(1019)$ respectively $\omega(783)$.

Then, one has the following $SU(3)$ -invariant pair-interaction Hamiltonians:

1. $J^{PC} = 0^{+-}$: $SU(3)$ -singlet couplings $S_\beta^\alpha = \delta_\beta^\alpha \sigma / \sqrt{3}$,

$$\mathcal{H}_{S_1PP} = \frac{g_{S_1PP}}{\sqrt{3}} \{ \boldsymbol{\pi} \cdot \boldsymbol{\pi} + 2K^\dagger K + \eta_8 \eta_8 \} \cdot \sigma$$

2. $J^{PC} = 0^{++}$: $SU(3)$ -octet symmetric couplings I, $S_\beta^\alpha = (S_8)_\beta^\alpha \Rightarrow (1/4)\text{Tr}\{S[P, P]_+\}$,

$$\begin{aligned}\mathcal{H}_{S_8PP} &= \frac{g_{S_8PP}}{\sqrt{6}} \left\{ (\mathbf{a}_0 \cdot \boldsymbol{\pi}) \eta_8 + \frac{\sqrt{3}}{2} \mathbf{a}_0 \cdot (K^\dagger \boldsymbol{\tau} K) \right. \\ &\quad + \frac{\sqrt{3}}{2} \{ (K_0^\dagger \boldsymbol{\tau} K) \cdot \boldsymbol{\pi} + h.c. \} \\ &\quad - \frac{1}{2} \{ (K_0^\dagger K) \eta_8 + h.c. \} \\ &\quad \left. + \frac{1}{2} f_0 (\boldsymbol{\pi} \cdot \boldsymbol{\pi} - K^\dagger K - \eta_8 \eta_8) \right\}\end{aligned}$$

3. $J^{PC} = 1^{+-}$: $SU(3)$ -octet symmetric couplings II, $S_\beta^\alpha = (B_8)_\beta^\alpha \Rightarrow (1/4)\text{Tr}\{B^\mu[V_\mu, P]_+\}$,

$$\begin{aligned}\mathcal{H}_{B_8VP} &= \frac{g_{B_8VP}}{\sqrt{6}} \left\{ \frac{1}{2} [(\mathbf{B}_1^\mu \cdot \boldsymbol{\rho}_\mu) \eta_8 + (\mathbf{B}_1^\mu \cdot \boldsymbol{\pi}_\mu) \phi_8] \right. \\ &\quad + \frac{\sqrt{3}}{4} [\mathbf{B}_1 \cdot (K^{*\dagger} \boldsymbol{\tau} K) + h.c.] \\ &\quad + \frac{\sqrt{3}}{4} [(K_1^\dagger \boldsymbol{\tau} K^*) \cdot \boldsymbol{\pi} + (K_1^\dagger \boldsymbol{\tau} K) \cdot \boldsymbol{\rho} + h.c.] \\ &\quad - \frac{1}{4} [(K_1^\dagger \cdot K^*) \eta_8 + (K_1^\dagger \cdot K) \phi_8 + h.c.] \\ &\quad \left. + \frac{1}{2} H^0 \left[\boldsymbol{\rho} \cdot \boldsymbol{\pi} - \frac{1}{2} (K^{*\dagger} \cdot K + K^\dagger \cdot K^*) - \phi_8 \eta_8 \right] \right\}\end{aligned}$$

4. $J^{PC} = 1^{--}$: $SU(3)$ -octet a-symmetric couplings I, $A_\beta^\alpha = (V_8)_\beta^\alpha \Rightarrow (-i/\sqrt{2})\text{Tr}\{V^\mu[P, \partial_\mu P]_-\}$,

$$\begin{aligned}\mathcal{H}_{V_8PP} &= g_{A_8PP} \left\{ \frac{1}{2} \boldsymbol{\rho}_\mu \cdot \boldsymbol{\pi} \times \overleftrightarrow{\partial}^\mu \boldsymbol{\pi} + \frac{i}{2} \boldsymbol{\rho}_\mu \cdot (K^\dagger \boldsymbol{\tau} \overleftrightarrow{\partial}^\mu K) \right. \\ &\quad + \frac{i}{2} \left(K_\mu^{*\dagger} \boldsymbol{\tau} (K \overleftrightarrow{\partial}^\mu \boldsymbol{\pi}) - h.c. \right) + i \frac{\sqrt{3}}{2} \left(K_\mu^{*\dagger} \cdot \right. \\ &\quad \left. (K \cdot \overleftrightarrow{\partial}^\mu \eta_8) - h.c. \right) + \frac{i}{2} \sqrt{3} \phi_\mu (K^\dagger \overleftrightarrow{\partial}^\mu K) \left. \right\}\end{aligned}$$

5. $J^{PC} = 1^{++}$ $SU(3)$ -octet a-symmetric couplings II, $A_\beta^\alpha = (A_8)_\beta^\alpha \Rightarrow (-i/\sqrt{2})\text{Tr}\{A^\mu[P, V_\mu]_-\}$:

$$\begin{aligned}\mathcal{H}_{A_8VP} &= g_{A_8VP} \left\{ \mathbf{A}_1 \cdot \boldsymbol{\pi} \times \boldsymbol{\rho} \right. \\ &\quad + \frac{i}{2} \mathbf{A}_1 \cdot [(K^\dagger \boldsymbol{\tau} K^*) - (K^{*\dagger} \boldsymbol{\tau} K)] \\ &\quad - \frac{i}{2} \left([(K^\dagger \boldsymbol{\tau} K_A) \cdot \boldsymbol{\rho} + (K_A^\dagger \boldsymbol{\tau} K^*) \cdot \boldsymbol{\pi}] - h.c. \right) \\ &\quad - i \frac{\sqrt{3}}{2} \left([(K^\dagger \cdot K_A) \phi_8 + (K_A^\dagger \cdot K^*) \eta_8] - h.c. \right) \\ &\quad \left. + \frac{i}{2} \sqrt{3} f_1 [K^\dagger \cdot K^* - K^{*\dagger} \cdot K] \right\}\end{aligned}$$

The relation with the pair-couplings used in this paper and paper I, see also [31], I is $g_{S_1 PP}/\sqrt{3} = g_{(\pi\pi)_0}/m_\pi$, $g_{A_8 VP} = g_{(\pi\rho)_1}/m_\pi$ etc.

where $n = 0, 1$ refers to the $(1/M)$ -order, and the subscript $\sigma + T$ indicates that only the spin-spin and tensor contributions are given here and not the spin-orbit potentials.

Appendix B: $J^{PC} = 1^{+-}$ Axial-pair Potentials

In this appendix we document the $J^{PC} = 1^{+-}$ -axial $(\pi\omega)$ 1-pair potentials, which have not been reported elsewhere yet. The involved meson-pairs can be read off from the SU(2) structure of the interaction Hamiltonian (4.27).

Below, we denote the type of potentials by writing $V_{\sigma+T}^{(n)}$,

1. NN-Potentials ($S = 0, I = 1$)-exchange, $(\pi\omega_1)$ etc.

To be specific, consider $(\pi\omega)_1$ -exchange for NN and elastic ΣN potentials. One obtains:

1. The leading, i.e. $(1/M)^0$ -terms in momentum and configuration space are

$$\tilde{V}_{\sigma+T}^{(0)}(\mathbf{q}, \mathbf{k}) = +g_{(\pi\omega)_1; NN} f_{NN\pi} G_{NN\omega} \left(\boldsymbol{\sigma}_1 \cdot \mathbf{k} \boldsymbol{\sigma}_2 \cdot \mathbf{k}_1 + \boldsymbol{\sigma}_1 \cdot \mathbf{k}_1 \boldsymbol{\sigma}_2 \cdot \mathbf{k} \right) \times \frac{1}{\omega_1^2 \omega_2^2} \cdot \frac{1}{m_\pi^2 \mathcal{M}}, \quad (\text{B1a})$$

$$V_{\sigma+T}^{(0)}(r) = -2g_{(\pi\omega; NN)} f_{NN\pi} G_{NN\omega} \left[F_{B,\sigma}^{(0)}(r) \boldsymbol{\sigma}_1 \cdot \boldsymbol{\sigma}_2 + F_{B,T}^{(0)}(r) S_{12} \right] \cdot \frac{1}{m_\pi^2 \mathcal{M}}, \quad (\text{B1b})$$

where

$$F_{B,\sigma}^{(0)}(r) = \frac{1}{3} \left(\frac{2}{r} F' G + F' G' + F'' G \right), \quad F_{B,T}^{(0)}(r) = \frac{1}{3} \left(-\frac{1}{r} F' G + F' G' + F'' G \right). \quad (\text{B2a})$$

Above $\omega_1 = \sqrt{\mathbf{k}_1^2 + m_\pi^2}$ and $\omega_2 = \sqrt{\mathbf{k}_1^2 + m_\omega^2}$. For the Fourier transforms of the momentum pair-exchange potentials with gaussian form factors, we refer to the basic papers [31]. The superscript for the functions $F_{B,\sigma,T}$ refers to the denominators $1/\omega_1^2 \omega_2^2$ in (B1). For these denominators, in the notation of [31], the functions F and G are

$$F(r) = I_2(r, m_\pi, \Lambda_\pi), \quad G(r) = I_2(r, m_\omega, \Lambda_\omega). \quad (\text{B3})$$

Similar formulas apply to e.g. ΣN -potentials, and also to $(K^* K)_1$ -pair exchange.

2. The non-leading, i.e. $(1/M)$ -terms, are

$$\tilde{V}_{\sigma+T}^{(1)}(\mathbf{q}, \mathbf{k}) = -g_{(\pi\omega)_1; NN} f_{NN\pi} G_{NN\omega} \frac{1}{2M_N} \left(\boldsymbol{\sigma}_1 \cdot \mathbf{k} \boldsymbol{\sigma}_2 \cdot \mathbf{k}_2 + \boldsymbol{\sigma}_1 \cdot \mathbf{k}_2 \boldsymbol{\sigma}_2 \cdot \mathbf{k} \right) \times \frac{1}{\omega_1 \omega_2 (\omega_1 + \omega_2)} \cdot \frac{1}{m_\pi^2 \mathcal{M}}, \quad (\text{B4a})$$

$$V_{1/M, \sigma+T}^{(1)}(r) = +2g_{(\pi\omega)_1; NN} f_{NN\pi} G_{NN\omega} \frac{m_\pi}{2M_N} \left[F_{B,\sigma}^{(1)}(r) \boldsymbol{\sigma}_1 \cdot \boldsymbol{\sigma}_2 + F_{B,T}^{(1)}(r) S_{12} \right] \cdot \frac{1}{m_\pi^3 \mathcal{M}}, \quad (\text{B4b})$$

where now superscript for the functions $F_{B,\sigma,T}^{(1)}$ refers to the denominators $1/\omega_1 \omega_2 (\omega_1 + \omega_2)$ in (B4). For this denominator the basic Fourier transform is [31]

$$F_B^{(1)}(r) = \frac{2}{\pi} \int_0^\infty d\lambda F(\Lambda, r) G(\lambda, r), \quad (\text{B5})$$

where the functions F and G are

$$F(r) = I_2(r, m_\pi(\lambda), \Lambda_\pi), \quad G(r) = I_2(r, m_\omega(\lambda), \Lambda_\omega), \quad (\text{B6})$$

with the understanding that under the λ -integral in (B5) there occur the combinations

$$F_{B,\sigma}^{(1)}(r) = \frac{1}{3} \left(\frac{2}{r} F G' + F' G' + F G'' \right), \quad F_{B,T}^{(1)}(r) = \frac{1}{3} \left(-\frac{1}{r} F G' + F' G' + F G'' \right). \quad (\text{B7a})$$

3. The symmetric spin-orbit $(1/M)^2$ -terms, are

$$\tilde{V}_{SLS}^{(2)}(\mathbf{q}, \mathbf{k}) = -g_{(\pi\omega)_1; NN} f_{NN\pi} G_{NN\omega} \frac{1}{M_N^2} \frac{i}{2} (\boldsymbol{\sigma}_1 + \boldsymbol{\sigma}_2) \cdot \mathbf{q} \times \mathbf{k}_2 \times \frac{1}{\omega_2^2}, \quad (\text{B8a})$$

$$V_{SLS}^{(2)}(r) = -g_{(\pi\omega)_1; NN} f_{NN\pi} G_{NN\omega} \frac{1}{m_\pi^2 M_N^2} I_0(m_\pi, r) \left(-\frac{1}{r} \frac{d}{dr} I_2(m_\omega, \Lambda_V, r) \right) \mathbf{L} \cdot \mathbf{S}, \quad (\text{B8b})$$

where

$$I_0(\Lambda_P, r) = \frac{1}{4\pi} \frac{1}{2\sqrt{\pi}} \left(\frac{\Lambda_P}{m_\pi} \right)^3 \exp \left(-\frac{1}{4} \Lambda_P^2 r^2 \right). \quad (\text{B9})$$

We note that important contributions to the anti-symmetric spin-orbit potentials are proportional to $(1/M_N - 1/M_Y) \sim 1/M^2$. Also, spin-orbit potentials from OBE are order $1/M^2$. Therefore, we included this SLS-potential in the ESC08-model.

2. YN-potentials, (S=0, I=0)-Exchange, $(\pi\rho)_0$ etc.

The above given potentials also occur in YN- and YY-channels, of course. In this subsection we give as an illustration only the $1/M$ -contribution for the spin-spin and tensor. Again, to be specific, now we consider $(\pi\rho)_0$ -exchange for ΛN potentials. We obtain:

$$\tilde{V}_{\sigma+T}^{(1)}(\mathbf{q}, \mathbf{k}) = -2g_{\Lambda\Lambda;(\pi\rho)_0} f_{NN\pi} G_{NN\rho} \frac{1}{2M_N} [\boldsymbol{\sigma}_1 \cdot \mathbf{k} \boldsymbol{\sigma}_2 \cdot \mathbf{k}_2] \times \frac{1}{\omega_1 \omega_2 (\omega_1 + \omega_2)}, \quad (\text{B10a})$$

$$\tilde{V}_{\sigma+T}^{(1)}(\mathbf{q}, \mathbf{k}) = -2g_{NN;(\pi\rho)_0} f_{\Lambda\Sigma\pi} G_{\Lambda\Sigma\rho} \frac{1}{M_\Lambda + M_\Sigma} [\boldsymbol{\sigma}_1 \cdot \mathbf{k}_2 \boldsymbol{\sigma}_2 \cdot \mathbf{k}] \times \frac{1}{\omega_1 \omega_2 (\omega_1 + \omega_2)}. \quad (\text{B10b})$$

In configuration space we get

$$V_{\sigma+T}^{(1)}(r) = +2g_{\Lambda\Lambda;(\pi\rho)_0} f_{NN\pi} G_{NN\rho} \frac{1}{2M_N} \left[G_{B,\sigma}^{(1)}(r) \boldsymbol{\sigma}_1 \cdot \boldsymbol{\sigma}_2 + G_{B,T}^{(1)}(r) S_{12} \right], \quad (\text{B11a})$$

$$V_{\sigma+T}^{(1)}(r) = +2g_{NN;(\pi\rho)_0} f_{\Lambda\Sigma\pi} G_{\Lambda\Sigma\rho} \frac{1}{M_\Lambda + M_\Sigma} \left[G_{B,\sigma}^{(1)}(r) \boldsymbol{\sigma}_1 \cdot \boldsymbol{\sigma}_2 + G_{B,T}^{(1)}(r) S_{12} \right], \quad (\text{B11b})$$

where

$$G_{B,\sigma}^{(1)}(r) = \frac{1}{3} \left(\frac{2}{r} F_\pi \otimes F'_\omega + F'_\pi \otimes F'_\omega + F_\pi \otimes F''_\omega \right), \quad (\text{B12a})$$

$$G_{B,T}^{(1)}(r) = \frac{1}{3} \left(-\frac{1}{r} F_\pi \otimes F'_\omega + F'_\pi \otimes F'_\omega + F \otimes_\pi F''_\omega \right). \quad (\text{B12b})$$

Here, again the superscript on the G-functions refers to the denominator in momentum space. For the denominators in (B10) the functions $F \otimes g$ are given by[31]

$$F_\alpha \otimes F_\beta(r) = \frac{2}{\pi} \int_0^\infty d\lambda F_\alpha(\lambda, r) F_\beta(\lambda, r), \quad (\text{B13})$$

where

$$F_\alpha(\lambda, r) = e^{-\lambda^2/\Lambda_\alpha^2} I_2(\sqrt{m_\alpha^2 + \lambda^2}, r). \quad (\text{B14})$$

3. YN-potentials, (S = ±1, I = 1/2)-Exchange, $(\pi K^*)_{1/2}$ etc.

Again, to be specific, consider $(\pi K^*)_{1/2}$ -exchange for ΛN potentials. One obtains:
The leading, i.e. $(1/M)^0$ -potentials

$$\tilde{V}_{\sigma+T}^{(1)}(\mathbf{q}, \mathbf{k}) = +g_{(\pi K^*); \Lambda N} f_{NN\pi} G_{N\Lambda K^*} \left(\boldsymbol{\sigma}_1 \cdot \mathbf{k} \boldsymbol{\sigma}_2 \cdot \mathbf{k}_1 + \boldsymbol{\sigma}_1 \cdot \mathbf{k}_1 \boldsymbol{\sigma}_2 \cdot \mathbf{k} \right) \times \frac{1}{\omega_1^2 \omega_2^2} \cdot \mathcal{P}_f, \quad (\text{B15a})$$

$$\tilde{V}_{\sigma+T}^{(1)}(\mathbf{q}, \mathbf{k}) = +g_{(\pi K^*); \Lambda N} f_{\Lambda\Sigma\pi} G_{N\Sigma K^*} \left(\boldsymbol{\sigma}_1 \cdot \mathbf{k} \boldsymbol{\sigma}_2 \cdot \mathbf{k}_1 + \boldsymbol{\sigma}_1 \cdot \mathbf{k}_1 \boldsymbol{\sigma}_2 \cdot \mathbf{k} \right) \times \frac{1}{\omega_1^2 \omega_2^2} \cdot \mathcal{P}_f. \quad (\text{B15b})$$

The configuration space potentials are:

$$V_{\sigma+T}^{(1)}(r) = -2g_{(\pi K^*); \Lambda N} f_{NN\pi} G_{N\Lambda K^*} \left(F_{B,\sigma}^{(0)}(r) \boldsymbol{\sigma}_1 \cdot \boldsymbol{\sigma}_2 + F_{B,T}^{(0)}(r) S_{12} \right) \cdot \mathcal{P}_f, \quad (\text{B16a})$$

$$V_{\sigma+T}^{(1)}(r) = -2g_{(\pi K^*); \Lambda N} f_{\Lambda\Sigma\pi} G_{N\Sigma K^*} \left(F_{B,\sigma}^{(0)}(r) \boldsymbol{\sigma}_1 \cdot \boldsymbol{\sigma}_2 + F_{B,T}^{(0)}(r) S_{12} \right) \cdot \mathcal{P}_f. \quad (\text{B16b})$$

The non-leading, i.e. $(1/M)^1$ -potentials are

$$\tilde{V}_{\sigma+T}^{(1)}(\mathbf{q}, \mathbf{k}) = -g_{(\pi K^*); \Lambda N} f_{NN\pi} G_{N\Lambda K^*} \frac{1}{2M_N} \left[\left(\boldsymbol{\sigma}_1 \cdot \mathbf{k} \boldsymbol{\sigma}_2 \cdot \mathbf{k}_2 + \boldsymbol{\sigma}_1 \cdot \mathbf{k}_2 \boldsymbol{\sigma}_2 \cdot \mathbf{k} \right) \right] \frac{1}{\omega_1 \omega_2 (\omega_1 + \omega_2)} \cdot \mathcal{P}_f, \quad (\text{B17a})$$

$$\tilde{V}_{\sigma+T}^{(1)}(\mathbf{q}, \mathbf{k}) = -g_{(\pi K^*); \Lambda N} f_{\Lambda \Sigma \pi} G_{N\Sigma K^*} \frac{1}{M_\Lambda + M_\Sigma} \left(\boldsymbol{\sigma}_1 \cdot \mathbf{k} \boldsymbol{\sigma}_2 \cdot \mathbf{k}_2 + \boldsymbol{\sigma}_1 \cdot \mathbf{k}_2 \boldsymbol{\sigma}_2 \cdot \mathbf{k} \right) \frac{1}{\omega_1 \omega_2 (\omega_1 + \omega_2)} \cdot \mathcal{P}_f. \quad (\text{B17b})$$

The configuration space potentials are:

$$V_{\sigma+T}^{(1)}(r) = +2g_{(\pi K^*); \Lambda N} f_{NN\pi} G_{N\Lambda K^*} \frac{m_\pi}{2M_N} \left(G_{B,\sigma}^{(1)}(r) \boldsymbol{\sigma}_1 \cdot \boldsymbol{\sigma}_2 + G_{B,T}^{(1)}(r) S_{12} \right) \cdot \mathcal{P}_f, \quad (\text{B18a})$$

$$V_{\sigma+T}^{(1)}(r) = +2g_{(\pi K^*); \Lambda N} f_{\Lambda \Sigma \pi} G_{N\Sigma K^*} \frac{m_\pi}{M_\Lambda + M_\Sigma} \left(G_{B,\sigma}^{(1)}(r) \boldsymbol{\sigma}_1 \cdot \boldsymbol{\sigma}_2 + G_{B,T}^{(1)}(r) S_{12} \right) \cdot \mathcal{P}_f. \quad (\text{B18b})$$

Above, \mathcal{P}_f is the flavor-exchange operator, discussed in [12, 25]. In addition, we have to multiply these potentials with the isoscalar factors appearing in the Hamiltonian (4.26). For example for $K - \rho$ and $K - \phi$ pairs this factor is $+\sqrt{3}/4$ respectively $-1/4$, etc.

Appendix C: Exchange Potentials

In this section we follow our multi-channel description formalism in the treatment of the exchange potentials [7].

In the case of the anti-symmetric spin-orbit the exchange potential requires some attention, because their special features. The potentials in configuration space are described in Pauli-spinor space as follows

$$V = V_C + V_\sigma \boldsymbol{\sigma}_1 \cdot \boldsymbol{\sigma}_2 + V_T S_{12} + V_{SL} \mathbf{L} \cdot \mathbf{S}_+ + V_{AL} \mathbf{L} \cdot \mathbf{S}_- + V_Q Q_{12}. \quad (\text{C1})$$

Here, the definition of the matrix elements of the spin operators are defined as follows

$$\left(\chi_{m'}^\dagger(\Lambda) \chi_{n'}^\dagger(N) | \boldsymbol{\sigma}_1 \cdot \boldsymbol{\sigma}_2 | \chi_m^\dagger(\Lambda) \chi_n^\dagger(N) \right) \equiv \left(\chi_{m'}^\dagger(\Lambda) | \boldsymbol{\sigma}_1 | \chi_m^\dagger(\Lambda) \right) \cdot \left(\chi_{n'}^\dagger(N) | \boldsymbol{\sigma}_2 | \chi_n^\dagger(N) \right), \quad (\text{C2})$$

and similarly for the SU(2) and SU(3) operator matrix elements. In Fig. 8 the labels (m, n, m', n') refer to the spin, and the labels $(\alpha, \beta, \alpha', \beta')$ refer to unitary spin, like SU(2) or SU(3). The momenta on line 1 are \mathbf{p} and \mathbf{p}' for respectively the initial and the final state. Likewise, the momenta on line 2 are $-\mathbf{p}$ and $-\mathbf{p}'$ for respectively the initial and the final state.

In graph Fig. 8 we encounter the matrix elements

Properties of this operator are

$$\begin{aligned} (\boldsymbol{\sigma}_1)_{m',m} &= \left(\chi_{m'}^\dagger(N) | \boldsymbol{\sigma}_1 | \chi_m^\dagger(\Lambda) \right), \\ (\boldsymbol{\sigma}_2)_{n',n} &= \left(\chi_{n'}^\dagger(\Lambda) | \boldsymbol{\sigma}_2 | \chi_n^\dagger(N) \right) \end{aligned} \quad (\text{C3})$$

1. Spin-Exchange Potentials

In order to project the exchange potentials on the forms in (C1) we have to rewrite these matrix elements in terms of those occurring in (C2). This can be done using the spin-exchange operator P_σ :

$$P_\sigma = \frac{1}{2} (1 + \boldsymbol{\sigma}_1 \cdot \boldsymbol{\sigma}_2). \quad (\text{C4})$$

$$\begin{aligned} P_\sigma^\dagger &= P_\sigma, \quad P_\sigma^2 = 1, \\ P_\sigma \chi_{1,m} \chi_{2,n} &= \chi_{1,n} \chi_{2,m}, \\ P_\sigma \sigma_{1,k} P_\sigma &= \sigma_{2,k}, \\ P_\sigma \sigma_{2,k} P_\sigma &= \sigma_{1,k}. \end{aligned}$$

Similar properties hold for the flavor-exchange operator P_f , but then for the SU(2) isospin operators τ_k , or the SU(3) octet operators λ_k .

In the following we make only explicit the spin labels, but similar operations apply to the SU(2) or SU(3) labels.

Using this spin-exchange operator, we find that

$$\begin{aligned} &\left(\chi_{1,m'}^\dagger(N) \chi_{2,n'}^\dagger(\Lambda) | \boldsymbol{\sigma}_1 \otimes 1_2 - 1_1 \otimes \boldsymbol{\sigma}_2 | \chi_{1,m}^\dagger(\Lambda) \chi_{2,n}^\dagger(N) \right) = \\ &\left(\chi_{2,n'}^\dagger(N) \chi_{1,m'}^\dagger(\Lambda) | P_\sigma^\dagger \left(\boldsymbol{\sigma}_1 \otimes 1_2 - 1_1 \otimes \boldsymbol{\sigma}_2 \right) P_\sigma | \chi_{1,m}^\dagger(\Lambda) \chi_{2,n}^\dagger(N) \right) = \\ &- \left(\chi_{1,m'}^\dagger(\Lambda) \chi_{1,n'}^\dagger(N) | (\boldsymbol{\sigma}_1 \otimes 1_2 - 1_1 \otimes \boldsymbol{\sigma}_2) P_\sigma | \chi_{1,m}^\dagger(\Lambda) \chi_{2,n}^\dagger(N) \right). \end{aligned} \quad (\text{C5})$$

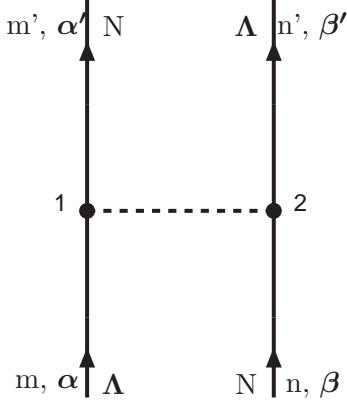


FIG. 8: Particle- and spin-exchange for ΛN .

Above, we added the subscripts 1 and 2 to indicate explicitly the baryon line that is involved.

2. Spin- and Strangeness-Exchange Potentials

In addition to the spin-exchange, we also have the flavor-exchange operator P_f active here. So, in total we have to apply $-P_\sigma P_f = P_x$, i.e. the space-exchange operator. This latter relation follows from the anti-symmetry of the two-baryon states, which implies that only states with $P_f P_\sigma P_x = -1$ are physical. All this implies

1. For the ALS-potential derived in K-exchange etc. one has in (C1), considering both spin- and flavor-exchange, the operator

$$\text{ALS} \Rightarrow \frac{1}{2} (\boldsymbol{\sigma}_1 - \boldsymbol{\sigma}_2) \cdot \mathbf{L} P_x \quad (\text{C6})$$

2. For the SLS-potential derived in K-exchange etc. one has in (C1), considering both spin- and flavor-exchange, the operator $P_f P_\sigma$, but since

$$\begin{aligned} \boldsymbol{\sigma}_1 \cdot \boldsymbol{\sigma}_2 \sigma_{1,k} &= \sigma_{2,k} + i\epsilon_{klm} \sigma_{1,l} \sigma_{2,m} , \\ \boldsymbol{\sigma}_1 \cdot \boldsymbol{\sigma}_2 \sigma_{2,k} &= \sigma_{1,k} + i\epsilon_{klm} \sigma_{2,l} \sigma_{1,m} , \end{aligned}$$

one derives easily that

$$P_\sigma (\boldsymbol{\sigma}_1 + \boldsymbol{\sigma}_2) \cdot \mathbf{L} = (\boldsymbol{\sigma}_1 + \boldsymbol{\sigma}_2) \cdot \mathbf{L} , \quad (\text{C7})$$

and therefore, similarly to (C5) we have, with the inclusion of the flavor labels,

$$\begin{aligned} & \left(\chi_{1,m'\alpha'}^\dagger(N) \chi_{2,n'\beta'}^\dagger(\Lambda) | \boldsymbol{\sigma}_1 \otimes 1_2 + 1_1 \otimes \boldsymbol{\sigma}_2 | \chi_{1,m\alpha}^\dagger(\Lambda) \chi_{2,n\beta}^\dagger(N) \right) = \\ & \left(\chi_{2,n'\beta'}^\dagger(N) \chi_{1,m'\alpha'}^\dagger(\Lambda) | P_f^\dagger P_\sigma^\dagger \left(\boldsymbol{\sigma}_1 \otimes 1_2 + 1_1 \otimes \boldsymbol{\sigma}_2 \right) | \chi_{1,m\alpha}^\dagger(\Lambda) \chi_{2,n\beta}^\dagger(N) \right) = \\ & \left(\chi_{1,m'\alpha'}^\dagger(\Lambda) \chi_{1,n'\beta'}^\dagger(N) | (\boldsymbol{\sigma}_1 \otimes 1_2 + 1_1 \otimes \boldsymbol{\sigma}_2) P_f | \chi_{1,m\alpha}^\dagger(\Lambda) \chi_{2,n\beta}^\dagger(N) \right) . \end{aligned} \quad (\text{C8})$$

So, for the SLS-potential derived in K-exchange etc. one has in (C1), considering both spin- and flavor-exchange, the operator

$$\text{SLS} \Rightarrow \frac{1}{2} (\boldsymbol{\sigma}_1 + \boldsymbol{\sigma}_2) \cdot \mathbf{L} P_f \quad (\text{C9})$$

This treatment for the SLS-potential also applies to the central-, spin-spin-, tensor-, and quadratic-spin-orbit potentials as well, of course.

We conclude this section by noticing that we have found, using our multi-channel set-up the same prescriptions for the treatment of the flavor-exchange potentials as in [25]. For the treatment of the ALS-potential for $S = \pm 1$ -exchange, our prescription here is more clear. For example in the case of the coupled $^1P_1 - ^3P_1$ system our prescription is unambiguous, and given by the P_x -operator, which is the same for both partial-waves coupled in this case.

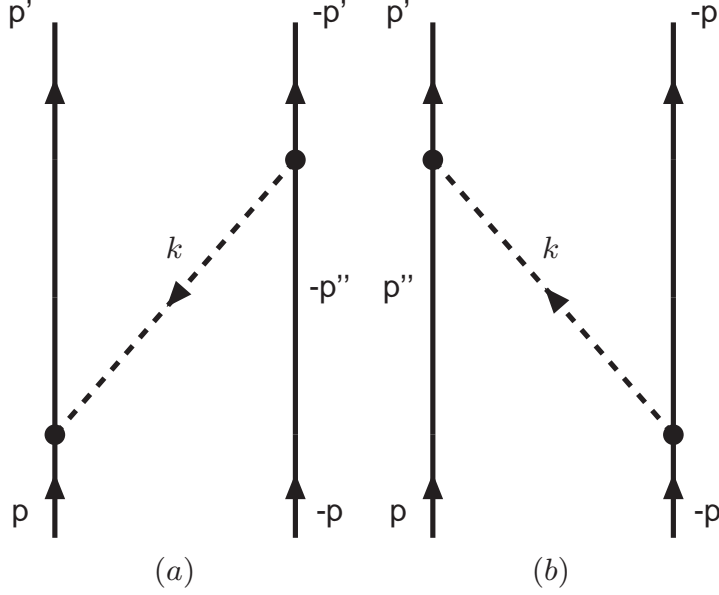


FIG. 9: K- and K*-exchange time-ordered graphs (a) and (b).

Appendix D: Derivation BDI ALS-potentials for strange-meson-exchanges

The contributions to the P_8 -spinor invariant, see [26],

$$P_8 = 2 \left(\sigma_1 \cdot \mathbf{q} \sigma_2 \cdot \mathbf{k} - \sigma_1 \cdot \mathbf{k} \sigma_2 \cdot \mathbf{q} \right), \quad (\text{D1})$$

for (K, K^*) -exchange were given by Brown, Downs, and Iddings [16]. Here we derive these for (K, K^*, K_1, K_2) , and in particular for the pseudoscalar K within the ps-pv theory.

1. K-exchange ALS-potential (PS-PV Theory)

We derive the K-exchange potential using the PV-theory, and show that we get the BDI-answer for the anti-symmetric spin-orbit potential (ALS). For graph (a) we get from the vertices the matrix element

$$\begin{aligned} (a) &: -\frac{f_P^2}{m_\pi^2} \left[\sigma_1 \cdot \mathbf{k} + \frac{2\omega}{M_\Lambda + M_N} \sigma_1 \cdot \mathbf{q} \right] \left[-\sigma_2 \cdot \mathbf{k} + \frac{2\omega}{M_\Lambda + M_N} \sigma_2 \cdot \mathbf{q} \right] \cdot \frac{1}{2\omega} \frac{-1}{\omega - a} \\ &= -\frac{f_P^2}{m_\pi^2} \left[\sigma_1 \cdot \mathbf{k} \sigma_2 \cdot \mathbf{k} - \frac{2\omega}{M_\Lambda + M_N} (\sigma_1 \cdot \mathbf{k} \sigma_2 \cdot \mathbf{q} - \sigma_1 \cdot \mathbf{q} \sigma_2 \cdot \mathbf{k}) \right] \cdot \frac{1}{2\omega(\omega - a)}, \end{aligned} \quad (\text{D2a})$$

$$\begin{aligned} (b) &: -\frac{f_P^2}{m_\pi^2} \left[\sigma_1 \cdot \mathbf{k} - \frac{2\omega}{M_\Lambda + M_N} \sigma_1 \cdot \mathbf{q} \right] \left[-\sigma_2 \cdot \mathbf{k} - \frac{2\omega}{M_\Lambda + M_N} \sigma_2 \cdot \mathbf{q} \right] \cdot \frac{1}{2\omega} \frac{-1}{\omega + a} \\ &= -\frac{f_P^2}{m_\pi^2} \left[\sigma_1 \cdot \mathbf{k} \sigma_2 \cdot \mathbf{k} + \frac{2\omega}{M_\Lambda + M_N} (\sigma_1 \cdot \mathbf{k} \sigma_2 \cdot \mathbf{q} - \sigma_1 \cdot \mathbf{q} \sigma_2 \cdot \mathbf{k}) \right] \cdot \frac{1}{2\omega(\omega + a)}, \end{aligned} \quad (\text{D2b})$$

where $a = M_\Lambda - M_N$. Summing these contributions gives

$$\begin{aligned}\tilde{V}_K(\mathbf{q}, \mathbf{k}) &= -\frac{f_P^2}{m_\pi^2} \left[\frac{1}{2\omega} \left\{ \frac{1}{\omega - a} + \frac{1}{\omega + a} \right\} \boldsymbol{\sigma}_1 \cdot \mathbf{k} \boldsymbol{\sigma}_2 \cdot \mathbf{k} \right. \\ &\quad \left. + \frac{1}{M_\Lambda + M_N} \left\{ \frac{1}{\omega - a} - \frac{1}{\omega + a} \right\} (\boldsymbol{\sigma}_1 \cdot \mathbf{k} \boldsymbol{\sigma}_2 \cdot \mathbf{q} - \boldsymbol{\sigma}_1 \cdot \mathbf{q} \boldsymbol{\sigma}_2 \cdot \mathbf{k}) \right] \mathcal{P}_f \\ &= -\frac{f_P^2}{m_\pi^2} \left[\boldsymbol{\sigma}_1 \cdot \mathbf{k} \boldsymbol{\sigma}_2 \cdot \mathbf{k} - 2 \frac{M_\Lambda - M_N}{M_\Lambda + M_N} (\boldsymbol{\sigma}_1 \cdot \mathbf{k} \boldsymbol{\sigma}_2 \cdot \mathbf{q} - \boldsymbol{\sigma}_1 \cdot \mathbf{q} \boldsymbol{\sigma}_2 \cdot \mathbf{k}) \right] \mathcal{P}_f \cdot \frac{1}{\omega^2 - a^2}\end{aligned}\quad (\text{D3})$$

We notice that this result corresponds with the answer in the PS-PS theory. All this in the approximation $(M_\Lambda + M_N)^{-1} = (1/M_\Lambda + 1/M_N)/4$. Now, using the definitions in [12, 26] we have

$$\begin{aligned}P_8 &= 2 \left(\boldsymbol{\sigma}_1 \cdot \mathbf{q} \boldsymbol{\sigma}_2 \cdot \mathbf{k} - \boldsymbol{\sigma}_1 \cdot \mathbf{k} \boldsymbol{\sigma}_2 \cdot \mathbf{q} \right), \\ P_6 &= (i/2) (\boldsymbol{\sigma}_1 - \boldsymbol{\sigma}_2) \cdot \mathbf{n}, \quad \mathbf{n} = \mathbf{p} \times \mathbf{p}' = \mathbf{q} \times \mathbf{k},\end{aligned}$$

with the relation [16] $P_8 = -(1 + \boldsymbol{\sigma}_1 \cdot \boldsymbol{\sigma}_2) P_6 = 2\mathcal{P}_x \mathcal{P}_f P_6$. This leads to the following expression

$$\tilde{V}_K(\mathbf{q}, \mathbf{k}) = -\frac{f_P^2}{m_\pi^2} \left[\boldsymbol{\sigma}_1 \cdot \mathbf{k} \boldsymbol{\sigma}_2 \cdot \mathbf{k} + 2 \frac{M_\Lambda - M_N}{M_\Lambda + M_N} \cdot (i/2) (\boldsymbol{\sigma}_1 - \boldsymbol{\sigma}_2) \cdot \mathbf{n} \mathcal{P}_x \mathcal{P}_f \right] \mathcal{P}_f \cdot \frac{1}{\omega^2 - a^2} \quad (\text{D4})$$

2. K^* -exchange ALS-potential

Upon inspection, we find that the only contribution to the P_8 -invariant is given by

$$\begin{aligned}\tilde{V}_{K^*}(\mathbf{q}, \mathbf{k}) &\approx \frac{1}{4} \frac{G_{13} G_{24}}{\omega^2 - a^2} \boldsymbol{\sigma}_1 \cdot \left(\frac{\mathbf{p}}{M_N} - \frac{\mathbf{p}'}{M_\Lambda} \right) \boldsymbol{\sigma}_2 \cdot \left(\frac{\mathbf{p}}{M_\Lambda} - \frac{\mathbf{p}'}{M_N} \right) \mathcal{P}_f \\ &= \frac{1}{4} \frac{G_{13} G_{24}}{\omega^2 - a^2} \left[\boldsymbol{\sigma}_1 \cdot \left\{ \left(\frac{1}{M_N} - \frac{1}{M_\Lambda} \right) \mathbf{q} - \frac{1}{2} \left(\frac{1}{M_N} + \frac{1}{M_\Lambda} \right) \mathbf{k} \right\} \cdot \right. \\ &\quad \left. \boldsymbol{\sigma}_2 \cdot \left\{ \left(\frac{1}{M_\Lambda} - \frac{1}{M_M} \right) \mathbf{q} - \frac{1}{2} \left(\frac{1}{M_\Lambda} + \frac{1}{M_N} \right) \mathbf{k} \right\} \right] \mathcal{P}_f \\ &= \frac{1}{4} \frac{G_{13} G_{24}}{\omega^2 - a^2} \left[\frac{1}{4} \left(\frac{1}{M_N} + \frac{1}{M_\Lambda} \right)^2 \boldsymbol{\sigma}_1 \cdot \mathbf{k} \boldsymbol{\sigma}_2 \cdot \mathbf{k} - \left(\frac{1}{M_N} - \frac{1}{M_\Lambda} \right)^2 \boldsymbol{\sigma}_1 \cdot \mathbf{q} \boldsymbol{\sigma}_2 \cdot \mathbf{q} \right. \\ &\quad \left. - \frac{1}{2} \left(\frac{1}{M_N^2} - \frac{1}{M_\Lambda^2} \right) (\boldsymbol{\sigma}_1 \cdot \mathbf{q} \boldsymbol{\sigma}_2 \cdot \mathbf{k} - \boldsymbol{\sigma}_1 \cdot \mathbf{k} \boldsymbol{\sigma}_2 \cdot \mathbf{q}) \right] \mathcal{P}_f,\end{aligned}\quad (\text{D5})$$

which gives the anti-symmetric spin-orbit potential

$$\tilde{V}_{K^*}(\mathbf{q}, \mathbf{k}) = \frac{1}{4} \frac{G_{13} G_{24}}{\omega^2 - a^2} \left(\frac{1}{M_N^2} - \frac{1}{M_\Lambda^2} \right) (i/2) (\boldsymbol{\sigma}_1 - \boldsymbol{\sigma}_2) \cdot \mathbf{n} \mathcal{P}_x. \quad (\text{D6})$$

Finally, we mention the relation with another sometimes used form for the antisymmetric spin-orbit. Namely, we have $\boldsymbol{\sigma}_1 \cdot \boldsymbol{\sigma}_2 (\boldsymbol{\sigma}_1 \times \boldsymbol{\sigma}_2) = -2i(\boldsymbol{\sigma}_1 - \boldsymbol{\sigma}_2) - \boldsymbol{\sigma}_1 \times \boldsymbol{\sigma}_2$, so that

$$(\boldsymbol{\sigma}_1 - \boldsymbol{\sigma}_2) = iP_\sigma (\boldsymbol{\sigma}_1 \times \boldsymbol{\sigma}_2). \quad (\text{D7})$$

Acknowledgments

We wish to thank E. Hiyama, K. Itonaga, T. Motoba, and H.-J. Schulze for many stimulating discussions.

[1] M.M. Nagels, Th.A. Rijken, and Y. Yamamoto, *Extended-soft-core Baryon-Baryon Model ESC08, I. Nucleon-Nucleon Scattering*, arXiv:nucl-th/1408.4825

(2014)
[2] M.M. Nagels, Th.A. Rijken, and Y. Yamamoto, *Extended-soft-core Baryon-Baryon Model ESC08, II.*

- Hyperon-Nucleon Interactions*, this paper preprint 2014.
- [3] M.M. Nagels, Th.A. Rijken, and Y. Yamamoto, *Extended-soft-core Baryon-Baryon Model ESC08, III. $S=-2$ Hyperon-hyperon/nucleon Interactions*, preprint 2014.
 - [4] Th.A. Rijken, M.M. Nagels, and Y. Yamamoto, *Progr. Theor. Phys.* **185**, 14 (2010); Y. Yamamoto, T. Motoba, and Th.A. Rijken, *ibid* 72; E. Hiyama, M. Kamimura, Y. Yamamoto, T. Motoba, and Th.A. Rijken, *ibid* 106.
 - [5] Th.A. Rijken, *Phys. Rev.* **C73**, 044007 (2006).
 - [6] Th.A. Rijken and Y. Yamamoto, *Phys. Rev.* **C73**, 044008 (2006).
 - [7] Th.A. Rijken and Y. Yamamoto, *Extended-soft-core baryon-baryon model III, hyperon-hyperon/nucleon interactions*, arXiv:nucl-th/060807 (2006)
 - [8] L. Micu, *Nucl. Phys.* **B10** (1969) 521; R. Carlitz and M. Kislinger, *Phys. Rev. D* **2** (1970) 336.
 - [9] A. Le Yaouanc, L. Oliver, O. Pène, and J.-C. Raynal, *Phys. Rev. D* **8** (1973) 2223; *Phys. Rev. D* **11** (1975) 1272.
 - [10] N. Isgur and J. Paton, *Phys. Rev.* **D31**, 2910 (1985); R. Kokoski and N. Isgur, *Phys. Rev.* **D35**, 907 (1987).
 - [11] M.M. Nagels, T.A. Rijken, and J.J. de Swart, *Phys. Rev. D* **17** (1978) 768.
 - [12] P.M.M. Maessen, Th.A. Rijken, and J.J. de Swart, *Phys. Rev. C* **40** (1989) 2226.
 - [13] Th.A. Rijken, V.G.J. Stoks, and Y. Yamamoto, *Phys. Rev. C* **59**, 21, (1999).
 - [14] E. Hiyama, M. Kamimura, T. Motoba, T. Yamada, and Y. Yamamoto, *Phys. Rev. Lett.* **85** (2000) 270.
 - [15] O. Hashimoto and H. Tamura, *Progr. Part. Phys.* **57** (2006) 564.
 - [16] J.T. Brown, B.W. Downs, and C.K. Iddings, *Ann. Phys. (N.Y.)* **60**, 148 (1970).
 - [17] For the OBE-potentials we have included the Brown-Downs-Iddings anti-symmetric spin-orbit potentials from pseudo-scalar, vector-, and scalar- meson exchange [16]. Also we derived new anti-symmetric spin-orbit contributions from MPE. Since we do not fit P-waves for YN, these play no role in the construction of the ERSC07-model. Therefore, these potentials will be published elsewhere.
 - [18] In principle, the off-mass-shell $J=0$ contribution from the tensor-meson nonet A_2, K_2 etc. is included with the diffractive soft-core potentials, see e.g. [11, 12]. Although the couplings are zero in ESC08 models, we include these potentials in the text for completeness.
 - [19] For a review see: C. Ewerz, *The Odderon in Quantum Chromodynamics*, hep-ph/0306137.
 - [20] M. Oka, K. Shimizu, and K. Yazaki, *Progr. Theor. Phys., Suppl.* **137**, p. 1 (2000).
 - [21] Y. Fujiwara, Y. Suzuki, and C. Nakamoto, *Progr. in Part. and Nuclear Physics*, **58** (2007) 439.
 - [22] R. Tamagaki and H. Tanaka, *Progr. Theor. Physics*, **34**, 191 (1965); R. Tamagaki, *Suppl. Progr. Theor. Phys., Extra Number*, p.242, 1968; R. Tamagaki, *Progr. Theor. Phys.* **39**, 91 (1968).
 - [23] J. Dabrowski, *Phys. Rev. C* **60** (1999) 025205.
 - [24] H. Noumi et al., *Phys. Rev. Lett.* **89** (2002) 072301.
 - [25] M.M. Nagels, T.A. Rijken, and J.J. de Swart, *Phys. Rev. D* **15** (1977) 2547.
 - [26] J.J. de Swart, M.M. Nagels, T.A. Rijken, and P.A. Verhoeven, *Springer Tracts in Modern Physics*, **60**, 138 (1971).
 - [27] M.M. Nagels, T.A. Rijken, and J.J. de Swart, *Ann. Phys. (N.Y.)* **79**, 338 (1973).
 - [28] R.H. Dalitz and F. von Hippel, *Phys. Lett.* **10**, 153 (1964).
 - [29] C. Itzykson and J-B. Zuber, *Quantum Field Theory*, section 2-3-2, McGraw-Hill Inc. 1980.
 - [30] Th.A. Rijken, *Ann. Phys. (N.Y.)*, **208**, 253 (1991).
 - [31] Th.A. Rijken and V.G.J. Stoks, *Phys. Rev. C* **54** (1996) 2869; *ibid. C* **54** (1996) 2869.
 - [32] E. Hiyama, T. Motoba, Y. Yamamoto, and Th.A. Rijken, in preparation.
 - [33] V.G.J. Stoks, R.A.M. Klomp, M.C.M. Rentmeester, and J.J. de Swart, *Phys. Rev. C* **48** (1993) 792.
 - [34] R.A.M. Klomp, private communication (unpublished).
 - [35] J.K. Ahn et al., *Nucl. Phys. A* **761** (2005) 41.
 - [36] J.A. Kadyk, G. Alexander, J.H. Chan, P. Gaposchkin and G.H. Trilling, *Nucl. Phys.* **B27** (1971) 13.
 - [37] Y. Kondo et al., *Nucl. Phys. A* **676** (2000) 371.
 - [38] T. Takahashi et al., *Phys. Rev. Lett.* **87** (2001) 212502.
 - [39] E. Hiyama, M. Kamimura, T. Motoba, T. Yamada, and Y. Yamamoto, *Phys. Rev. C* **66** (2002) 024007.
 - [40] P. Khaustov et al., *Phys. Rev. C* **61** (2000) 054603.
 - [41] V.G.J. Stoks, R. Timmermans, and J.J. de Swart, *Phys. Rev. C* **47** (1993) 512.
 - [42] V.G.J. Stoks, R.A.M. Klomp, C.P.F. Terheggen, and J.J. de Swart, *Phys. Rev. C* **49** (1994) 2950.
 - [43] R.A. Bryan and A. Gersten, *Phys. Rev. D* **6** (1972) 341.
 - [44] V.G.J. Stoks and Th.A. Rijken, *Nucl. Phys. A* **613** (1997) 311.
 - [45] G. Alexander, U. Karshon, A. Shapira, G. Yekutieli, R. Engelmann, H. Filthuth, and W. Lughofer, *Phys. Rev.* **173**, 1452 (1968).
 - [46] B. Sechi-Zorn, B. Kehoe, J. Twitty, and R.A. Burnstein, *Phys. Rev.* **175**, 1735 (1968).
 - [47] F. Eisele, H. Filthuth, W. Fölisch, V. Hepp, E. Leitner, and G. Zech, *Phys. Lett.* **37B**, 204 (1971).
 - [48] F.E. Close, and R.G. Roberts, *Phys. Lett. B* **316**, 165 (1993).
 - [49] R. Engelmann, H. Filthuth, V. Hepp, and E. Kluge, *Phys. Lett.* **21**, 587 (1966).
 - [50] V. Hepp and M. Schleich, *Z. Phys.* **214**, 71 (1968).
 - [51] D. Stephen, Ph.D. thesis, University of Massachusetts, 1970. *Z. Phys.* **214**, 71 (1968).
 - [52] T. Inoue et al, *Nucl. Phys. A* **881** (2012) 28.
 - [53] Y. Yamamoto and H. Bandō, *Prog. Theor. Phys. Suppl.* **No.81** (1985), 9.
 - [54] Y. Yamamoto, T. Motoba, H. Himeno, K. Ikeda and S. Nagata, *Prog. Theor. Phys. Suppl.* **No.117** (1994), 361.
 - [55] Y. Yamamoto, T. Motoba, Th.A. Rijken, *Prog. Theor. Phys. Suppl.* **No.185** (2010), 72.
 - [56] Y. Yamamoto, T. Furumoto, N. Yasutake and Th.A. Rijken, *Phys. Rev. C* **88** (2013), 022801(R).
 - [57] Y. Yamamoto, T. Furumoto, N. Yasutake and Th.A. Rijken, *Phys. Rev. C* **90** (2014), 045805.
 - [58] T. Harada and Y. Hirabayashi, *Nucl. Phys. A* **759**, 143 (2005).
 - [59] M. Kohno, Y. Fujiwara, Y. Watanabe, K. Ogata and M. Kawai *Phys. Rev.* **C74** (2006), 064613.
 - [60] R.R. Scheerbaum, *Nucl. Phys. A* **257** (1976), 77.
 - [61] O. Hashimoto and H. Tamura *Prog. Part. Nucl. Phys.* **57** (2006), 564.
 - [62] T. Fukuda *et al.*, *Phys. Rev.* **C58** (1998), 1306.
 - [63] P. Khaustov *et al.*, *Phys. Rev.* **C61** (2000), 054603.
 - [63] T. Gogami, PhD-thesis, Tohoku University 2014.

- [64] G.A. Miller, Phys. Rev. **C** (1989) 1563.
- [65] Th.A. Rijken and Y. Yamamoto, Proceedings of *The IX International Conference on Hypernuclear and Strange Particle Physics*, edited by J. Pochodzalla and Th. Walcher, October 10-14, 2006, p. 279. ISBN-10 3-540-76365-1 Springer Berlin Heidelberg New York.